

JOYCE DITS



OCULAR
STABILITY

3^{IN}-D
SPACE

Ocular Stability in Three-Dimensional Space

Joyce Dits

ISBN: 978-94-6169-497-3

Layout and printing: Optima Grafische Communicatie, Rotterdam, The Netherlands

Printing of this thesis was financially supported by: Chipsoft b.v, Erasmus Universiteit Rotterdam and Ikazia Ziekenhuis Rotterdam

Ocular Stability in Three-Dimensional Space

Stabiliteit van het oog in de driedimensionale ruimte

Proefschrift

ter verkrijging van de graad van doctor aan de
Erasmus Universiteit Rotterdam
op gezag van de
rector magnificus Prof.dr. H.A.P. Pols
en volgens besluit van het College voor Promoties.

De openbare verdediging zal plaatsvinden op
dinsdag 22 april 2014 om 15:30 uur

door

Joyce Dits

Geboren te Rotterdam



PROMOTIECOMMISSIE:

Promotor: Prof.dr. J. van der Steen

Co-promotor: Dr.ir. J.J.M. Pel

Overige leden: Prof.dr. J.G.G. Borst

Prof.dr.ir. M. Mulder

Prof.dr. R.J. Baatenburg de Jong

CONTENTS

| | | |
|-----------|---|-----|
| Chapter 1 | General Introduction | 7 |
| Chapter 2 | Binocular eye movement control and motion perception: What is being tracked? <i>Investigative Ophthalmology and Visual Science 2012</i> | 19 |
| Chapter 3 | Version-vergence interactions during memory-guided binocular gaze shifts. <i>Investigative Ophthalmology and Visual Science 2013</i> | 37 |
| Chapter 4 | Three dimensional vestibular ocular reflex testing using a six degrees of freedom motion platform. <i>Journal of Visualized Experiments 2013</i> | 59 |
| Chapter 5 | Scaling of compensatory eye movements during translations: virtual versus real depth. <i>Neuroscience 2013</i> | 79 |
| Chapter 6 | Memory-guided saccade-vergence interactions after passive whole-body rotations and translations. <i>Submitted Neuroscience 2014</i> | 97 |
| Chapter 7 | General discussion | 117 |
| Chapter 8 | Summary / Samenvatting | 129 |
| | Curriculum Vitae | 137 |
| | PhD Portfolio | 139 |
| | List of Publications | 141 |
| | Dankwoord | 141 |



1

General introduction

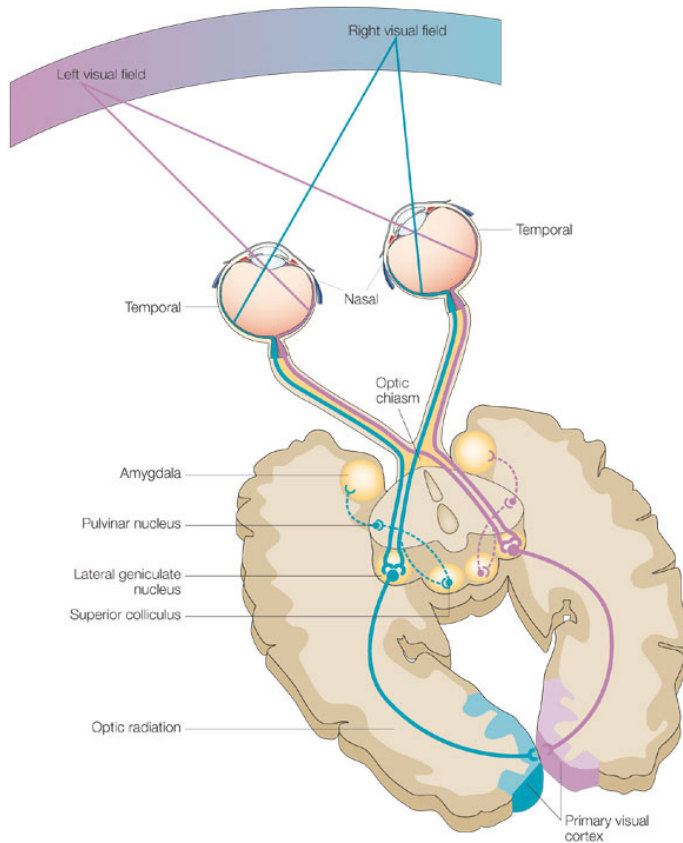
During natural movement, we visually orient ourselves continuously to objects in our environment that are located in different directions and at different viewing distances from our body. Since humans have their eyes placed frontally, we have the ability to look at these objects using combined images of two eyes. This is called binocular vision. Visual information that enters each eye remains segregated in the primary pathways up to the visual cortex. In the primary visual cortex the information of the two eyes are merged, which enables humans to perceive depth. There is a caveat in having binocular vision. To obtain sharp vision, objects of interest have to be projected on the fovea of both retinas, where photoreceptor density is largest. During movement, it is essential to keep track of the objects around us and to maintain clear and sharp binocular vision. The most essential tool in accomplishing these goals is making eye movements. Eye movements are necessary to compensate for motion and direct the lines of sight of both eyes to new objects of interest. This interaction between processing of visual information and making eye movements is an ongoing process, which allows us to continuously update all changes in our visual environment. Thus, eye movements can be regarded as 'the motor system that sees the world'. There are two types of eye movements; stabilizing and voluntary eye movements. Stabilizing eye movements, especially in association with the vestibular system, are necessary to maintain sharp vision during movement. Voluntary eye movements are used to shift gaze to new objects of interest. Voluntary eye movements can be triggered from visual, auditory or tactile stimuli, or from memory.

This thesis focuses on the accuracy and dynamics of binocular eye movements to objects at varying distances in three-dimensional space. The interaction between the direction of gaze of both eyes (version) and the angle between both eyes (vergence) was studied under different visual conditions, under memory guided conditions, when eye movements interact with the vestibular system and when whole body movements intervene with visual spatial memory. In the next chapters, an overview is presented of the characteristics of binocular vision, binocular eye movements, vestibulo-ocular reflex (VOR) and visual spatial memory.

BINOCULAR VISION

Central visual pathways

To understand the neural basis for arrangement of inputs from two eyes, the projection of images on the retina and central visual processing in the brain should be considered. Images of an object fall on the retinas of two eyes, producing two visual fields in which the position of that object is coded with respect to the fovea of each eye (see figure 1). Although the two visual fields partially overlap, the bilateral optic nerves contain the visual information of each eye. In the chiasm the fibers of the optic nerve are re-organized in the optic tracts, such that after the decussation, each optic tract carries a complete representation of one



Nature Reviews | Neuroscience

Figure 1: Visual pathways. Images of an object fall on the retinas of two eyes. Bilateral optic nerves are re-organized in the optic tracts, that project to the lateral geniculate nucleus of the thalamus. The optic radiation carries the contralateral hemifield information to the primary visual cortex (V1). [source: 1]

half of the binocular visual field. The two optic tracts project to subcortical targets. The most important one is the lateral geniculate nucleus of the thalamus, where left and right eye inputs terminate in different layers. Although the input from each eye is still segregated at this point, a complete retinotopic presentation of the contralateral visual field from both eyes is created. The lateral geniculate nucleus carries the contralateral hemifield information to the primary visual cortex (V1) which is the first stage for cortical visual information processing that ultimately leads to perception and motor action, i.e. making of eye movements.

One of the important properties of neurons in V1 is that many neurons are binocular, responding to stimulation of both left and right eyes. The axons of the geniculate neurons, which contain segregated information of the left and right eye, terminate within cortical layer 4 of the striate cortex in alternating eye-specific ocular dominance columns. Thus, layer 4 of V1 is the place where the visual information from the two eyes converges for the first

time. This combination of visual input from two eyes is a necessary first step for binocular vision and stereopsis [2, 3].

Perception of depth

Binocular view, or stereopsis, depends on the view on the world with each eye at a slightly different position. For three-dimensional depth vision, the visual system has to convert the two-dimensional images from each retina using monocular and binocular cues. The fixation point is the point of focus where images fall on corresponding places of the retina of both eyes. Objects in front or behind the fixation plane, project to non-corresponding points on the two retinas producing binocular disparity (presented in figure 2). This difference in image

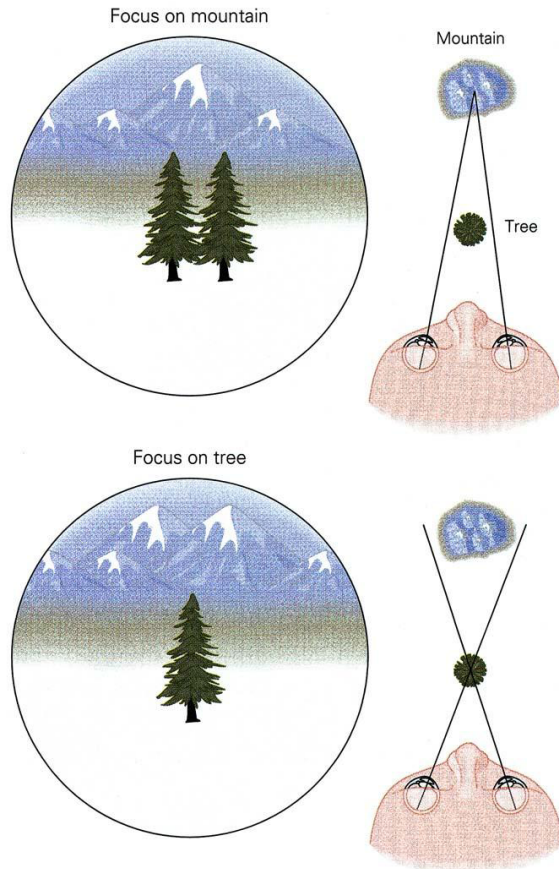


Figure 2: Disparity. When the eyes focus on the distant mountain, the nearer tree occupies relative different retinal position, resulting in disparity and double vision. When the eyes focus on the tree, the mountains appear double. [source: 2]

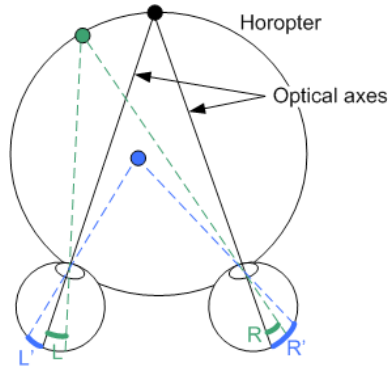


Figure 3: Horopter. Green: corresponding points on retina, same vergence angle, sharp vision; Blue: non-corresponding points, different vergence angle, double vision. (source <http://doc.instantreality.org/tutorial/stereo-basics/horopter.png>)

location of an object seen by the left and right eye is referred to as binocular disparity. This disparity results in double vision, or diplopia, and is a strong interpreter of depth [2, 3].

As the eyes fixate on a visual target, the locus of all points in space that make the same angles between the two eyes as the fixation target, produce sharp binocular vision. These points in space are located on one radius, a so-called horopter (or Vieth-Muller / iso-vergence circle) and project to corresponding locations on the retina, presented in figure 2. Targets located on the horopter produce zero disparity. Certain neurons in V1 respond selectively to disparity, while other neurons respond to zero disparity. Specific cells that respond to stimuli at a range of disparities in front or beyond the fixation plane are present in the striate and extrastriate cortex. Besides the perception of depth, disparity is also important for alignment of the eyes (convergence and divergence as will be discussed below) [4].

Besides binocular cues for processing perception of depth, additional information is acquired from monocular cues. An important monocular cue is the phenomenon that objects closer to the eye seem to move faster than objects at farther distance, as the observer moves. This phenomenon is referred to as motion parallax. Other examples of monocular cues are familiar size, shadow or linear perspective.

BINOCULAR EYE MOVEMENTS

Types of eye movements

For sharp vision, the object of interest has to be projected on the fovea, where photoreceptor density is greatest. During head motion, compensatory eye movements are required to stabilize gaze and keep images steady on the retina (vestibulo-ocular reflex, optokinetic reflex and smooth-pursuit). Voluntary eye movements are used to change the angle of gaze

and shift the line of sight to a new object of interest and are discussed here. To binocularly view an object of interest conjugate and disjunctive eye movements are made. Saccades are conjugate eye movements, which are fast, brief and accurate, used to change the line of sight in different direction in absence of head movements. They can be triggered by visual stimuli, auditory stimuli, or from memory (see below, spatial memory). Depending on the type of visual stimulus presentation, a delay of 100-200ms passes before the saccade is initiated. This period is necessary for processing the visual information and activating the ocular motor system to generate a saccade. The peak velocity of a saccade depends on size of saccades and has in humans a maximum of 500 degree/second. Saccades are short, not longer than 100ms, preventing interference with vision and because of this visual feedback cannot be used to adjust the amplitude or direction.

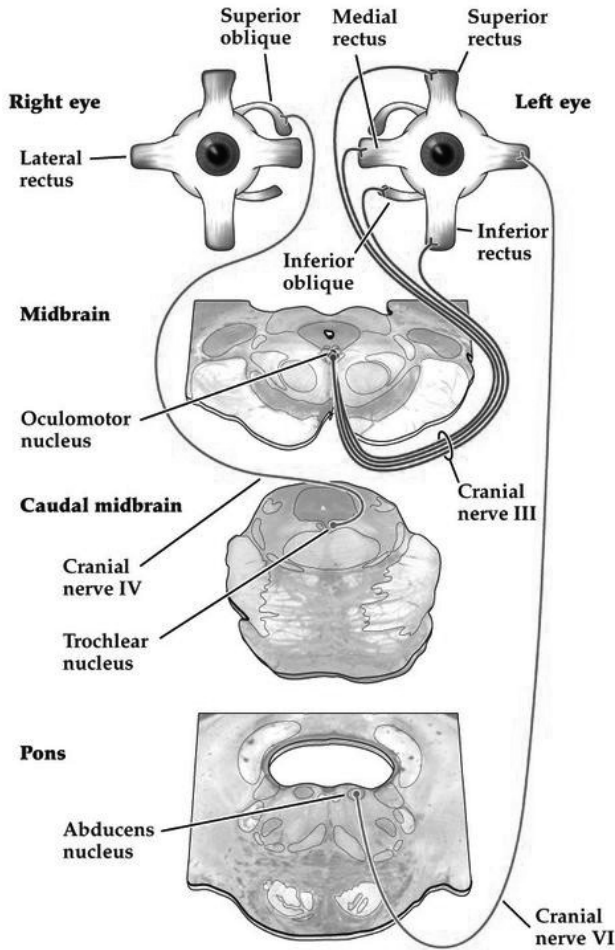
Gaze is shifted to different distances by vergence eye movements. Vergence eye movements are disjunctive (disconjugate) and rotate the eyes in opposite direction to change the angle between the eyes. Vergence movements are crucial for depth vision. When gaze is shifted from a visual target at far distance to a target closer, the angle between the eyes increases and a convergence eye movement is made. When the opposite occurs and the angle between the eyes decreases, a divergence eye movement is made. There are two important stimuli for vergence: the first stimulus is disparity between the projections on two retinas, and the second is accommodation (pupil constriction) in response to a near target. In contrast to saccades, vergence eye movements are slow movements in isolation and have lower peak-velocities [5].

The extraocular muscles and their innervations

Eye movements can be performed along three axes: horizontal, toward the nose (adduction) or toward temporal (abduction); vertical, elevation or depression; and torsional. Three antagonistic pairs of muscles control the eye movements. The medial and lateral rectus muscles control horizontal movements. Vertical movements are controlled by the superior and inferior rectus muscle, as well as by the oblique muscles. Torsional movements are generated by the inferior and superior oblique muscle. The innervation of the extraocular muscles is achieved by three cranial nerves, illustrated in figure 3. The abducens nerve (VI) innervates the lateral rectus muscle, which is responsible for abduction of the eye. The trochlear nerve (IV) innervates the superior oblique muscle. The oculomotor nerve (III) innervates the other muscles [3].

Control of binocular eye movements

During natural gaze shifts, we change our visual fixation between objects that lie in different direction and at different distances in the environment. To voluntarily accomplish these gaze



NEUROSCIENCE 5e, Figure 20.3

© 2012 Sinauer Associates, Inc.

Figure 4: Extraocular muscles and innervations. The innervation of the extraocular muscles is achieved by three cranial nerves. The abducens nerve (VI) innervates the lateral rectus muscle. The trochlear nerve (IV) innervates the superior oblique muscle. The oculomotor nerve (III) innervates the other muscles. [source: 3]

shifts, a combination of saccadic (conjugate) and vergence (disjunctive) eye movements is required. How binocular eye movements are coordinated remains an issue of discussion. The most accepted theory is Hering's law that describes different vergence and conjugate neuronal controllers that are summed by the motor neurons of each eye [6, 7]. Horizontal conjugate motor commands are generated in the paramedian pontine reticular formation (PPRF), known as the conjugate gaze center, whereas vergence command signals are generated in the midbrain [8-11]. Despite functional and anatomical differences between the two subsystems, there is also a close interaction. Helmholtz stated that each eye is individually

controlled and binocular coordination is learned behavior [12]. Saccadic and vergence movements are seldom made in isolation, but combinations are made continuously. During disjunctive saccadic gaze shifts, the dynamic properties of the vergence and conjugate components are altered; saccades are slowed down and vergence becomes faster, than if either movement was made in isolation [5, 13].

VESTIBULO-OCULAR REFLEX

Vestibular system and function

As stated, compensatory eye movements are made to maintain stable gaze during head and body movements. The vestibulo-ocular reflex (VOR) is an important mechanism for generating these movements. To understand the VOR and its relation to binocular vision, a short overview of the vestibular system is presented.

The peripheral vestibular organ, the labyrinth, is located in the temporal bone connected to the cochlea. Two otolith organs (the utricle and saccule) respond to linear (translational) accelerations and head position relative to gravity. The three semicircular canals are specialized for responding to rotational (angular) acceleration. Specialized sensory cells (hair cells) are activated by movements of endolymph fluid stimulating the vestibular nerve (n.VIII). The vestibulo-ocular reflex produces fast eye movements that counter head movements, permitting gaze to be fixed on a particular point in space. For example, activity in the right horizontal canal, induced by rightward rotation of the head, excites the right vestibular nucleus producing an eye movement to the left. Although the VOR is mainly vestibular driven and works even in total darkness, visual input increases its quality, expressed in terms of gain, the ratio between eye and head velocity. [3, 5]

Translational versus angular vestibulo-ocular reflex

Besides the difference in peripheral detection of translational and rotational head movements, the properties and goals of the compensating eye movements are also different. The rotational VOR stabilizes gaze during rotations, by producing eye movement that are opposite to head movements. Thus, the rotational VOR can stabilize the whole visual field on the retina. The translational VOR detects linear accelerations and its function is to decrease retinal slip and minimize binocular disparity during self or passive motion. In contrast to the rotational VOR, compensatory eye movements during the translational VOR are dependent on direction of gaze to keep images stable on the two foveae [14-16]. Only images in one particular spatial location in the visual field can remain stable. Thus, the translational VOR is

also dependent on viewing distance, which is in its turn proportional to vergence angle. This is necessary to compensate for motion parallax [17].

SPATIAL MEMORY

Visually versus memory-guided eye movements

When we orient ourselves, we direct our eye movements to targets that are present in our visual field, but also to remembered targets that are no longer in view. Memory-guided saccades are saccades generated to a location in which a target was previously presented. The dorsolateral prefrontal cortex plays an important role in programming saccades to remembered locations of targets [18, 19]. Memory-guided saccades are less accurate and have lower peak-velocity and longer duration than visually-guided saccades [20, 21]. There is, however, very little knowledge on combined saccade-vergence movements from memory. When vergence movements are made from memory, visual feedback and herewith visual disparity is lacking. Since visual disparity is one of the most effective stimuli for vergence movements, saccade-vergence interactions may be different when binocular gaze shifts towards remembered visual targets are made.

Visuospatial memory

Our brain is capable of storing a three dimensional representation of space. This is called spatial memory. Even as we move, we have no difficulty in keeping track of an object, even when that object is temporarily out of sight. To maintain accurate orientation, we constantly have to update our spatial memory. Sensory and motor information is used to form and update a spatial representation. Retinal errors and disparity provide important information on target locations. Other cues such as accommodation, vergence angle and efference copy signals of motor commands are also used. How the information is stored, more precisely, what frames of reference are used, is still under debate. Different egocentric (self-centered) or allocentric (world-centered) frames to store spatial representations might be used [22, 23].

Spatial updating after passive displacement

During memory-guided gaze shifts, not only information stored from visual memory is used, but also extra-retinal signals are important. Memory-guided saccades can be made after intervening active (i.e. self-induced locomotion) or passive (e.g. whole body displacements) movements of the head or body. For such movements the vestibular system is likely to be involved. In natural movements in life (e.g. walking) we do not only undergo rotations, but

also translations through space. Spatial updating after translational movements is more complicated than after rotational movement. For rotations, amplitude and direction of the intervening movement is required for updating. However, during translations, images of objects closer to the eyes move faster across our retinas than the images of far objects (motion parallax, perception of depth). This information has to be taken into account for accurate spatial updating after translation. Furthermore, as we translate through space, the distance of an object from the observer changes, so vergence angles have to be adjusted. This is a difficult process and computation of binocular updating is still only partially understood [22, 24].

MAIN OBJECTIVE

In this thesis the interaction between the gaze direction of both eyes (version) and the angle between both eyes (vergence) is studied. The main question addressed is: How do binocular eye movements interact with visual spatial memory, (intervening) whole body movements and the vestibular system? In this thesis, the focus is on binocular eye movements in healthy human volunteers, to targets that are close to our eyes in 3-dimensional space.

The following research questions are addressed in the next chapters:

Chapter 2; Can humans make independent slow phase eye movements using a two-dimensional visual stimulation paradigm?

Chapter 3; What is the accuracy and the contribution of the abducting and adducting eye during memory-guided combined saccadic-vergence movements?

Chapter 4; How is the three-dimensional vestibulo-ocular reflex measured in humans, using a six degree of freedom motion platform?

Chapter 5; What is the influence of vergence angle and target distance on gaze stabilization during translations in humans?

Chapter 6; What are the differences between spatial memory updating after rotational and translational passive whole body movements?

REFERENCES

1. Hannula, D.E., D.J. Simons, and N.J. Cohen, Imaging implicit perception: promise and pitfalls. *Nat Rev Neurosci*, 2005. 6(3): p. 247-55.
2. Kandel, E.R., J.H. Schwartz, and T.M. Jessell, Principles of neural science. 4th ed2000, New York: McGraw-Hill, Health Professions Division. xli, 1,414 p.
3. Purves, D., Neuroscience. 4th ed2008, Sunderland, Mass.: Sinauer. xvii, 857 p. 52 p.
4. Howard, I.P., B.J. Rogers, and Oxford University Press., Seeing in depth2008, New York: Oxford University Press. 1275.
5. Leigh, R.J. and D.S. Zee. The neurology of eye movements. 2006; 4th:[x, 763].
6. Hering, E., Die Lehre vom binokularen Sehen1868: Leipzig: Engleman.
7. Hering, E., The theory of binocular vision1977: New York: Plenum.
8. Goebel, H.H., et al., Lesions of the pontine tegmentum and conjugate gaze paralysis. *Arch Neurol*, 1971. 24(5): p. 431-40.
9. Hepp, K. and V. Henn, Spatio-temporal recoding of rapid eye movement signals in the monkey paramedian pontine reticular formation (PPRF). *Exp Brain Res*, 1983. 52(1): p. 105-20.
10. Mays, L.E., Neural control of vergence eye movements: convergence and divergence neurons in midbrain. *J Neurophysiol*, 1984. 51(5): p. 1091-1108.
11. Mays, L.E., et al., Neural control of vergence eye movements: neurons encoding vergence velocity. *J Neurophysiol*, 1986. 56(4): p. 1007-21.
12. Helmholtz, H., Helmholtz's treatise on physiological optics (English translation of "Handbuch der physiologischen Optik", 1910),1910/1962, New York: Dover.
13. King, W.M., Binocular coordination of eye movements – Hering's Law of equal innervation or unio-ocular control? *Eur J Neurosci*, 2011. 33(11): p. 2139-46.
14. Angelaki, D.E., H.H. Zhou, and M. Wei, Foveal versus full-field visual stabilization strategies for translational and rotational head movements. *J Neurosci*, 2003. 23(4): p. 1104-8.
15. Seidman, S.H., G.D. Paige, and D.L. Tomko, Adaptive plasticity in the naso-occipital linear vestibulo-ocular reflex. *Exp Brain Res*, 1999. 125(4): p. 485-94.
16. Tomko, D.L. and G.D. Paige, Linear vestibuloocular reflex during motion along axes between naso-occipital and interaural. *Ann NY Acad Sci*, 1992. 656: p. 233-41.
17. Angelaki, D.E., Eyes on target: what neurons must do for the vestibuloocular reflex during linear motion. *J Neurophysiol*, 2004. 92(1): p. 20-35.
18. Pierrot-Deseilligny, C., D. Milea, and R.M. Muri, Eye movement control by the cerebral cortex. *Curr Opin Neurol*, 2004. 17(1): p. 17-25.
19. Pierrot-Deseilligny, C., et al., Decisional role of the dorsolateral prefrontal cortex in ocular motor behaviour. *Brain*, 2003. 126(Pt 6): p. 1460-73.
20. Baker, J.T., T.M. Harper, and L.H. Snyder, Spatial memory following shifts of gaze. I. Saccades to memorized world-fixed and gaze-fixed targets. *J Neurophysiol*, 2003. 89(5): p. 2564-76.
21. White, J.M., D.L. Sparks, and T.R. Stanford, Saccades to remembered target locations: an analysis of systematic and variable errors. *Vision Res*, 1994. 34(1): p. 79-92.
22. Klier, E.M. and D.E. Angelaki, Spatial updating and the maintenance of visual constancy. *Neuroscience*, 2008. 156(4): p. 801-18.
23. Medendorp, W.P., Spatial constancy mechanisms in motor control. *Philos Trans R Soc Lond B Biol Sci*, 2011. 366(1564): p. 476-91.
24. Klier, E.M., B.J. Hess, and D.E. Angelaki, Human visuospatial updating after passive translations in three-dimensional space. *J Neurophysiol*, 2008. 99(4): p. 1799-809.



2

Binocular eye movement control and motion perception: What is being tracked?

Johannes van der Steen and Joyce Dits

Department of Neuroscience, Erasmus MC, Rotterdam, The Netherlands.

Adapted from:

Investigative Ophthalmology and Visual Science (IOVS). 2012 Oct; 53(11): 7268-75.

ABSTRACT

Purpose: To investigate under what conditions humans can make independent slow phase eye movements. The ability to make independent movements of the two eyes is generally attributed to few specialized lateral eyed animal species, e.g. chameleons. In this study we show that also humans can move the eyes in different directions. To maintain binocular retinal correspondence independent slow phase movements of each are produced.

Method: We used the scleral search coil method to measure binocular eye movements in response to dichoptically viewed visual stimuli oscillating in orthogonal direction.

Results: Correlated stimuli led to orthogonal slow eye movements, while the binocularly perceived motion was the vector sum of the motion presented to each eye. The importance of binocular fusion on independency of the movements of the two eyes was investigated with anti-correlated stimuli. The perceived global motion pattern of anti-correlated dichoptic stimuli was both perceived as an oblique oscillatory motion, as well resulted in a conjugate oblique motion of the eyes.

Conclusions: We propose that the ability to make independent slow phase eye movements in humans is used to maintain binocular retinal correspondence. Both eye-of-origin and binocular information are used during the processing of binocular visual information and it is decided at an early stage whether binocular or monocular motion information and independent slow phase eye movements of each eye are produced during binocular tracking.

INTRODUCTION

The ability to move the eyes independently from one another in different directions is generally restricted to specialized lateral eyed animal species, e.g. chameleons. In contrast, humans with frontally placed eyes are considered to have a tight coupling between the two eyes, although there are exceptions [1]. Normally humans coordinate their eye movements in such a way that each eye is aimed at the same point at a given distance in visual space [2]. Association of visual inputs derived from corresponding retinal locations provides the brain with a binocular unified image of the visual world [3]. From the retinal images of the two eyes a binocular single representation of the visual world is constructed based on binocular retinal correspondence [4]. To achieve this the brain has to use the visual information from each eye to stabilize the two retinal images relative to each other. Imagine that one holding two laser pointers, one in each hand, and one has to project the two beams precisely on top of each other on a wall.

Eye movements contribute to binocular vision using visual feedback from image motion of each eye and from binocular correspondence. It is generally believed that the problem of binocular correspondence is solved in V1 [5, 6]. Neurons in V1 process both monocular and binocular visual information [7]. At subsequent levels of processing eye-of-origin information is lost and the perception of the binocular world is invariant for eye movements and self-motion [8-11].

An important question is to what extent binocular and/or monocular visual information is used. Binocular vision relies heavily on disparity, which only works within limits of fusion [12, 13]. Neurons used for binocular disparity were first described in primary visual cortex in the cat [14, 15] and were later found in many other visual cortical areas: V1 to V5 (= MT) and in area MST [6, 10, 11, 16-19]. Although most is known about the neural substrate of horizontal disparities there is also evidence for vertical disparity sensitive neurons in visual cortex [7, 20].

The variation in sensitivity of cortical areas to specific stimulus attributes also suggests a hierarchical structure for motion processing. First-order motion energy detectors in striate areas are at the basis for initial ocular following responses [21]. In area MT cortical neurons are not only tuned to binocular disparity but also to orientation, motion direction and speed [16, 22]. Perception of depth and motion in depth occurs outside area V1 [5, 9, 10, 23, 24].

Although it has been suggested that V1 is responsible for generating input signals for the control of vergence during binocular vision [6, 25], and there is evidence for disparity energy sensing [26], it is unknown how visual disparity signals from V1 are connected to oculomotor command centers in the brainstem.

Also at the brainstem level the monocular or binocular organization of oculomotor signals is still controversial (for a review see [27]). On one hand there is strong support for conjugate control using separate version and vergence centers, such as the mesencephalic reticular

formation [28]. On the other hand there are also examples of a more independent control [1]. Several lines of evidence suggest that at the premotor level abducens burst neurons can be divided in left and right eye bursters, and thus have a monocular component [29-32].

In humans there is behavioral evidence for asymmetrical vergence [8, 33]. Recently a dual visual-local feedback model of the vergence movement system was proposed that can account for both binocular as well as monocular driven vergence responses [34].

To investigate to what extent humans have independent binocular control and what are the required conditions for this behavior, we used a two-dimensional dichoptic visual stimulation paradigm. With this paradigm we demonstrate in humans that 1) To sustain binocular vision, they can generate slow phase eye movements with independent motion directions and 2) The perceived direction of binocular motion can be dissociated from control of eye movement.

METHODS

Subjects

Six subjects participated in the experiments (age 20 to 52 years). None of them had a history of ocular or oculomotor pathology. Visual acuities varied between 0.8 and 1.0 (Snellen acuity chart). Stereopsis was better than 60 sec of arc (measured with the TNO test for stereoscopic vision). None of the subjects had ocular dominance (tested at viewing distance of 2 m with polaroid test). Subjects were naïve to the goal of the experiment with exception of one of the authors. All experiments were carried out according to the Declaration of Helsinki.

Stimulus presentation

Subjects faced a tangent screen (dimensions 2.5 x 1.8 m) at a distance of 2 m.

Visual stimuli were generated by a visual workstation (Silicon Graphics) and back-projected on the tangent screen by a high-resolution projector provided with a wide-angle lens (JVC D-ILA projector, contrast ratio 600:1).

The viewing angle of the whole stimulus was 60°, whereas each dot subtended 1.2° visual angle.

The visual stimulus consisted of two overlaid random dot patterns (figure 1, left panels).

One pattern oscillated horizontally, the other oscillated vertically. We stimulated with three different frequencies ($f=0.16, 0.32$ and 0.64 Hz, with amplitudes of respectively $1.72^\circ, 0.86^\circ$ and 0.43°).

Stimuli were either correlated or anti-correlated random dot patterns. Left and right eye image separation by the filters was better than 99%. In the experiments described in this

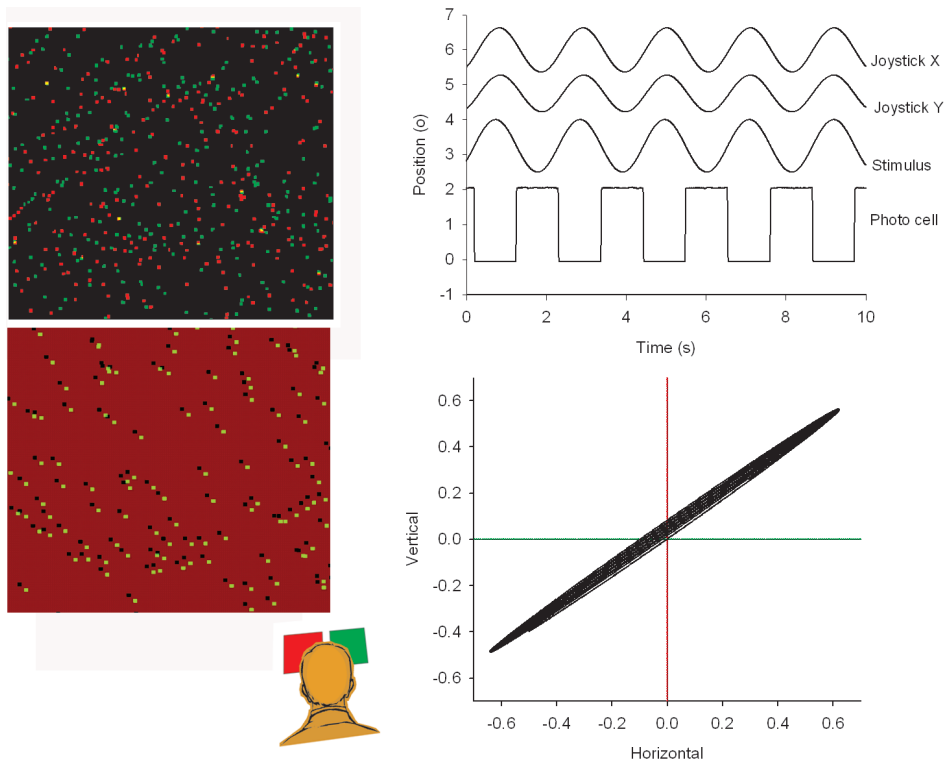


Figure 1: Left panel: Cartoon of the correlated (upper panel) and anti-correlated (lower panel) stimulus displays from a subject's point of view. From behind the red and green filters the left and right eye saw the stimulus oscillating between up and down and between left and right, respectively. Subjects tracked the perceived stimulus motion with a joystick. Amplitudes of the joystick signal were scaled to the actual stimulus amplitude. The upper right panel shows the perceived direction of motion of the pattern in relation to the stimulus motion. The signal labeled "stimulus" was reconstructed from the square wave photocell signal, in which each flank corresponds to a zero crossing of the sinusoidal motion. The lower right panel shows the perceived vectorial motion direction of the stimulus and the actual motion components.

study subjects viewed the stimuli under dichoptic (separated by red and green filters) conditions. They were instructed to stare at the presented visual stimuli while trying to maintain binocular fusion. Correlated dot patterns consisted of randomly distributed red and green dots against a black background (figure 1, left upper panel). Correlated patterns with 1000 elements in each pattern were used with both identical as two different frequencies. Standard procedure was to present the horizontal stimulus to the right eye and the vertical stimulus to the left eye. Reversing this order had no effect on the general outcome of the data.

Anti-correlated stimuli consisted of random dot patterns against a red and green background with opposite contrast of the dots (figure 1, left lower panel). When viewed through red-green anaglyphic glasses dots appeared as light and dark dots against a grey background.

Anti-correlated stereograms have the property that they cannot be fused and do not lead to depth perception[35], although they can evoke vergence eye movements with opposite sign [7, 25]. Performance between correlated and anti-correlated stimuli was compared using 200 element stimuli.

To synchronize stimulus presentation with the eye movement recordings we projected a small alternating black and white square in the lower right corner of the screen. The square was covered with a black cardboard at the front side of the screen to make it invisible to the subject. The black to white transitions corresponded to the zero crossings of the oscillating patterns. A photo detector, placed directly in front of the black and white square, produced an analog voltage proportional to the luminance of the square. This voltage was sampled together with the eye movement signals (see figure 1, upper right panel). In this way we were able to synchronize our sampled eye movements with the presentation onset of the stimulus on the screen within 1 ms precision.

Eye movement and perceived movement registration

Binocular eye movements of human subjects were measured using the two-dimensional magnetic search coil method [36], which has a resolution of 20 seconds of arc. Subjects indicated the perceived motion with a joystick (figure 1, bottom right panel). Analog signals were sampled at 1000 Hz with 16-bit precision by a PC based data acquisition system (CED1401, Cambridge, UK). Prior to digitization, signals were fed through a low-pass filter with a cut-off frequency of 250 Hz. The overall noise level was less than 1.5 min of arc.

Zero crossings in the sampled photocell signal were determined by the computer, and used to reconstruct the stimulus. The signal was also used to verify that no frames had been skipped. The next step of the analysis consisted of a saccade removal of the eye coil signals. Saccades were identified with the following criteria: velocity threshold $12^\circ/s$, minimum amplitude 0.2° , acceleration threshold $1000^\circ/s^2$ and subsequently removed from the raw eye movement signal (for a detailed description see [37]). In- and output relations between stimulus and smooth eye movement signals, i.e. gain and phase, were computed from the cross- and auto-spectral densities of the FFT transformed signals [38].

RESULTS

Orthogonal stimulation with correlated random-dot images

All subjects fused the two correlated stimulus patterns without binocular rivalry. The combination of the horizontal pattern motion presented to one eye and vertical pattern motion to

the other eye was seen as an oblique sinusoidal movement, corresponding to the vector sum of the motions presented to each eye.

The two orthogonally oscillating visual stimuli elicited smooth tracking eye movements interrupted by small saccades. Figure 2 (left panels) shows an example of the differences in amplitudes of the horizontal and vertical component of each eye. The right eye was tracking the horizontal motion and the left eye the vertical motion. The disconjugacy between left and right eye was restricted to the smooth components. Saccades were conjugate (differences in saccade amplitude were less than 0.1 degrees) and corrected for drift in the smooth signals (see the traces of left and right eye before and after saccade removal in figure 2 left panel, traces labeled "raw" and "smooth"). In all subjects there was an upward drift in one eye

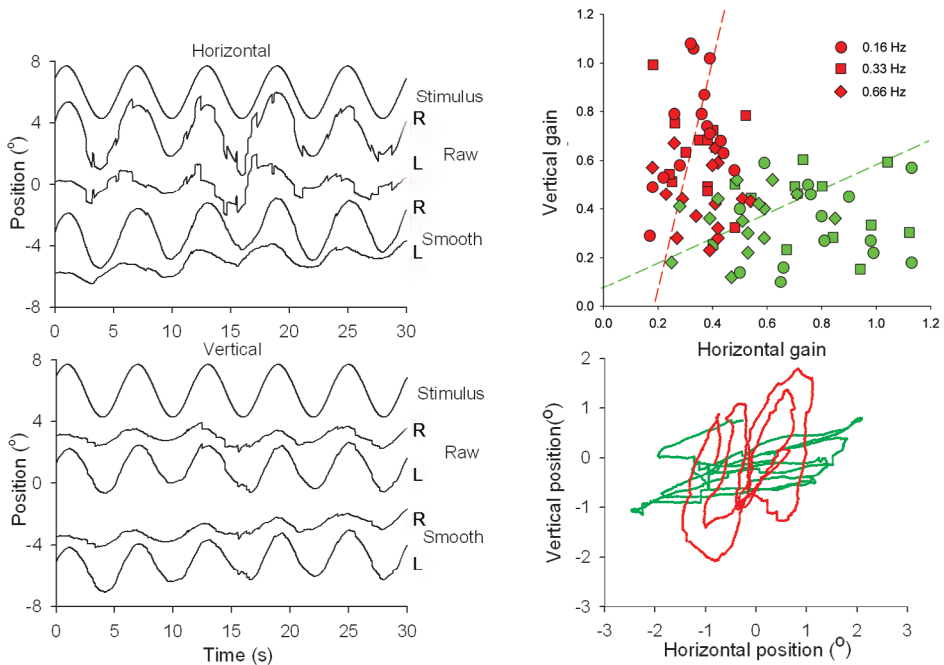


Figure 2: Eye movements in response to orthogonally oscillating patterns ($f=0.16$ Hz, $A=1.72^\circ$). Left panels show from top to bottom: stimulus motion, horizontal and vertical movements of right (R) and left (L) eye. Positive values of horizontal and vertical eye movement traces correspond to rightward and upward positions, respectively. Traces labeled "Raw" show eye movements with saccades, whereas in the traces labeled "Smooth", saccades have been digitally removed. The XY-plot at the lower right panel shows an example of the horizontal and vertical excursions of the two eyes. The top right panel shows a scatter plot of the horizontal versus vertical gain of left eye (red symbols) and right eye (green symbols) of all six subjects for three different frequencies (circles 0.16 Hz; squares 0.33 Hz and diamonds 0.66 Hz). Pooled data points for all three frequencies were fitted with an orthogonal fit procedure, minimizing errors in both x and y direction.

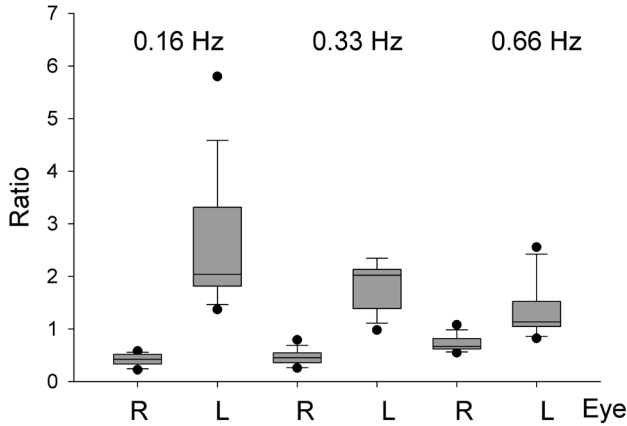


Figure 3: Box plots based on the ratios of horizontal versus vertical amplitudes of left and right eye. The plot shows three pairs of box plots for three stimulus frequencies alternatingly for left and right eye. Note that differences between left and right eye ratios decrease as a function of stimulus frequency.

and a nasally directed drift in the other eye (see smooth traces in figure 2), which did not change when we reversed the movement presented to each eye.

The lower right panel of figure 2 shows examples of motion trajectories of the left and right eye in one subject. The upper right panel of figure 2 summarizes the differences in motion direction of left and right eye for all six subjects. Here we plotted the gain of the horizontal against vertical smooth eye movements of the left and right eye for three different frequencies and amplitudes. The movement directions of the left and right eye were not exactly orthogonal to each other. The orthogonal regression lines fitted through all data points are described by the following functions: $V_R = 0.51 * H_R + 0.05$ and $V_L = 4.72 * H_L - 0.93$, where V_R , V_L , H_R and H_L are the right and left eye vertical and horizontal gain, respectively. To test if the motion directions of left and right eye were significantly different, we calculated the horizontal versus vertical amplitude ratio (xy-ratio) of the left and right eye. We then compared the left and right eye ratios different for the three stimulus frequencies. For all three frequencies the left and right eye ratios were significantly different ($P < 0.001$, Rank Sum test) (see box plots in figure 3).

Orthogonal stimulation with anti-correlated random-dot images

None of the subjects ($N=6$) reported to suppress one of the images or have binocular rivalry when viewing the anti-correlated stereograms. When they looked at the global pattern, they perceived an oblique motion, whereas when they shifted their attention to a single dot, only its local horizontal or vertical motion was seen.

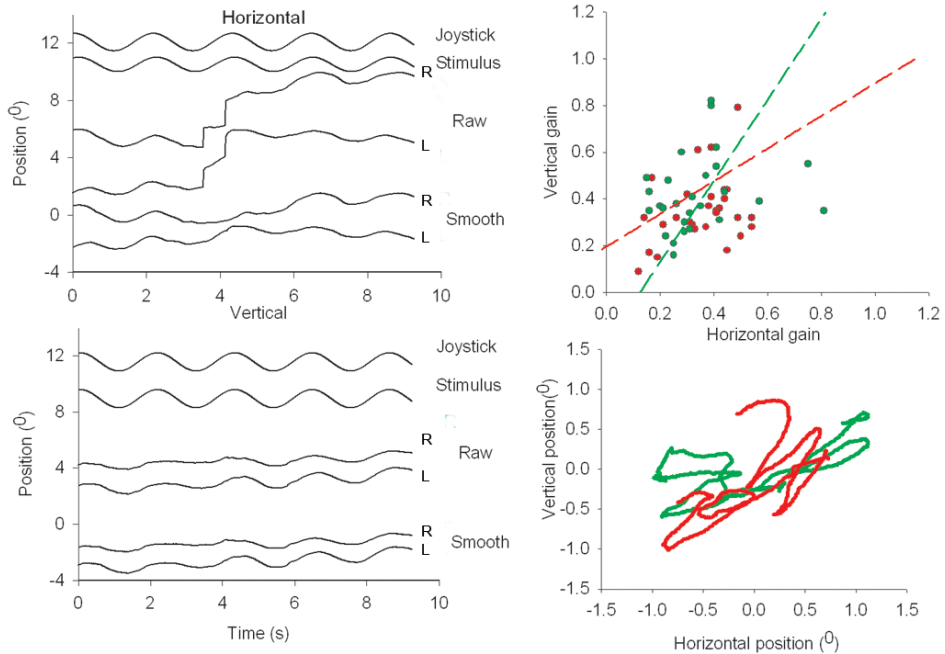


Figure 4: Eye movements in response to the orthogonally oscillating 200 dot anti-correlated stereogram. Left panels show horizontal (middle panel) and vertical (lower traces) raw and smooth eye movements. Top two traces at each of the two left panels show stimulus motion and perceived movement indicated with a joystick. The XY-plot at the lower right panel shows an example of the horizontal and vertical excursions of the smooth components of the two eyes. Top right panel shows a scatter plot of the horizontal versus vertical gain of left (closed circles) and right (open circles) eye of all six subjects. Data points are fitted with an orthogonal fit procedure, minimizing errors in both x and y direction.

An example of eye movements evoked in response to the anti-correlated pattern is shown in figure 4 (left panels). The lower right panel shows a xy-plot of the right and left eye horizontal and vertical movements. Both eyes oscillate with a diagonal trajectory and were largely conjugate. The amplitude of the response was about 50 % compared to the correlated stereograms. The upper right panel of figure 4 shows the orthogonal regression lines fitted through the gain values of the horizontal against vertical smooth eye movements of the left and right eye for all frequencies and amplitudes.

The orthogonal regression lines are described by the following functions: $V_R = 0.82 * H_R - 0.04$, Left eye: $V_L = 0.55 * H_L + 0.17$. We also calculated the xy-ratio of the left and right eye. Motion directions for left and right eye data were not significantly different ($P = 0.087$, Rank sum test).

We compared the tracking performance of the perceived motion for correlated and anti-correlated 200 dot stimuli at different frequencies by having our subjects track the direction of perceived motion with a joystick. We concentrated on the timing of the tracking response and not on response amplitude because we expected a considerable individual variability

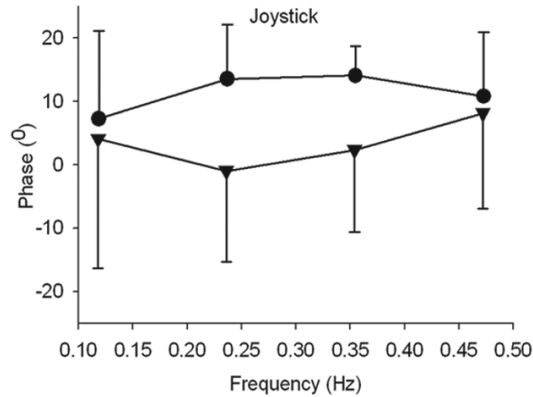


Figure 5: Mean phase and standard deviation of perceived movement as a function of stimulus frequency. Subjects (N=6) tracked the direction of perceived motion with a joystick. Positive values indicate a phase lead, negative values a phase lag. Closed triangles: Correlated stimulus patterns, closed circles: anti-correlated stimulus patterns

in response amplitude due to the subjective scaling. Under both conditions the tracking was in the same direction as the perceived motion. The phase of the tracking responses across frequencies is shown at the right panel of figure 5 and was different for the two types of stimuli. Correlated stimuli were tracked with a mean phase lead of $3.4^\circ \pm 3.8^\circ$, whereas anti-correlated stimuli were tracked across frequencies with a mean phase lead of $11.6^\circ \pm 3.13^\circ$. Differences between correlated and uncorrelated stimuli values were not significantly different (paired t-test, $p > 0.05$).

Frequency response of left and right eye during orthogonal movements

To estimate the contribution of monocular and binocular slow phase eye movement components to the response, we also determined the frequency response of the left and right eye in two dimensions.

Firstly, we determined the gain and phase characteristics of the monocular (left and right eye) and binocular (version and vergence) eye movement components. For all six subjects we analyzed the responses to orthogonal stimulation for the three different frequencies (0.16, 0.32 and 0.66 Hz) and amplitudes (1.72° , 0.86° and 0.63°). Gain and phase were calculated from the Fast Fourier Transformed stimulus signal and the smooth eye movement components. Average values (N=6) are shown in figure 6. Each data point is based on 18 measurements.

Figure 6 shows that each monocular presented stimulus evoked not only a movement confined to the direction of the stimulated eye, but in addition a smaller gain component in the other eye (see also figure 2). Across all subjects the gain of the movement of the viewing eye in the plane of stimulus motion was significantly larger than in the other eye. With increase

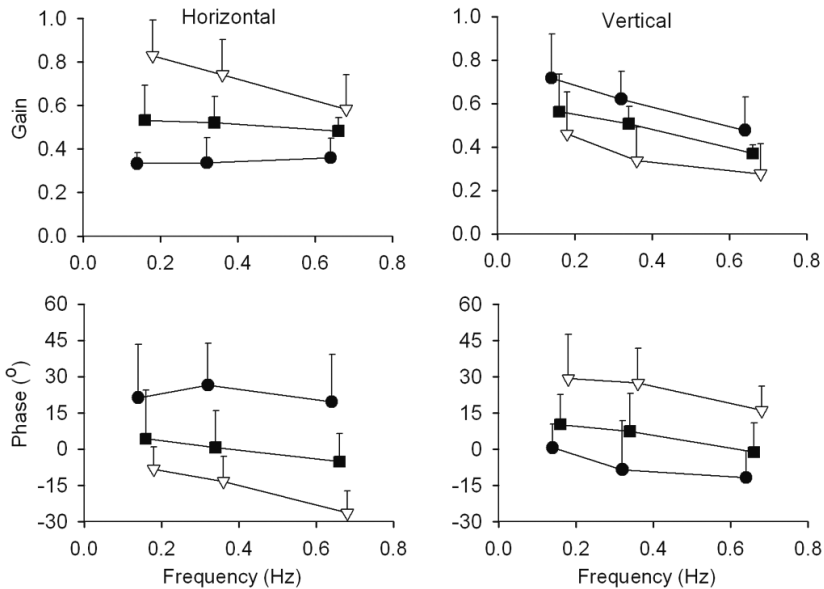


Figure 6: Gain and phase plots of the smooth left and right eye movements in response to sinusoidal stimulation with three different frequencies. Top panels show the mean ($N=6$) gain \pm 1 S.D. of left eye (closed circles), right eye (open triangles) and version signals (closed squares) in horizontal and vertical direction. Lower panels present the phase of the left eye, right eye and version smooth eye movements. Note the phase lag and phase lead in the lower left panel of the horizontal left and right eye, respectively. The reverse applies to the vertical eye movements (lower right panel). The individual curves have shifted along the x-axis with respect to each other to visualize the error bars.

in stimulus frequency, gain decreased from 0.83 to 0.58 in horizontal direction. The gain of the vertical component ranged between 0.72 and 0.48. The gain of the non-stimulated eye movement averaged over subjects and amplitudes varied from 0.33 and 0.36 for horizontal (figure 6, top left panel, closed circles) and from 0.46 to 0.28 for vertical stimulation (figure 6, top right panel, open triangles).

The movement components of the left and right eye in the direction of stimulus motion lagged the stimulus motion (figure 6, lower left panel, open triangles and lower right panel, closed circles). Phase lag increased with frequency from -8.3 to -26° for horizontal and from $+0.6$ to -12° for vertical motion. In contrast, the “cross-talk” horizontal or vertical movement of the other eye had a phase lead which varied between $+16$ and $+29^\circ$. Version gain (figure 6, closed squares) ranged between 0.53 and 0.48 for horizontal and between 0.58 and 0.37 for vertical stimulus motion. Phase was close to zero (mean $0.1^\circ \pm 4.8^\circ$ for horizontal, and $5.5^\circ \pm 6.0^\circ$ for vertical).

In summary, this gain and phase analysis shows that each eye produced a movement with a high gain and a frequency dependent phase lag in the direction of its own stimulus motion. This is in line with the xy-ratio analysis (see figure 3). The gain-phase analysis shows in addition that there is a low gain response and a phase lead of the “cross-talk” movement in

the other eye. For version, gain equals to the mean of left and right eye. Phase errors of the version signal were close to zero.

DISCUSSION

In this study we show that, with orthogonally oscillating dichoptic stimuli correlated images within limits of fusion are tracked with slow phase eye movements in the direction and at the frequency of the stimulus presented to that eye. The perceived direction of motion was the vector sum of the motion of the two images presented to each eye. We conclude that these disjunctive eye movements help to maximize binocular correspondence and to minimize binocular correspondence errors. In our study anti-correlated stimuli evoked a similar motion percept as the correlated stimuli, but the elicited eye movements were conjugate and moved obliquely in correspondence with the perceived direction of motion.

Binocular eye movement control

The neural control of binocular eye movements is a controversial issue in oculomotor physiology. Behavioral and electrophysiological evidence shows that separate version and vergence neuronal control systems exist with different dynamics [39-41] [28] [42]. Horizontal version signals are mediated by the paramedian pontine reticular formation (PPRF), whereas vergence command centers are located in the mesencephalic region. The main body of the discussion has been so far on whether burst neurons in the paramedian pontine reticular formation (PPRF) carry conjugate or monocular command signals [27].

The oculomotor behavior described in our study implies that the vergence center must be able to send an adjustable distribution of signals to left and right oculomotor neurons. The idea of adjustable distribution was suggested earlier for horizontal binocular eye movements by Erkelens [33]. From our data it follows that this property not only applies to horizontal but also to vertical binocular eye movements. The gain and phase plots we constructed from our data are consistent with simulated data from a recent model on the vergence eye movement system [34].

Several studies have suggested that disparity-sensitive cells operate in the binocular servo control of disjunctive eye movements [5, 8, 43]. Disparity sensitive cells in V1 are not only sensitive to horizontal but also to vertical disparities [14]. We propose that depending on whether the two retinal images are fusible or not, disparity sensitive cells or monocular sensitive cells are in the feedback loop to the mesencephalic region. This way V1 not only acts as a gatekeeper for the perception of motion [44], but also controls left and right eye movement related activity to maintain binocular correspondence. This results in paradoxically independent left and right eye movements to minimize the retinal errors between the

two patterns. Such a scheme explains why in the absence of fusion only conjugate motor command signals are generated for both eyes.

Binocular motion perception

Maintaining fusion of binocularly perceived images involves sensory fusion mechanisms based on retinal correspondence, as well as oculomotor control mechanisms to keep the retinas of the two eyes within fusional limits.

Erkelens and Collewijn [45] were the first to show that large dichoptically presented random-dot stereograms with equal but opposite horizontal motion were perceived as stationary while these patterns elicited ocular vergence movements. Their conclusion was that the visual system strived for a situation in which both binocular disparity as well as retinal slip were reduced to a minimum [8]. Our data are in line with their findings and show that this is not restricted to horizontal eye movements, but also applies to combined horizontal and vertical slow phase version and vergence.

The perceived motion directions of our correlated stimuli are in line with evidence that under dichoptic viewing conditions the motion components presented separately to the two eyes are integrated by the visual system into a single perceived motion [46, 47].

An important question is how the control mechanisms of binocular eye movements and motion perception interact. During the processing of binocular visual information, binocular retinal correspondence is already achieved in V1 by an early stage correlation of the two retinal images. It has also been suggested that binocular visual signals in V1 may be used for vergence control [6]. However, several investigators claimed that the control mechanisms for binocular eye movements also have access to eye-of-origin information [33, 48]. We argue that the decision on the use of eye-of-origin information for eye movement depends on the fusibility of the two images. Although it is unlikely that V1 is actually the place where perception occurs [19], part of the decision process could take place at this level. In V1 disparity detectors exist which are sensitive to absolute local disparities [9]. Recent evidence suggests that decisions leading to visual awareness of motion are taken in V1 [44]. Thus, the function of V1 could not only be to gate visual perception to higher areas, but also to gate signals to the oculomotor system.

How do anti-correlated stimuli fit in with this scheme? Normally, if the visual inputs of the two eyes do not match, a situation of binocular rivalry results. In such conditions cellular activity in extrastriate areas is related to the perceptually dominating pattern [49, 50]. Anti-correlated patterns are a special case. Anti-correlated patterns can cause a perception of motion or depth in the reverse direction [51]. It has been argued that perceived motion direction depends on spatial frequency [52].

In our experiments both the correlated and anti-correlated random-dot patterns we used in our experiment yielded a global motion percept consistent with the vector sum of the

inputs to the two eyes. This suggests a high order grouping of local motion vectors independent from disparity. This global motion integration may occur in extrastriate areas, e.g. area MT, which is known to have disparity selection and motion selectivity [10, 16, 22].

REFERENCES

1. MacAskill, M.R., K. Koga, and T.J. Anderson, Japanese street performer mimes violation of Hering's Law. *Neurology*, 2011. 76(13): p. 1186-7.
2. Erkelens, C.J., et al., Ocular vergence under natural conditions. I. Continuous changes of target distance along the median plane. *Proc R Soc Lond B Biol Sci*, 1989. 236(1285): p. 417-40.
3. Howard, I.P. and B.J. Rogers, *Seeing in Depth* 2002, Toronto: Porteous I.
4. Westheimer, G., Three-dimensional displays and stereo vision. *Proceedings. Biological sciences / The Royal Society*, 2011. 278(1716): p. 2241-8.
5. Cumming, B.G. and A.J. Parker, Responses of primary visual cortical neurons to binocular disparity without depth perception. *Nature*, 1997. 389(6648): p. 280-3.
6. Cumming, B.G. and A.J. Parker, Local disparity not perceived depth is signaled by binocular neurons in cortical area V1 of the Macaque. *J Neurosci*, 2000. 20(12): p. 4758-67.
7. Poggio, G.F., Mechanisms of stereopsis in monkey visual cortex. *Cerebral Cortex*, 1995. 5: p. 193-204.
8. Erkelens, C.J. and H. Collewijn, Eye movements and stereopsis during dichoptic viewing of moving random-dot stereograms. *Vision Res*, 1985. 25(11): p. 1689-700.
9. Cumming, B.G. and A.J. Parker, Binocular neurons in V1 of awake monkeys are selective for absolute, not relative, disparity. *J Neurosci*, 1999. 19(13): p. 5602-18.
10. DeAngelis, G.C., B.G. Cumming, and W.T. Newsome, Cortical area MT and the perception of stereoscopic depth. *Nature*, 1998. 394(6694): p. 677-80.
11. Parker, A.J. and B.G. Cumming, Cortical mechanisms of binocular stereoscopic vision. *Prog Brain Res*, 2001. 134: p. 205-16.
12. Schor, C., T. Heckmann, and C.W. Tyler, Binocular fusion limits are independent of contrast, luminance gradient and component phases. *Vision Res*, 1989. 29(7): p. 821-35.
13. Erkelens, C.J., Fusional limits for a large random-dot stereogram. *Vision Res*, 1988. 28(2): p. 345-53.
14. Barlow, H.B., C. Blakemore, and J.D. Pettigrew, The neural mechanism of binocular depth discrimination. *J Physiol*, 1967. 193(2): p. 327-42.
15. Pettigrew, J.D., T. Nikara, and P.O. Bishop, Binocular interaction on single units in cat striate cortex: simultaneous stimulation by single moving slit with receptive fields in correspondence. *Exp Brain Res*, 1968. 6(4): p. 391-410.
16. DeAngelis, G.C. and W.T. Newsome, Organization of disparity-selective neurons in macaque area MT. *J Neurosci*, 1999. 19(4): p. 1398-415.
17. Maunsell, J.H. and D.C. Van Essen, Functional properties of neurons in middle temporal visual area of the macaque monkey. II. Binocular interactions and sensitivity to binocular disparity. *J Neurophysiol*, 1983. 49(5): p. 1148-67.
18. Poggio, G.F., F. Gonzalez, and F. Krause, Stereoscopic mechanisms in monkey visual cortex: binocular correlation and disparity selectivity. *J Neurosci*, 1988. 8(12): p. 4531-50.
19. Backus, B.T., et al., Human cortical activity correlates with stereoscopic depth perception. *J Neurophysiol*, 2001. 86(4): p. 2054-68.
20. Durand, J.B., et al., Neurons in parafoveal areas V1 and V2 encode vertical and horizontal disparities. *J Neurophysiol*, 2002. 88(5): p. 2874-9.
21. Masson, G.S., D.S. Yang, and F.A. Miles, Reversed short-latency ocular following. *Vision Research*, 2002. 42(17): p. 2081-7.
22. DeAngelis, G.C. and W.T. Newsome, Perceptual "Read-Out" of Conjoined Direction and Disparity Maps in Extrastriate Area MT. *PLoS Biol*, 2004. 2(3): p. E77.

23. Uka, T. and G.C. DeAngelis, Linking neural representation to function in stereoscopic depth perception: roles of the middle temporal area in coarse versus fine disparity discrimination. *The Journal of neuroscience: the official journal of the Society for Neuroscience*, 2006. 26(25): p. 6791-802.
24. Neri, P., H. Bridge, and D.J. Heeger, Stereoscopic processing of absolute and relative disparity in human visual cortex. *Journal of neurophysiology*, 2004. 92(3): p. 1880-91.
25. Masson, G.S., C. Busettini, and F.A. Miles, Vergence eye movements in response to binocular disparity without depth perception. *Nature*, 1997. 389(6648): p. 283-6.
26. Miura, K., et al., The initial disparity vergence elicited with single and dual grating stimuli in monkeys: evidence for disparity energy sensing and nonlinear interactions. *Journal of neurophysiology*, 2008. 100(5): p. 2907-18.
27. King, W.M. and W. Zhou, New ideas about binocular coordination of eye movements: is there a chameleon in the primate family tree? *Anat Rec*, 2000. 261(4): p. 153-61.
28. Mays, L.E. and P.D. Gamlin, Neuronal circuitry controlling the near response. *Curr Opin Neurobiol*, 1995. 5(6): p. 763-8.
29. Zhou, W. and W.M. King, Premotor commands encode monocular eye movements. *Nature*, 1998. 393(6686): p. 692-5.
30. King, W.M. and W. Zhou, Neural basis of disjunctive eye movements. *Annals of the New York Academy of Sciences*, 2002. 956: p. 273-83.
31. King, W.M. and W. Zhou, Initiation of disjunctive smooth pursuit in monkeys: evidence that Hering's law of equal innervation is not obeyed by the smooth pursuit system. *Vision Research*, 1995. 35(23-24): p. 3389-400.
32. Cullen, K.E. and M.R. Van Horn, The neural control of fast vs. slow vergence eye movements. *The European journal of neuroscience*, 2011. 33(11): p. 2147-54.
33. Erkelens, C.J., Pursuit-dependent distribution of vergence among the two eyes. *Current Oculomotor Research*, ed. W.D. Becker, T. Mergner, T. 1999, New York: Plenum Press. 145-152.
34. Erkelens, C.J., A dual visual-local feedback model of the vergence eye movement system. *Journal of vision*, 2011. 11(10).
35. Julesz, B., *Foundations of Cyclopean Perception* 1971, Chicago: The University of Chicago Press.
36. Collewijn, H., F. Van der Mark, and T. Jansen, C, Precise recording of human eye movements. *Vision Research*, 1975. 15: p. 447-450.
37. van der Steen, J. and P. Bruno, Unequal amplitude saccades produced by aniseikonic patterns: effects of viewing distance. *Vision Res*, 1995. 35(23-24): p. 3459-71.
38. Van der Steen, J. and H. Collewijn, Ocular stability in the horizontal, frontal and sagittal planes in the rabbit. *Exp Brain Res*, 1984. 56(2): p. 263-74.
39. Rashbass, C. and G. Westheimer, Independence of conjugate and disjunctive eye movements. *J Physiol*, 1961. 159: p. 361-4.
40. Rashbass, C. and G. Westheimer, Disjunctive eye movements. *J Physiol*, 1961. 159: p. 339-60.
41. Mays, L.E. and J.D. Porter, Neural control of vergence eye movements: activity of abducens and oculomotor neurons. *J Neurophysiol*, 1984. 52(4): p. 743-61.
42. Mays, L.E., et al., Neural control of vergence eye movements: neurons encoding vergence velocity. *J Neurophysiol*, 1986. 56(4): p. 1007-21.
43. Poggio, G.F. and B. Fischer, Binocular interaction and depth sensitivity in striate and prestriate cortex of behaving rhesus monkey. *J Neurophysiol*, 1977. 40(6): p. 1392-405.
44. Silvanto, J., et al., Striate cortex (V1) activity gates awareness of motion. *Nat Neurosci*, 2005. 8(2): p. 143-4.

45. Erkelens, C.J. and H. Collewijn, Motion perception during dichoptic viewing of moving random-dot stereograms. *Vision Res*, 1985. 25(4): p. 583-8.
46. Alais, D., et al., Monocular mechanisms determine plaid motion coherence. *Vis Neurosci*, 1996. 13(4): p. 615-26.
47. Andrews, T.J. and C. Blakemore, Form and motion have independent access to consciousness. *Nat Neurosci*, 1999. 2(5): p. 405-6.
48. Howard, I.P. and B.J. Rogers, *Binocular Vision and Stereopsis*. 1995, Oxford: Oxford University Press.
49. Logothetis, N.K. and J.D. Schall, Neuronal correlates of subjective visual perception. *Science*, 1989. 245(4919): p. 761-3.
50. Logothetis, N.K., D.A. Leopold, and D.L. Sheinberg, What is rivalling during binocular rivalry? *Nature*, 1996. 380(6575): p. 621-4.
51. Sato, T., Reversed apparent motion with random dot patterns. *Vision research*, 1989. 29(12): p. 1749-58.
52. Read, J.C. and R.A. Eagle, Reversed stereo depth and motion direction with anti-correlated stimuli. *Vision research*, 2000. 40(24): p. 3345-58.



3

Version-vergence interactions during memory-guided binocular gaze shifts

Joyce Dits, Johan J. Pel, Angelique Remmers and Johannes van der Steen.

Department of Neuroscience, Erasmus MC, Rotterdam, The Netherlands.

Adapted from:

Investigative Ophthalmology and Visual Science (IOVS). 2013 Mar; 54(3): 1656-64.

ABSTRACT

Purpose: Visual orientation towards remembered or visible visual targets requires binocular gaze shifts that are accurate in direction (version) and ocular distance (vergence). We determined the accuracy of combined version and vergence movements and the contribution of abducting and adducting eye during gaze shifts towards memorized and visual targets in three-dimensional space.

Methods: Subjects fixated either a “far” (94 cm) or “near” (31 cm) fixation LED placed in front of the left eye. Next, in the memory-guided experiment, a target LED was lit for 80 ms (13 cm to the left or right and at 45 cm viewing distance). Subjects were instructed to make a saccade to the (remembered) target LED location. In the visually guided experiment, the target LED remained illuminated during the task. In both conditions gaze shifts consisted of version and vergence movements.

Results: Visually guided gaze shifts had both a fast intra-saccadic and slow post-saccadic vergence component and were most accurate. During memory-guided gaze shifts, the abducting eye was more accurate than the adducting eye. Distance correction was achieved by slow post-saccadic vergence of the adducting eye. Memory-guided gaze shifts that required convergence lacked an intra-saccadic vergence component and were less accurate compared to memory-guided gaze shifts that required divergence.

Conclusions: Visually guided binocular gaze shifts are faster and more accurate than memory-guided binocular gaze shifts. During memory-guided gaze shifts the abducting eye has a leading role and an intra-saccadic vergence enhancement during convergence is reduced.

INTRODUCTION

In our daily environment, visual targets are located in different directions and at different viewing distances relative to our body. To binocularly view an object of interest, two different types of eye movements are used: saccades and vergence. Saccades are the rapid conjugate component of eye movements used to orient the eyes towards a new direction by rotating both eyes with similar angles. Vergence eye movements are used to bring the focal point of binocular gaze to a different viewing point in depth by disjunctively rotating the eyes.

Saccades and vergence eye movements have different dynamic properties and they are assumed to be controlled by independent subsystems [1, 2]. Lesion and physiological data have shown that different neuronal populations exist for conjugate gaze and vergence. Motor commands for conjugate gaze shifts are assembled in the paramedian pontine reticular formation (PPRF) [3-5], whereas vergence command signals are generated in the midbrain [6, 7]. Despite functional and anatomical differences between the two subsystems, there is also a close interaction. In natural gaze shifts, saccadic and vergence movements are seldom made in isolation, but combinations are made continuously, altering the dynamic properties of the eye movements. Saccades are slowed down when they are combined with vergence, while vergence movements during the intrasaccadic period become faster in combination with saccades [8, 9]. There are different explanations for saccade-vergence interactions. One mechanism is an interaction between conjugate saccade command centers and vergence burst neurons [10], whereas others suggest that combined saccade-vergence eye movements are generated via monocular saccadic burst neurons [11-13].

Binocular disparity, which refers to the difference in image location of an object seen by the left and right eye resulting from the eyes' horizontal separation, is one of the most effective stimuli for vergence movements [14, 15]. For this reason, visual information about the target location in 3D space was continuously available in most experimental studies. Most modelling studies also assume that vergence is controlled by continuous disparity feedback [16]. Visual feedback is also implicitly assumed in more recent models that have embedded both attentive (target vergence) and inattentive mechanisms (global disparity) driving version-vergence voluntary gaze shifts [17]. However, saccade-vergence interactions may be different when binocular gaze shifts towards remembered visual targets are made. In this situation eye movement command signals lack visual feedback information on where a target is located in 3D space. Both direction and distance information to drive version and vergence eye movements, has to be retrieved entirely from memory. The characteristics of memory-guided saccades without vergence have been studied extensively. Memory-guided saccades are less accurate and have lower peak velocities and longer duration than visually guided saccades [18-20]. However, little is known about the dynamics of memory-guided eye movements with a combination of saccades and vergence. Kumar et al. [21] found differences in version/vergence peak velocity ratios between memory-guided and visually-guided gaze

shifts. The memory-guided eye movements showed a larger slowing of the convergence components than of the corresponding saccadic components, resulting in a smaller saccade/vergence peak velocity ratio. Taken together the findings suggest that different interactions exist between version and vergence under visually and memory-guided conditions.

In most experiments on spatial memory (updating) during binocular vision, monocular movements of each eye have been combined and results have been described in terms of vergence (right eye – left eye) and conjugate gaze or version ((right eye + left eye) / 2) components [22, 23]. The aim of the present paper was to determine the accuracy and contribution of the abducting and adducting eye during binocular gaze shifts towards memorized and visual 3D targets that were presented in three-dimensional space. To our knowledge this is the first study to quantify the contribution of vergence and of each eye separately during combined saccade-vergence gaze shifts from memory.

METHODS

Subjects

Eye movements were recorded from eight subjects (5 males, 3 female, age 40 ± 15 years) who were naïve with respect to the goal of the experiment. Three of the eight subjects also participated in the control trials. Written informed consent was obtained from all subjects prior to the experiments. None of the subjects had a history of ocular pathology or impaired stereoscopic vision and all subjects had normal or corrected-to-normal vision. The mean inter-ocular distance of the subjects was 6.5 ± 0.2 cm. Phoria was measured before the experiment with the Maddox-Rod test at 6 and 1 meter distance. As an additional measure we determined in three subjects the change in vergence over a period of 4 seconds following switching-off the fixation target. Eye dominance was determined with a variant of the hole-in-the-card test by looking through a hole made with the hands. An individually moulded bite board and a vacuum cushion that was placed around the back of the subject's neck were used to restrain the head. Experimental procedures were approved by the Medical Ethical Committee of Erasmus MC and adhered to the Declaration of Helsinki for research involving human subjects.

Experimental setup

Eye movement recordings

Eye positions were recorded with scleral search coils. We used a standard 25-kHz two-field coil system (Model EMP3020; Skalar Medical, Delft, The Netherlands) based on the amplitude detection method by Robinson [24]. Standard dual coils embedded in a silicone annulus

(Skalar Medical, The Netherlands) were inserted in each eye. Before insertion, the eyes were anesthetized with a few drops of oxybuprocain (0.4%) in HCl (pH 4.0). Both coils were calibrated in vitro by mounting them on a gimbal system placed in the center of the magnetic fields. Search coil data were sampled at 1000 Hz on a CED system (Cambridge Electronic Design, Cambridge, UK). At the beginning of each experiment an in vivo calibration was performed. Subjects were instructed to fixate a series of five targets (central target and a target at 10 degrees left, right, up and down). Targets were back projected onto a translucent screen at 186 cm distance. The subjects fixated each target for ten seconds. Data were stored on a hard disk for further off-line analysis.

Visual targets

During the experiment, a subject was seated in a chair that was placed in a completely darkened room. Three Light-Emitting Diodes (LEDs) placed at eye level at different viewing distance from the subject served as visual stimuli (figure 1). One of two red LEDs in front of the subject aligned with the subject's left eye one at respectively 94 cm (far) and 31 cm (near) viewing distance, functioned as fixation point (fixation LED). The third (white) LED served as visual target (target LED). The target LED was suspended from the ceiling 45 cm in front and 13 cm to the left relative to the subject's left eye.

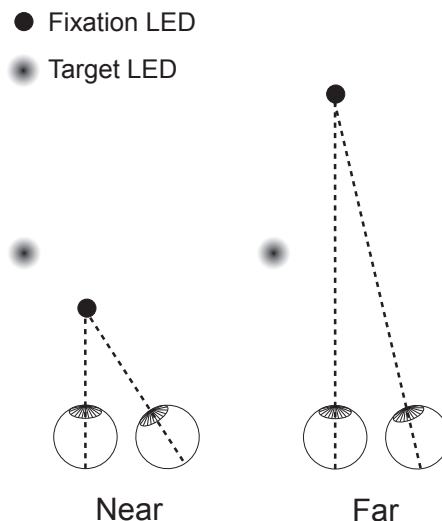


Figure 1: Schematic top view of visual targets. The fixation LEDs (black closed circles) were placed in line with the subject's left eye: one target was at a distance of 94 cm ("far") and one at a distance of 31 cm ("near") in depth. The target LED (grey closed circles) was located at a distance of 45 cm in front and 13 cm to the left relative to the subject's left eye.

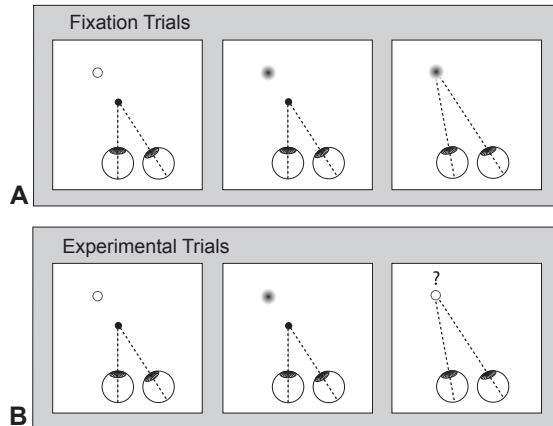


Figure 2: Setup of trials. Trials are illustrated for the “near” condition. A. Fixation trials: The subjects were instructed to fixate the target LED that was presented for 5 seconds. Fixation trials were used to calculate the errors in horizontal gaze and vergence towards the target LED. B. Memory-guided trials: The subjects were asked to fixate the fixation LED while the target LED was turned on for 80 ms. Subjects had to maintain fixation on the fixation LED, and at the same time remember the location of the peripheral flashed target LED. 1800 ms after the target LED was extinguished, the fixation LED was turned off and he subject had to make a saccade to the remembered location of the target LED.

Experimental procedures

Memory-guided gaze shifts

In the memory-guided experiment, subjects were instructed to make eye movements guided from memory (see figure 2B). The subjects were asked to fixate one of the two fixation targets. At a random interval during this fixation period the target LED was flashed for 80 ms. Subjects had to maintain fixation while remembering the location of the target LED.

The fixation LED was switched off 1800 ms after the target LED was extinguished, upon which the subject had to make a saccade to the remembered location of the target in 3D space. Twenty trials were recorded per experimental session and all conditions were presented in randomized order. This resulted in 10 repetitions of each condition. No visual feedback of the location of the flash fixed target was provided after each trial. Data were analyzed post-hoc for a possible learning effect. The trials were preceded by two fixation trials (figure 2A). In these two trials the subjects had to fixate the target LED that was presented for 5 seconds. Fixation trials were used to calculate the errors in horizontal gaze and vergence toward the flashed target (see data analysis).

Control experiments

Three control experiments were performed in which 3 subjects participated:

- (1) Visually guided gaze shifts:

The experiment is similar to the memory-guided experiment, except that the target LED was turned on again, at the same time the fixation LED was turned off. The subjects were asked to make an eye movement toward the target LED after the fixation target was switched off.

(2) Lateralization effects:

To exclude possible left-right differences in performance due to eye dominance, we presented the flash target on the right side of the subject. Test conditions and trial numbers were identical to the memory-guided gaze shift trials, except that the flash target was placed 45 cm in depth and 13 cm to the right relative to the right eye.

(3) Peripheral visual cueing effects:

To test the influence of depth cues on localization of the flash target, a light source consisting of 8 bright white LEDs was placed on a frame above the subject's head. The light source illuminated the environment before and during the period the flash target was turned on.

Data analysis

Data were analyzed off-line using self-written Matlab (Mathworks) routines. Eye movements to the 5-point calibration pattern, retrieved during the calibration task, were used to transform voltage into Fick angles. Trials were excluded when: 1) the subject did not keep their eyes aimed at the fixation target, 2) the subject did not make a saccade after the fixation target was extinguished or 3) when the subject made a saccade before the fixation target was extinguished. We computed the horizontal gaze position of the left and right eye separately. We determined horizontal gaze and vergence at fixed points during each task (figure 3): the initial gaze position when the eyes were fixated on the fixation target (t_1) and after

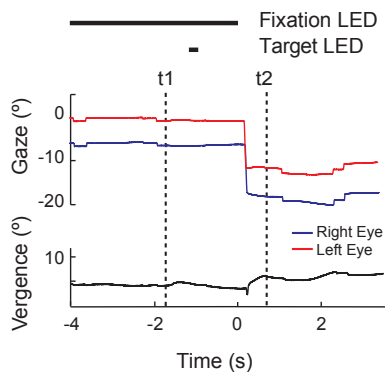


Figure 3: Points in time used for error calculation. Simulation of horizontal gaze (top panel) and vergence (bottom panel) against time. We determined horizontal gaze and vergence at fixed points during each task: the initial position when the eyes were fixated on the fixation LED (t_1) and after the memory-guided eye movement, but before slow drifting eye movements (t_2).

the memory-guided eye movement (t_2). In the case of a single memory-guided saccade t_2 was selected after the saccade, but before slow (drifting) eye movements occurred. In those cases where multiple saccades were made to reach the memorized location of the target, we defined t_2 as the first moment after the last of the series of saccades within a time frame of 1 second where gaze reached a stable value. Saccades were detected by calculating the horizontal angular eye velocity signal from the position signal. Peak velocities were calculated from the selected saccade signals. Vergence angles were calculated as the difference between right and left (L-R) horizontal gaze. Version was calculated as the average of left and right horizontal gaze $((R+L)/2)$.

Errors in horizontal gaze (direction)

After retrieving horizontal gaze at time t_1 and t_2 , we calculated the errors for all trials. Absolute errors were calculated for each eye by subtracting correct gaze that was obtained during the fixation trials, from the actual horizontal gaze at t_2 :

$$\text{Gaze error} = \text{horizontal gaze } (t_2) - \text{horizontal gaze (fixation trial)} \quad \text{equation 1}$$

We also determined gaze errors for version using the following equation:

$$\text{Version error} = \text{version } (t_2) - \text{version (fixation trial)} \quad \text{equation 2}$$

Subject specific correct gaze values were obtained during the fixation trials. A negative error for gaze or version indicates that the leftward memory-guided eye movement was too large, whereas a positive error indicates that the eye movement was too small.

Errors in vergence (depth)

Absolute vergence errors were calculated using the following equation:

$$\text{Vergence error} = \text{vergence } (t_2) - \text{vergence (fixation trial)} \quad \text{equation 3}$$

Subject specific correct vergence angle was obtained during the fixation trials. Negative vergence errors indicate that the vergence angle is too small, while positive errors indicate that the vergence angle is too large.

Statistics

The mean and standard deviation of gaze and vergence errors of each specific spatial task was group-wise calculated and tested for a normal distribution. To test for a possible learning effect during the experiment, regression lines were fitted to vergence errors as a function of trial number for each subject. The significance of version, gaze and vergence errors was

tested using the one-sample t-tests by comparing the results with the test value set to zero. The differences between the errors of each eye were tested for significance using a trial-based paired-sample t-test. To test the influence of fixation distance and the influence of each eye on the errors, we performed univariate analysis of variance (ANOVA) analyses. The differences between left-right eye the peak velocities were tested for significance with a trial-based paired-sample t-test. We compared the memory-guided with the visually guided peak eye velocities using the independent sample t-test. The vergence errors with and without illumination of the environment were compared using independent sample t-tests. All statistical analyses (memory-guided trials and control trials) were performed on trial-based aggregated data of the subjects. Statistical analyses were performed in SPSS.

RESULTS

Memory-guided gaze shifts

All subjects had phoria values measured with the Maddox cross that were less than 1 degree. All subjects successfully fixated the flash target with high precision in the fixation trials immediately preceding the memory-guided experiment. When we switched off the fixation target, vergence remained fairly stable over a period of at least 4 seconds (mean vergence change 0.52 ± 0.8 degrees for the far target and 1.5 ± 1.2 for the near fixation target). About 15% of the memory-guided gaze shift trials were discarded, mostly because subjects started a saccade towards the target LED too early. The average horizontal gaze in the fixation trials was -16.30 ± 0.45 and -23.30 ± 0.89 degrees for the left and right eye respectively, while vergence was 7.02 ± 0.51 degrees. Parameters obtained from the fixation trials were subject specific and were used to calculate the performance of memory-guided eye movements. Subject specific average errors for horizontal gaze of each eye, for version and for vergence, including the number of analyzed trials, are listed in table 1. Also subject specific gaze, version and vergence obtained from the fixation trials, are given as well as eye dominance. To test for a possible learning effect during the experiment we also calculated vergence errors for each subject as a function of trial number. The fitted regression lines had an average slope of 0.00 ± 0.07 degrees, indicating that there was no learning effect that could have influenced the measurement series.

Horizontal gaze

In figure 4 and figure 5 examples of horizontal gaze against time for one subject (subject 6) for respectively the "near" and "far" memory-guided condition are plotted. The top panel shows the horizontal gaze for each eye separately. Figure 4 illustrates the "near" condition in which

Table 1: Average errors and standard deviation per subjects

| Subject | | | Error (°) ± SD | | Fixation trial | # trials | | Eye Dominance |
|---------|----------|-------|----------------|--------------|----------------|----------|-----|---------------|
| | | | Near | Far | | Near | Far | |
| 1 | Gaze | Left | -0.86 ± 2.10 | -0.94 ± 2.00 | -16.24 | 7 | 6 | Right |
| | | Right | -1.22 ± 2.23 | 2.26 ± 2.00 | -23.57 | | | |
| | Version | | -1.04 ± 2.05 | 0.66 ± 1.94 | -19.90 | | | |
| | Vergence | | 0.20 ± 1.50 | -3.30 ± 0.83 | 7.33 | | | |
| 2 | Gaze | Left | 2.31 ± 3.69 | 0.30 ± 2.76 | -17.31 | 8 | 8 | Right |
| | | Right | 2.88 ± 2.35 | 3.31 ± 2.61 | -24.79 | | | |
| | Version | | 2.59 ± 2.96 | 1.80 ± 2.66 | -21.06 | | | |
| | Vergence | | -0.71 ± 1.91 | -3.15 ± 0.61 | 7.48 | | | |
| 3 | Gaze | Left | -2.11 ± 1.49 | -2.97 ± 1.23 | -16.04 | 6 | 7 | Left |
| | | Right | -5.71 ± 2.50 | -5.04 ± 1.95 | -22.75 | | | |
| | Version | | -3.91 ± 1.87 | -4.00 ± 1.56 | -19.40 | | | |
| | Vergence | | 3.85 ± 1.63 | 2.29 ± 1.11 | 6.71 | | | |
| 4 | Gaze | Left | 2.22 ± 1.88 | 0.26 ± 1.38 | -16.24 | 10 | 10 | Right |
| | | Right | 3.56 ± 1.51 | 2.43 ± 1.39 | -22.97 | | | |
| | Version | | 2.89 ± 1.68 | 1.34 ± 1.36 | -19.61 | | | |
| | Vergence | | -1.35 ± 0.58 | -2.17 ± 0.53 | 6.73 | | | |
| 5 | Gaze | Left | -2.40 ± 1.54 | -3.50 ± 2.67 | -16.00 | 7 | 9 | Right |
| | | Right | -0.09 ± 1.35 | -0.02 ± 2.10 | -22.66 | | | |
| | Version | | -1.24 ± 1.42 | -1.76 ± 2.37 | -19.33 | | | |
| | Vergence | | -2.29 ± 0.52 | -3.46 ± 0.75 | 6.67 | | | |
| 6 | Gaze | Left | 2.81 ± 2.30 | 2.91 ± 2.53 | -15.95 | 9 | 8 | Right |
| | | Right | 4.37 ± 2.43 | 5.52 ± 2.83 | -22.59 | | | |
| | Version | | 3.59 ± 2.36 | 4.21 ± 2.67 | -19.38 | | | |
| | Vergence | | -1.57 ± 0.47 | -2.61 ± 0.51 | 6.85 | | | |
| 7 | Gaze | Left | 1.23 ± 2.43 | -4.21 ± 1.67 | -16.52 | 9 | 9 | Left |
| | | Right | 1.69 ± 2.21 | -2.03 ± 1.97 | -24.46 | | | |
| | Version | | 1.46 ± 1.46 | -3.12 ± 1.81 | -20.05 | | | |
| | Vergence | | -0.45 ± 0.58 | -2.17 ± 0.50 | 7.94 | | | |
| 8 | Gaze | Left | -1.31 ± 2.32 | 2.08 ± 1.88 | -16.08 | 7 | 8 | Right |
| | | Right | -0.07 ± 2.43 | 2.40 ± 1.45 | -22.55 | | | |
| | Version | | -0.69 ± 2.36 | 2.24 ± 1.59 | -19.32 | | | |
| | Vergence | | -1.34 ± 0.59 | -0.42 ± 1.14 | 6.47 | | | |

the fixation LED was placed in front of the target LED. Figure 5 illustrates the “far” condition in which the fixation LED was behind the target LED. The bars on top of the horizontal gaze traces indicate the moment in time that the fixation and target LED were illuminated. In all conditions shown in our plots, leftward eye movements were made towards the memorized

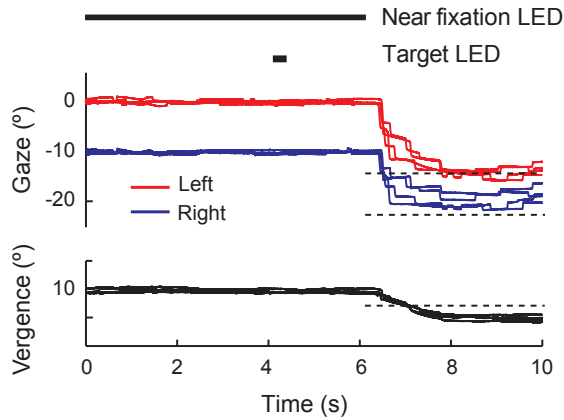


Figure 4: Example of memory-guided trials for the “near” condition. The examples of eye movements are obtained from subject 6. Horizontal gaze of both eyes is plotted against time in the top panel and vergence is plotted against time in the bottom panel. The bars on top of the horizontal gaze traces indicate the illumination of the fixation (“near”) and target LED. The dashed lines are the subject specific correct gaze and vergence values and that are retrieved from the fixation trials. Leftward eye movements are made towards the memorized location of the target LED. Gaze of the left eye (red traces) is more accurate than gaze of the right eye gaze (blue traces). Vergence decreased during the memory-guided eye movement.

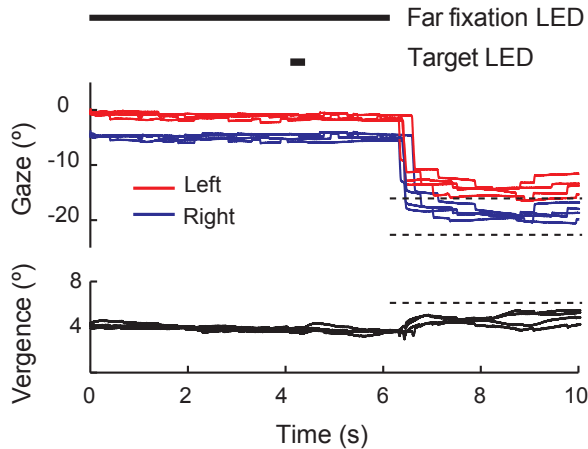


Figure 5: Example of memory-guided trials for the “far” condition. The examples of eye movements are obtained from subject 6. Horizontal gaze of both eyes is plotted against time in the top panel and vergence is plotted against time in the bottom panel. The bars on top of the horizontal gaze traces indicate the illumination of the fixation (“far”) and target LED. The dashed lines are the subject specific correct gaze and vergence values and that are retrieved from the fixation trials. Leftward eye movements are made towards the memorized location of the target LED. Gaze of the left eye (red traces) is more accurate than gaze of the right eye gaze (blue traces). Vergence increased during the memory-guided eye movement.

location of the target LED. The correct horizontal gaze values, retrieved from each subject in the fixation trials, are plotted as a reference.

Table 2: Horizontal gaze and vergence errors

| | Horizontal Gaze Error (°) | | Vergence Error (°) | |
|----------------------------|---------------------------|----------|--------------------|-----------|
| | Mean ± SD | P-value* | Mean ± SD | P-value* |
| Near fixation (divergence) | | | | |
| Left eye | 0.59 ± 2.97 | P=0.13 | -0.67 ± 1.83 | P < 0.01 |
| Right eye | 1.23 ± 3.44 | P < 0.01 | | |
| Version | 1.69 ± 3.10 | P < 0.05 | | |
| Far fixation (convergence) | | | | |
| Left eye | -0.67 ± 3.23 | P=0.11 | -2.12 ± 1.65 | P < 0.001 |
| Right eye | 1.42 ± 3.43 | P < 0.01 | | |
| Version | 1.22 ± 3.82 | P=0.37 | | |

*One sample t-test with 0.0.

Average gaze errors, calculated from all trials per condition, are expressed in degrees and presented in table 2 (left column). The tests of normality indicated that the data had normal distribution. In the “near” condition, mean gaze errors (mean ± SD) were 0.59 ± 2.97 and 1.23 ± 3.44 degrees, for the left and the right eye respectively. In “far” condition, mean gaze errors (mean ± SD) were -0.67 ± 3.23 and 1.42 ± 3.43 degrees for the left and the right eye respectively. In both conditions, the gaze error of the right eye was significantly different from zero ($P < 0.01$), whereas the gaze error of the left eye was not ($P=0.13$ and $P=0.11$ for “near” and “far” respectively). This indicates that the mean gaze errors of the left eye were smaller. We further evaluated this with a paired sample t-test, resulting in a significant difference between the left and right eye errors ($P < 0.01$ and $P < 0.001$, “near” and “far” respectively).

We also calculated gaze errors for the average of both eyes (version). These values are also shown in table 2. Version gaze errors (mean ± SD) were 1.69 ± 3.10 and 1.22 ± 3.82 degrees for the “near” and “far” condition respectively. Version gaze error in the “near” condition was significantly different from zero ($P < 0.05$), whereas the version gaze error in the “far” condition was not ($P=0.37$). A univariate ANOVA, with fixation LED (near / far) and horizontal gaze (left, right and version) as fixed factors and gaze error as dependent variable, indicated no effect of fixation LED ($F(1,366)=2.13$, $P=0.15$), but a significant effect of horizontal gaze ($F(2,366)=7.55$, $P < 0.01$). Post hoc Tukey test indicated that the error of the left eye was significant smaller than the error of the right eye and version (for left vs. right and left vs. version, $P < 0.01$).

Vergence

The bottom panels of figure 4 and 5 show examples of vergence for respectively the “near” and “far” memory-guided conditions. In the “near” condition (Figure 4) vergence decreased, because the flash LED was placed farther than the fixation LED, whereas in the “far” condition

(figure 5) the target LED was in front of the fixation LED. This required that a subject made a convergence eye movement toward the location of the remembered target.

Errors in vergence are shown in table 2 (right column). In the “near” condition vergence error (\pm SD) was -0.67 ± 1.83 degrees, this value was significantly different from zero ($P < 0.01$). This negative error indicates that vergence decreased too much: in other words, the divergence eye movement was too large. In the “far” condition vergence error (mean \pm SD) was -2.12 ± 1.65 degrees, which is also significantly different from zero ($P < 0.001$). The negative vergence error in the “far” condition indicates that the convergent eye movement was too small: vergence did not increase enough, resulting in a vergence undershoot. Vergence errors under the “near” and

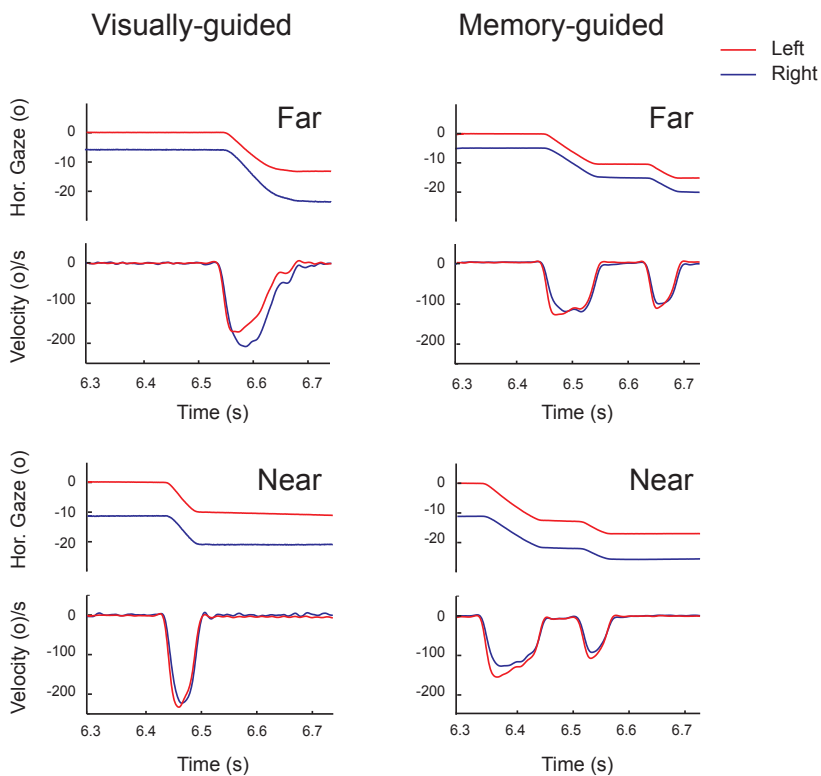


Figure 6: Example of visually versus memory-guided gaze shifts. The examples of eye movements are obtained from subject 1. Horizontal gaze (top panels) and eye velocity (bottom panels) of both eyes are plotted against time. The smaller inset in each panel shows the corresponding vergence position and velocity at a 2.5 times magnification along the Y-axis. Visually guided trials are presented in the left panels. During the “far” fixation LED, the gaze shift and peak velocity of the right eye was larger. In the “near” fixation condition intra-saccadic peak velocity of left eye was slightly larger than that of the right eye. Memory-guided trials are presented in the right panels. Both in the “near” and “far” fixation condition the left (abducting) eye was faster than the right (adducting) eye during the gaze shift to the target. Note that the peak velocities in the memory-guided trials were lower than in the visually guided trials.

“far” conditions were significantly different (unpaired t-test, $P < 0.001$). Errors were significantly smaller for divergent eye movements than for convergent eye movements.

Memory-guided versus visually guided gaze shift

The memory-guided experiment (with the target LED on the left side) was designed such that the right eye had to make a larger gaze shift than the left eye in the “far” condition. However, in the “near” condition, the left eye had to make a larger gaze shift than the right eye. One way to overcome this difference in amplitude between left and right eye, is to generate unequal saccades.

Examples of binocular gaze shifts under visually guided and memory-guided conditions from one subject (subject 1) are presented in figure 6. Visually guided gaze shifts and eye velocities are presented in the left panels. When the subject made a gaze shift under visually guided conditions, starting from the “far” fixation LED, the gaze shift made by the right was larger, resulting in higher peak velocity of the right eye. As expected, the opposite was found when gaze shifts were made from the “near” fixation LED to the target LED. Intra-saccadic peak velocity of left eye was slightly larger than that of the right eye. The differences in right versus left eye peak velocities were significant and consistent across all three subjects (paired sample T-test, $P < 0.001$). The average peak velocities from all subjects of each condition are presented in table 3.

For memory-guided binocular gaze shifts the situation was different (see figure 6, right panels). In the “far” condition, the left (abducting) eye was faster than the right (adducting) eye during the gaze shift to the target. Subjects used post-saccadic vergence mediated by the right (adducting) eye, to direct their binocular gaze to the memorized position in 3D space. In the “near” condition, the left and right eye had different peak velocities during the gaze shifts to the remembered target. Similar as in the visually guided saccades, the peak velocity of the right (adducting) eye was smaller than that of the left (abducting) eye. The difference in right versus left eye peak velocity was significant and consistent across all three subjects, see table 3 (paired sample T-test, $P < 0.001$).

Furthermore, we found that the peak velocities in the memory-guided trials were lower than in the visually guided trials (table 3). We compared the visually guided with the memory-guided peak velocities of each eye and found a significant difference in all conditions (independent sample t-test, $P < 0.001$). We also analyzed latencies (time between switching off the fixation LED and the initiation of an eye movement) in both the visually and memory-guided trials. In the memory-guided trials the average latency was $370 \text{ ms} \pm 8 \text{ ms SD}$ and in the visually guided trials a latency of $360 \text{ ms} \pm 8 \text{ ms SD}$ was found. The latencies were not significant different.

To compare the peak eye velocities, we expressed the differences between right and left eye peak velocities as right / left eye velocity ratios. The velocity ratios are presented in figure

Table 3: Peak velocities per subject

| Subject | | Peak velocity (°/s) ± SD | |
|-----------------|-----------|--------------------------|-----------------|
| | | Near | Far |
| Visually Guided | | | |
| 1 | Left eye | -192.29 ± 32.58 | -173.84 ± 20.96 |
| | Right eye | -172.51 ± 34.72 | -202.67 ± 19.36 |
| 2 | Left eye | -258.46 ± 28.76 | -337.02 ± 21.22 |
| | Right eye | -237.45 ± 27.40 | -340.14 ± 22.48 |
| 3 | Left eye | -369.86 ± 18.88 | -367.52 ± 11.02 |
| | Right eye | -360.59 ± 17.46 | -395.95 ± 15.18 |
| Memory-guided | | | |
| 1 | Left eye | -126.31 ± 23.57 | -145.55 ± 17.29 |
| | Right eye | -109.43 ± 18.78 | -136.67 ± 21.44 |
| 2 | Left eye | -165.34 ± 38.45 | -220.81 ± 49.67 |
| | Right eye | -144.18 ± 35.15 | -209.03 ± 46.19 |
| 3 | Left eye | -190.20 ± 47.81 | -205.03 ± 42.29 |
| | Right eye | -148.91 ± 40.36 | -180.56 ± 41.52 |

7. Only in the “far” visually guided condition, the velocity ratio was larger than 1 indicating that the peak velocity of the right (adducting) eye was larger. In all other conditions the left (abducting) eye had a larger peak velocity. All velocity ratios were significantly different from 1.0 (one sample T-test, $P < 0.001$). Both for the “far” and “near” condition, right/left eye velocity ratios between visually guided and memory-guided conditions were significantly different (independent sample t-test, $P < 0.001$).

Lateralization effects

To exclude that eye preferences influenced the memory-guided gaze shifts, we calculated gaze errors for both the “near” and “far” condition from the second control experiment, in which the target LED was placed on the right side. Gaze errors (mean ± SD) in the control experiment with “near” were not significantly different from zero: -0.83 ± 3.52 degrees ($P=0.21$) and 0.82 ± 4.60 degrees ($P=0.34$) for the left eye and right eye respectively. Gaze errors (± SD) in the “far” condition were significantly different from zero for the left eye (-3.61 ± 2.42 degrees, $P < 0.001$), but not for the right eye (-0.99 ± 3.30 degrees, $P=0.15$). Paired sample t-tests demonstrated significant differences between left and right eye gaze errors ($P < 0.001$ and $P < 0.001$ for both the “near” and “far” condition). A univariate ANOVA, with fixation LED (near / far) and horizontal gaze (left, right and version) as fixed factors and gaze error as dependent variables, indicated a significant effect of both fixation LED ($F(1,165) = 16.99$, $P < 0.001$) and horizontal gaze ($F(2,165) = 4.88$, $P < 0.01$). Post-hoc Tukey test indicated that the error of the right eye was significantly smaller than the error of the left eye (for left vs.

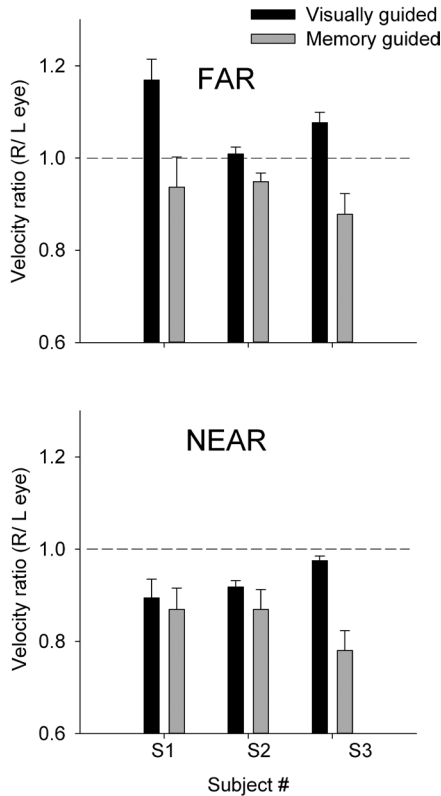


Figure 7: Eye velocity ratios. The differences between right and left eye peak velocities are plotted as right / left eye velocity ratios. Velocity ratios are plotted for each subject both for the visually (black bars) and memory-guided (grey bars) “near” (bottom) and “far” (top) fixation condition. In the “far” fixation visually guided condition, the velocity ratio was above 1 indicating that the peak velocity of the right (adducting) eye was larger. In all other conditions the left (abducting) eye had a larger peak velocity.

right, $P < 0.01$). The data show that differences in precision are based on differences between adducting and abducting eye, and not on eye preference.

Peripheral visual cueing effects

In the third control experiment we repeated the memory-guided gaze shift experiment by providing additional depth cues. Additional cues created by illuminating the environment while the target LED was turned on, did not improve the memory-guided vergence movements. In contrast, the vergence errors were larger than during the memory-guided trials without illumination of the environment. In the “near” condition, vergence errors were larger with illumination (mean = -1.14 , SD = 2.55 degrees) than without illumination (mean = -0.67 , SD = 1.83 degrees). This difference was not significant $t(84) = 0.96$, $p = 0.34$. In the “far” condition, vergence errors were also larger with illumination (mean = -3.26 , SD = 1.30 degrees)

than without illumination (mean = -2.12 , $SD = 1.65$ degrees). This difference was significant $t(29.09) = 2.95$, $p < 0.05$.

DISCUSSION

The aim of our experiments was to assess the accuracy and dynamics of binocular eye movements towards memorized targets in terms of direction and depth (version and vergence). We found significant differences in horizontal gaze errors between the left and the right eye that were related to viewing direction. When the memorized target was located on the left side of the subject, such that the left eye had to make an abducting movement (temporal) and the right eye an adducting (nasal) movement towards the remembered target, gaze error of the right eye was larger than that of the left eye. When the target LED was placed the right side of the subject the opposite was found; gaze errors were in this case significantly larger in the left (adducting) eye. This means that in orienting gaze towards memorized targets, the abducting eye is more accurate than the adducting eye. This also excludes the possibility that eye dominance influenced the task, because in the control experiment, in which the same subjects participated, the abducting eyes remained most accurate. Because version (the average gaze of both eyes) is a commonly used measure to quantify directional gaze shifts we also compared version with gaze of each eye separately. When version errors alone are used (shown in table 2), one may conclude that significant larger errors are made in the “near” condition, than in the “far” condition. However, gaze errors of each eye separately show that in both conditions equally large errors are made. Thus, when version alone is used to analyze memory-guided saccades, important information on the performance of each eye separately might be missed.

We also compared memory-guided binocular gaze shifts that had either a convergence or divergence component. In one condition the initial point of fixation of both eyes was at far distance, thus requiring convergent eye movements towards the remembered location of the target LED, whereas in the other situation the initial point of fixation was at near distance, requiring divergent memory-guided eye movements. We found that under the condition that required divergence, the error in vergence was significantly smaller than when convergence was required. Adding additional visual depth cues during the flash had no effect on vergence errors. In both the “near” and “far” condition, the remembered vergence angles toward the target LED were too small. One explanation is that the subject underestimated the target distance. However, this is contradicted by the fact that adding additional depth cues did not improve the vergence error. Another explanation might be that the eyes have a tendency to diverge because of a limitation in vergence control from memory. This suggests that passive release of vergence is an easier task than active increase of vergence. This is in line with the finding that without visual input the eyes have a physiological resting vergence position [25].

Because in our experiment gaze errors were unequal in both eyes, with the abducting eye being more accurate, vergence errors were mainly present in the adducting eye.

To our knowledge this difference in accuracy of abducting and adducting memory-guided eye movements has not been described before. The differences in neural pathways that are involved in the control of abducting and adducting eye movements offer a possible explanation for this finding. Innervation of the lateral rectus muscle, which abducts the eye, is a directly driven pathway by the abducens nucleus and nerve (VI), whereas the medial rectus muscle (which adducts the eye) is indirectly controlled by the abducens nucleus via the medial longitudinal fasciculus (MLF) and the oculomotor nucleus (III). The abducting eye has small gaze errors and its movement is also faster than that of the adducting eye. Differences in peak velocity were previously shown by Collewijn and colleagues using visually guided tasks [26].

The experimental design (with the target LED on the left side,) was such that based on geometry, different sized gaze shifts were required to fixate the target LED. When gaze shifts were made from the “far” fixation towards the target LED, the right (adducting) eye had to make a larger gaze shift than the left eye. However, in the “near” condition, the left eye (abducting eye) had to make a larger gaze shift than the right eye. Under visually guided conditions this amplitude difference between left and right eye was achieved by generating unequal sized saccades. For memory-guided saccades the abducting eye was always faster than the adducting eye. Thus, under this condition, subjects had to use post-saccadic vergence, mediated by the adducting eye, to direct their gaze to the memorized position in 3D space. Our data are consistent with the findings of Kumar et al. [21]. They, however, only considered peak saccade and peak vergence velocity ratios and did not analyze relative timing aspects. Our study shows that under visually guided conditions the abducting eye was initially faster, but that adducting eye continued to increase its velocity, reaching its peak after the peak velocity of the abducting eye.

Our data show that different strategies are used to achieve 3D gaze shifts under different conditions. An important issue is how our findings relate the long-standing debate on the internal organization of binocular oculomotor control. The prevailing theory is Hering's law that describes different vergence and conjugate commands that are summed by the motor neurons of each eye [1]. Helmholtz however, postulated that each eye is individually controlled [27]. In support of Hering's theory it has been shown that in the midbrain different types of neurons are involved in the control of vergence [6, 28, 29]. These studies have demonstrated that vergence tonic cells, located in the mesencephalon, either increase firing before convergence or before divergence eye movements. It is considered that these vergence signals are added to conjugate saccadic motor commands. Thus, in this view binocular saccadic eye movements are primarily controlled at the brainstem level by conjugate burst cells. However, more recently, monocular burst neurons encoding monocular commands for left and right eye saccades have been identified in the midbrain [13]. It has also been

demonstrated that the brain stem burst generators, which were commonly assumed to drive only the conjugate component of eye movements, carry substantial vergence-related information during disconjugate saccades [12]. As pointed out by Kumar et al [21], changes in binocular behavior that are quantitatively different for saccades and vergence are inconsistent with the independent eye control theory. Such changes were found during convergence, but not during divergence, both in our study and the study of Kumar et al. [21].

Our findings suggest that the internal circuitry for making 3D gaze shifts is dependent on continuous visual and local feedback when making intra-saccadic convergence eye movements during binocular gaze shifts. This does not exclude that there is also a memory system that keeps track where a target is in 3D space and that can be accessed by the oculomotor control system: Otherwise subjects could not make memory-guided binocular gaze shifts at all. A possible candidate is the caudal frontal eye field [30, 31]. However to use this information, the oculomotor system has to rely more on a sequential processing using fast and slow systems, than on a simultaneous processing of saccade and vergence commands. The fact that during divergence the situation is different may very well reflect the fact that for near vision there is already a state of tonic vergence. This is readily released at an early stage of the binocular gaze shift.

REFERENCES

1. Hering, E., *Die Lehre vom binokularen Sehen* 1868: Leipzig: Engleman.
2. Bridgeman, B.S., *The theory of binocular vision* 1977: New York: Plenum.
3. Goebel, H.H., et al., Lesions of the pontine tegmentum and conjugate gaze paralysis. *Arch Neurol*, 1971. 24(5): p. 431-40.
4. Hepp, K. and V. Henn, Spatio-temporal recoding of rapid eye movement signals in the monkey paramedian pontine reticular formation (PPRF). *Exp Brain Res*, 1983. 52(1): p. 105-20.
5. Zee, D.S., Brain stem and cerebellar deficits in eye movement control. *Trans Ophthalmol Soc U K*, 1986. 105 (Pt 5): p. 599-605.
6. Mays, L.E., Neural control of vergence eye movements: convergence and divergence neurons in midbrain. *J Neurophysiol*, 1984. 51(5): p. 1091-1108.
7. Mays, L.E., et al., Neural control of vergence eye movements: neurons encoding vergence velocity. *J Neurophysiol*, 1986. 56(4): p. 1007-21.
8. Collewijn, H., C.J. Erkelens, and R.M. Steinman, Voluntary binocular gaze-shifts in the plane of regard: dynamics of version and vergence. *Vision Res*, 1995. 35(23-24): p. 3335-58.
9. Zee, D.S., E.J. Fitzgibbon, and L.M. Optican, Saccade-vergence interactions in humans. *J Neurophysiol*, 1992. 68(5): p. 1624-41.
10. Busetini, C. and L.E. Mays, Saccade-vergence interactions in macaques. II. Vergence enhancement as the product of a local feedback vergence motor error and a weighted saccadic burst. *Journal of neurophysiology*, 2005. 94(4): p. 2312-30.
11. King, W.M. and W. Zhou, Neural basis of disjunctive eye movements. *Ann NY Acad Sci*, 2002. 956: p. 273-83.
12. Van Horn, M.R., P.A. Sylvestre, and K.E. Cullen, The brain stem saccadic burst generator encodes gaze in three-dimensional space. *J Neurophysiol*, 2008. 99(5): p. 2602-16.
13. Zhou, W. and W.M. King, Premotor commands encode monocular eye movements. *Nature*, 1998. 393(6686): p. 692-5.
14. Semmlow, J. and P. Wetzell, Dynamic contributions of the components of binocular vergence. *J Opt Soc Am*, 1979. 69(5): p. 639-45.
15. Westheimer, G. and D.E. Mitchell, The sensory stimulus for disjunctive eye movements. *Vision Res*, 1969. 9(7): p. 749-55.
16. Rashbass, C. and G. Westheimer, Disjunctive eye movements. *The Journal of physiology*, 1961. 159: p. 339-60.
17. Erkelens, C.J., A dual visual-local feedback model of the vergence eye movement system. *Journal of vision*, 2011. 11(10).
18. Baker, J.T., T.M. Harper, and L.H. Snyder, Spatial memory following shifts of gaze. I. Saccades to memorized world-fixed and gaze-fixed targets. *J Neurophysiol*, 2003. 89(5): p. 2564-76.
19. Leigh, R.J. and D.S. Zee. *The neurology of eye movements*. 2006; 4th:[x, 763].
20. White, J.M., D.L. Sparks, and T.R. Stanford, Saccades to remembered target locations: an analysis of systematic and variable errors. *Vision Res*, 1994. 34(1): p. 79-92.
21. Kumar, A.N., et al., Tests of Hering- and Helmholtz-type models for saccade-vergence interactions by comparing visually guided and memory-guided movements. *Ann NY Acad Sci*, 2005. 1039: p. 466-9.
22. Klier, E.M., B.J. Hess, and D.E. Angelaki, Differences in the accuracy of human visuospatial memory after yaw and roll rotations. *J Neurophysiol*, 2006. 95(4): p. 2692-7.

23. Klier, E.M., B.J. Hess, and D.E. Angelaki, Human visuospatial updating after passive translations in three-dimensional space. *J Neurophysiol*, 2008. 99(4): p. 1799-809.
24. Robinson, D.A., A Method Of Measuring Eye Movement Using A Scleral Search Coil In A Magnetic Field. *IEEE Trans Biomed Eng*, 1963. 10: p. 137-45.
25. Rosenfield, M., Tonic vergence and vergence adaptation. *Optom Vis Sci*, 1997. 74(5): p. 303-28.
26. Collewijn, H., C.J. Erkelens, and R.M. Steinman, Binocular co-ordination of human horizontal saccadic eye movements. *J Physiol*, 1988. 404: p. 157-82.
27. Helmholtz, H., Helmholtz's treatise on physiological optics (English translation of "Handbuch der physiologischen Optik", 1910),1910/1962, New York: Dover.
28. Zhang, Y., L.E. Mays, and P.D. Gamlin, Characteristics of near response cells projecting to the oculomotor nucleus. *J Neurophysiol*, 1992. 67(4): p. 944-60.
29. Judge, S.J. and B.G. Cumming, Neurons in the monkey midbrain with activity related to vergence eye movement and accommodation. *J Neurophysiol*, 1986. 55(5): p. 915-30.
30. Fukushima, J., et al., Neuronal activity in the caudal frontal eye fields of monkeys during memory-based smooth pursuit eye movements: comparison with the supplementary eye fields. *Cereb Cortex*, 2011. 21(8): p. 1910-24.
31. Fukushima, K., J. Fukushima, and T. Warabi, Vestibular-related frontal cortical areas and their roles in smooth-pursuit eye movements: representation of neck velocity, neck-vestibular interactions, and memory-based smooth-pursuit. *Front Neurol*, 2011. 2: p. 78.



4

Three dimensional vestibular ocular reflex testing
using a six degrees of freedom motion platform

Joyce Dits, Mark M. Houben and Johannes van der Steen.

Department of Neuroscience, Erasmus MC, Rotterdam, The Netherlands.

Adapted from:

Journal of Visualized Experiments. 2013 May;(75).

ABSTRACT

Short: A method is described to measure three-dimensional vestibulo ocular reflexes (3D VOR) in humans using a six degrees of freedom (6DF) motion simulator. The gain and misalignment of the 3D angular VOR provide a direct measure of the quality of vestibular function. Representative data on healthy subjects are provided.

Long: The vestibular organ is a sensor that measures angular and linear accelerations with six degrees of freedom 6DF. Complete or partial defects in the vestibular organ results in mild to severe equilibrium problems, such as vertigo, dizziness, oscillopsia, gait unsteadiness nausea and/or vomiting. A good and frequently used measure to quantify gaze stabilization is the gain, which is defined as the magnitude of compensatory eye movements with respect to imposed head movements. To test vestibular function more fully one has to realize that 3D VOR ideally generates compensatory ocular rotations not only with a magnitude (gain) equal and opposite to the head rotation but also about an axis that is co linear with the head rotation axis (alignment). Abnormal vestibular function thus results in changes in gain and changes in alignment of the 3D VOR response.

Here we describe a method to measure 3D VOR using whole body rotation on a 6DF motion platform. Although the method also allows testing translation VOR responses [1], we limit ourselves to a discussion of the method to measure 3D angular VOR. In addition, we restrict ourselves here to description of data collected in healthy subjects in response to angular sinusoidal and impulse stimulation.

Subjects are sitting upright and receive whole-body small amplitude sinusoidal and constant acceleration impulses. Sinusoidal stimuli ($f=1$ Hz, $A=4^\circ$) were delivered about the vertical axis and about axes in the horizontal plane varying between roll and pitch at increments of 22.5° in azimuth. Impulses were delivered in yaw, roll and pitch and in the vertical canal planes. Eye movements were measured using the scleral search coil technique [2]. Search coil signals were sampled at a frequency of 1 kHz. The input-output ratio (gain) and misalignment (co-linearity) of the 3D VOR were calculated from the eye coil signals. [3].

Gain and co-linearity of 3D VOR depended on the orientation of the stimulus axis. Systematic deviations were found in particularly during horizontal axis stimulation. In the light the eye rotation axis was properly aligned with the stimulus axis at orientations 0° and 90° azimuth, but gradually deviated more and more towards 45° azimuth.

The systematic deviations in misalignment for intermediate axes can be explained by a low gain for torsion (x-axis or roll-axis rotation) and a high gain for vertical eye movements (Y-axis or pitch-axis rotation (see figure 2). Because intermediate axis stimulation leads a compensatory response based on vector summation of the individual eye rotation components, the net response axis will deviate because the gain for x- and y-axis are different.

In darkness the gain of all eye rotation components had lower values. The result was that the misalignment in darkness and for impulses had different peaks and troughs than in the light: its minimum value was reached for pitch axis stimulation and its maximum for roll axis stimulation.

CASES PRESENTATION:

Nine subjects participated in the experiment. All subjects gave their informed consent. The experimental procedure was approved by the Medical Ethics Committee of Erasmus University Medical Center and adhered to the Declaration of Helsinki for research involving human subjects.

Control subjects:

Six subjects served as controls. Three subjects had a unilateral vestibular impairment due to a vestibular schwannoma. The age of control subjects (six males and three females)

ranged from 22 to 55 years. None of the controls had visual or vestibular complaints due to neurological, cardio vascular and ophthalmic disorders.

Patients:

The age of the patients with schwannoma varied between 44 and 64 years (two males and one female). All schwannoma subjects were under medical surveillance and/or had received treatment by a multidisciplinary team consisting of an otorhinolaryngologist and a neurosurgeon of the Erasmus University Medical Center. Tested patients all had a right side vestibular schwannoma and underwent a wait and watch policy (table 1; subjects N1-N3) after being diagnosed with vestibular schwannoma. Their tumors had been stable for over 8-10 years on magnetic resonance imaging.

PROCEDURE

1. 6DF motion platform

Vestibular stimuli were delivered with a motion platform (see figure 1) capable of generating angular and translational stimuli at a total of six degrees of freedom (FCS-MOOG, Nieuw-Venep, The Netherlands). The platform is moved by six electro-mechanical actuators connected

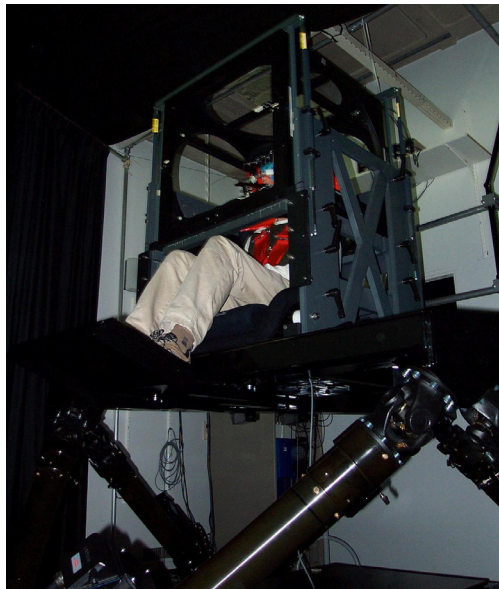


Figure 1: Experimental setup with the 6DF Motion platform

to a personal computer with dedicated control software. It generates accurate movements with six degrees of freedom. Sensors placed in the actuators continuously monitored the platform motion profile. The device has <0.5 mm precision for linear and $<0.05^\circ$ for angular movements. Vibrations during stimulation were 0.02° . Resonance frequency of the device was >75 Hz. Platform motion profile was reconstructed from the sensor information in the actuators using inverse dynamics and sent to the data collection computer. To synchronize platform and eye movement data, a laser beam was mounted at the backside of the platform and projected onto a small photocell (1 mm, reaction time 10 μ s). The output voltage of the photocell was sampled at a rate of 1 KHz together with the eye movement data and provided a real time indicator of motion onset with 1ms accuracy. During the offline analysis using Matlab (Mathworks, Natick, MA), the reconstructed motion profile of the platform based on the sensor information of the actuators in the platform was precisely aligned with the onset of platform motion.

2. Subjects

Seating

The subjects are seated on a chair mounted at the centre of the platform (figure 2). The subject's body was restrained with a four-point seatbelt as used in racing cars. The seatbelts were anchored to the base of the motion platform. The chair was surrounded by a PVC cubic frame and served as a support for the field coils. The field coil system was adjustable in height, such that the subject's eyes were in the centre of the magnetic field.

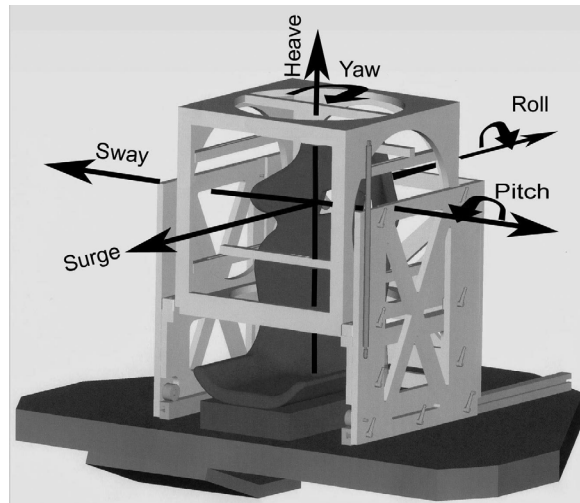


Figure 2: Schematic drawing of the electro magnetic field coil system surrounding the chair mounted on the 6DF motion platform. Arrows indicate the possible axes of rotation and translation of the platform.

Head fixation

The head is immobilized using an individually moulded dental-impression bite board, which was attached to the cubic frame via a rigid bar. A vacuum pillow folded around the neck and an annulus attached to the chair further ensured fixation of the subject (figure 1). In addition, to monitor spurious head movements during the stimulation, we attached two 3D sensors (Analog devices) directly to the bite board, one for angular and one for linear accelerations.

3. Coordinate system

Eye rotations are defined in a head-fixed right-handed coordinate system (figure 3). In this system from the subject's point of view a leftward rotation about the Z-axis (yaw), a downward rotation about the Y-axis (pitch) and rightward rotation about the X-axis (roll) are defined as positive. The planes orthogonal to the X, Y and Z rotation axes are respectively the roll, pitch and yaw planes (figure 3).

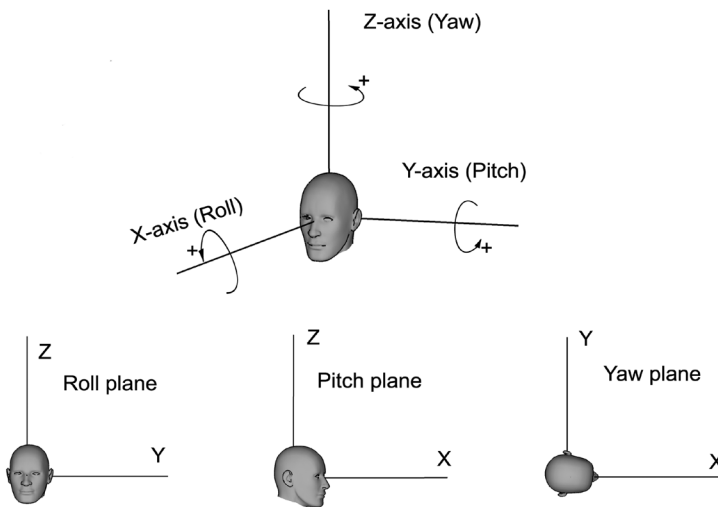


Figure 3: Directions of rotations around the cardinal axes according to the right hand rule. Bottom panels show the yaw, roll and pitch projection planes.

4. Eye movement recordings

Eye movements of both eyes were recorded with 3D scleral search coils (Skalar, Delft, The Netherlands) [4] using a standard 25 kHz two field coil system based on the amplitude detection method of Robinson (Model EMP3020, Skalar Medical, Delft, The Netherlands) [5]. The coil signals were passed through an analogue low-pass filter with cut-off frequency of 500 Hz

and sampled on-line and stored to hard disk at a frequency of 1000 Hz with 16 bit precision (CED system running Spike2 v6, Cambridge Electronic Design, Cambridge).

5. Search coil calibration

Prior to the experiments, the sensitivity and non-orthogonality of direction and torsion coils was verified in-vitro by mounting the coil on a Fick gimbal system placed in the centre of the magnetic field. By rotating the gimbal system about all cardinal axes we verified that all coils used in the experiments were symmetrical for all directions within 2%.

In vivo, the horizontal and vertical signals of both coils were individually calibrated by instructing the subject to successively fixate a series of five targets (central target and a target at 10 degrees left, right, up and down) for five seconds each. Calibration targets were projected onto a translucent screen at 186 cm distance. Post experiment analysis of the calibration data resulted in sensitivity and offset values for the each search coils. These values were then used in the analysis procedures written in Matlab [3]

6. Stimulation

Sinusoidal stimulation

The platform delivered whole-body sinusoidal rotations (1 Hz, $A=4^\circ$) were delivered about the three cardinal axes: The rostral-caudal or vertical axis (yaw), the interaural axis (pitch) and the nasal-occipital axis (roll), and about intermediate horizontal axes incremented in steps of 22.5° between roll and pitch.

Sinusoidal stimuli were delivered in light and darkness. In the light, subjects fixated a continuously lit visual target (a red LED, 2 mm diameter) located 177 cm in front of the subject at eye level (Fig 1C left panel). Head was positioned such that Reid's line was base (the imaginary line connecting the meatus externa with the lower orbital cantus) was within 6 degrees from earth-horizontal). During sinusoidal stimulation in the dark, the visual target was briefly presented (2 s) when the platform was stationary during each interval between two consecutive stimuli. To avoid spontaneous eye movements during the stimulation, subjects were instructed to fixate the imaginary location of the space fixed target during sinusoidal stimulation after the target had been switched off just prior to motion onset. We verified that the type of instruction mainly reduced the eye movements made in darkness, and had only a small effect on gain (< 10%). This variability occurred in all components (horizontal, vertical and torsion) simultaneously.

Impulse stimulation

Short duration whole body impulses were delivered in a dimly lit environment. The only visible stimulus available to the subject was a visual target located at 177 cm in front of the

subject at eye level. Each impulse was repeated six times and delivered in random order and with random timing of motion onset (intervals varied between 2.5 and 3.5 s). The profile of the impulses was a constant acceleration of $100^{\circ}\cdot\text{s}^{-2}$ during the first 100 ms of the impulse, followed by a gradual linear decrease in acceleration. This stimulus resulted in a linear increase in velocity reaching a velocity of $10^{\circ}\cdot\text{s}^{-1}$ after 100 ms. Aberrant head movements during vestibular stimulation measured by the angular rate and linear acceleration devices were less than 4% of stimulus amplitude. Peak velocity of the eye movements in response to these impulses was 100 times above the noise level of the coil signals.

7. Data analysis

Coil signals were converted into Fick angles and then expressed as rotation vectors [6, 7]. From the fixation data of the target straight ahead we determined the misalignment of the coil in the eye relative to the orthogonal primary magnetic field coils. Signals were corrected for this offset misalignment by three-dimensional counter rotation. It was also verified that no coil slippage had occurred during the experiment by verifying the position output during fixation of the target prior to each motion onset. To express 3D eye movements in the velocity domain, we converted rotation vector data back into angular velocity. Before conversion of rotation vector to angular velocity, we smoothed the data by zero-phase with a forward and reverse digital filter with a 20-point Gaussian window (length 20 ms).

8. Sinusoidal responses

Gain

The gain of each component and 3D eye velocity gain was calculated by fitting a sinusoid with a frequency equal to the platform frequency through the horizontal, vertical and torsion angular velocity components. The gain for each component defined as the ratio between eye component peak velocity and platform peak velocity was calculated separately for each eye.

Misalignment

The misalignment between the 3D eye velocity axis and head velocity axis was calculated using the approach of Aw and colleagues [8, 9] From the scalar product of two vectors the misalignment was calculated as the instantaneous angle in three dimensions between the inverse of the eye velocity axis and the head velocity axis. The 3D angular velocity gain and misalignment for each azimuthal orientation were compared to the gain and misalignment predicted from vector summation of the 0° (roll) and 90° (pitch) azimuth components [10]. From this vector summation it follows that when velocity gains for roll and pitch are equal, the orientation of the eye rotation axis aligns with the head rotation axis, when the two are

different, the maximum deviation between stimulus and eye rotation axis is expected at 45° azimuth.

9. Impulse responses

Left and right eye data traces of six presentations for each motion direction were separately analysed. Because left and right eye values were almost identical, the data from left and right eye were averaged to determine the gain of eye velocity in response to impulse stimulation. All traces were individually inspected on the computer screen. When the subject made a blink or saccade during the impulse that trace was manually discarded. Angular velocity components (N=5 to 6) during the first 100 ms after onset of the movement were averaged in time bins of 20 ms (providing an effective low pass filtering) and plotted as function of platform velocity [11, 12].

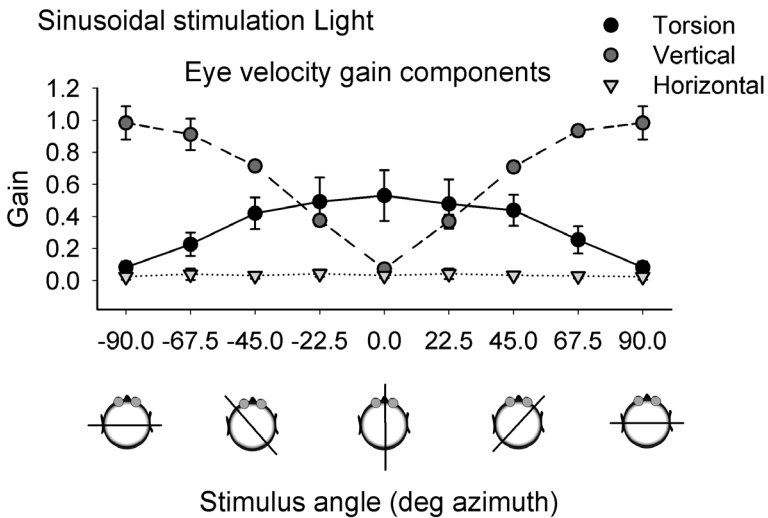


Figure 4: Mean gain of the horizontal, vertical and torsion eye velocity components. Results of horizontal axis sinusoidal stimulation for all tested horizontal stimulus axes averaged over all subjects (N=6) in the light. Cartoons underneath give a top view of the orientation of the stimulus axis with respect to the head.

OUTCOME AND REPRESENTATIVE RESULTS

Sinusoidal stimulation light

Figure 4 (top panel) shows for the control group the mean gain of the horizontal, vertical and torsion angular velocity components for all tested sinusoidal stimulations in the horizontal plane in the light. Torsion was maximal at 0° azimuth, whereas vertical had its maximum at

90°. Figure 5 shows the 3D eye velocity gain in the light. Gain varied between 0.99 ± 0.12 (pitch) and 0.54 ± 0.16 (roll). The measured data closely correspond to the predicted values calculated from the vector sum of torsion and vertical components (dashed line of Figure 5).

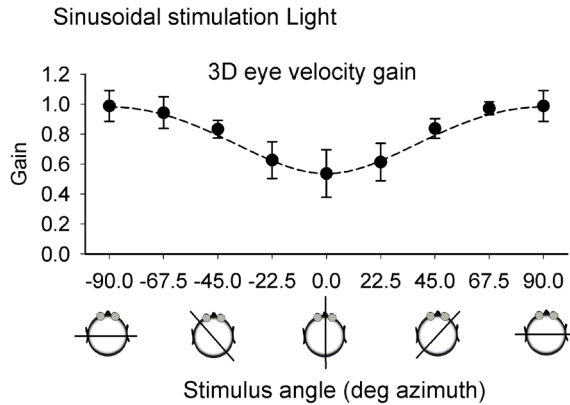


Figure 5: Mean 3D eye velocity gain for all tested horizontal stimulus axes averaged over all subjects (N=6) in the light. Dashed line is the vector eye velocity gain response predicted from the vertical and torsion components.

Cartoons underneath give a top view of the orientation of the stimulus axis with respect to the head.

The mean misalignment between stimulus and response axis averaged over six subjects is shown in Figure 6. In the light misalignment between stimulus and response axis was smallest (5.25°) during pitch and gradually increased towards roll until the orientation of the

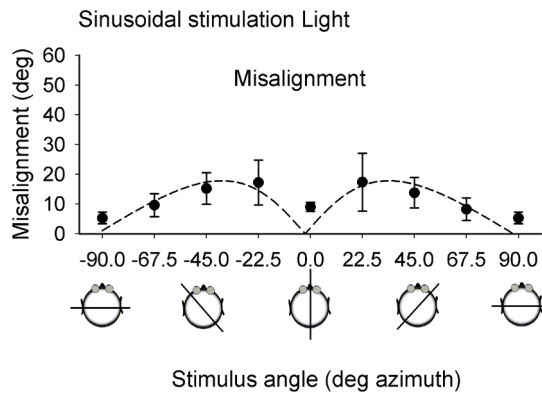


Figure 6: Misalignment of the response axis with respect to the stimulus axis during sinusoidal stimulation in the light. The dashed line in the lower panel represents the predicted misalignment calculated from the vector sum of only vertical and torsion eye velocity components in response to pure pitch and pure roll stimulation, respectively. Error bars indicate one standard deviation.

stimulus axis was oriented at 22.5° azimuth (maximum misalignment: 17.33°) and decreased towards the roll axis. These values for each horizontal stimulus angle correspond closely to what one would predict from linear vector summation of roll and pitch contributions (dashed line in figure 6).

Sinusoidal stimulation darkness

In darkness the maximum gain of both the vertical and torsion components was significantly lower (t-test $P < 0.001$) than in the light (vertical: 0.72 ± 0.19 torsion: 0.37 ± 0.09) (figure 7). Also the 3D eye velocity gain was significantly (t-test $P < 0.001$) lower than in the light (figure 8).

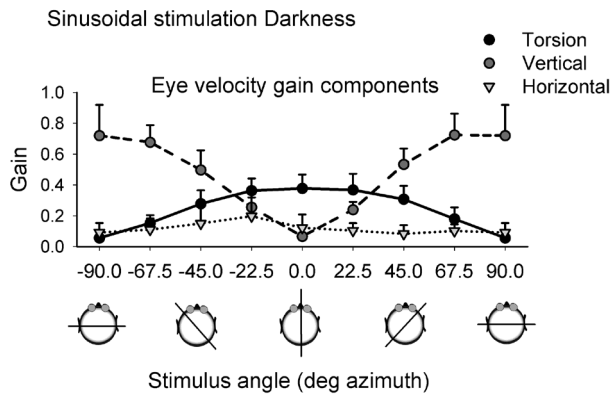


Figure 7: Mean gain of the horizontal, vertical and torsion eye velocity components. Results of horizontal axis sinusoidal stimulation for all tested horizontal stimulus axes averaged over all subjects (N=6) in darkness. Cartoons underneath give a top view of the orientation of the stimulus axis with respect to the head.

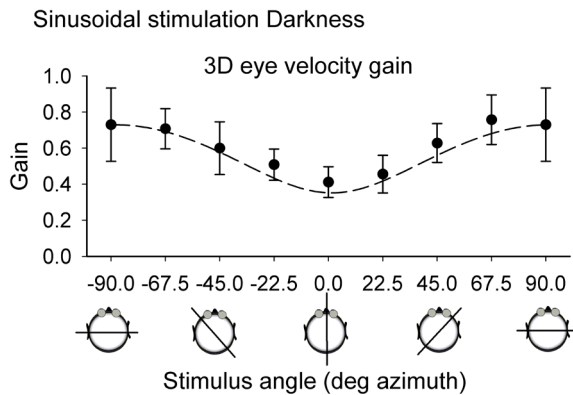


Figure 8: Mean 3D eye velocity gain for all tested horizontal stimulus axes averaged over all subjects (N=6) in darkness. Dashed line is the vector eye velocity gain response predicted from the vertical and torsion components.

Gain was slightly higher than predicted from the vertical and torsion components alone (dashed line in figure 8). In the dark the misalignment was minimal at 90° (pitch) and gradually increased to a peak around the 0° axis (roll). Due to the presence of a small horizontal component, the pattern of misalignment in the dark did not correspond to what one would predict from linear vector summation of only roll and pitch components (see figure 9).

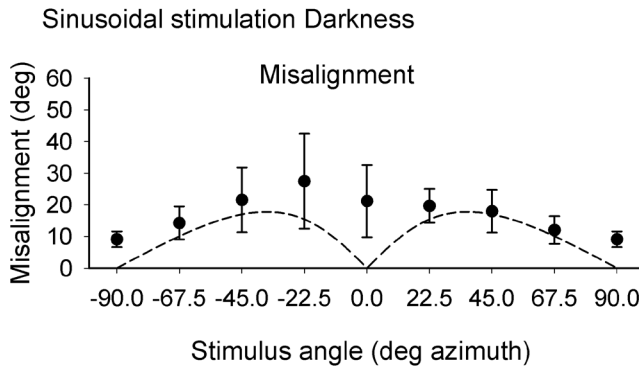


Figure 9: Misalignment of the response axis with respect to the stimulus axis during sinusoidal stimulation in darkness. The dashed line in the lower panel represents the predicted misalignment calculated from the vector sum of only vertical and torsion eye velocity components in response to pure pitch and pure roll stimulation, respectively. Error bars indicate one standard deviation

Impulse stimulation

Whole body impulses about the interaural axis (pitch) resulted in near unity gain for head up and a gain about 0.8 for head down impulses. Differences were significant ($P < 0.05$).

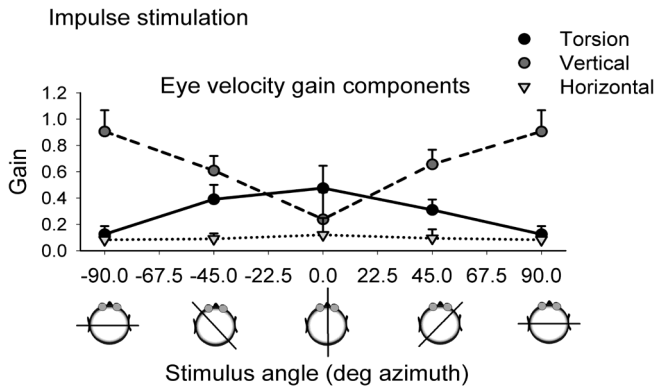


Figure 10: Mean gain of the horizontal, vertical and torsion eye velocity components in response to horizontal axis impulse stimulation. Responses are given for horizontal stimulus axes at 45 degree intervals averaged over all subjects ($N = 6$).

Horizontal, vertical and torsional gain components during impulse stimulation are shown in figure 10. Maximum mean gain for the vertical component alone was 0.85 for pitch (90° azimuth). Maximum gain for torsion was 0.42 for roll (0° azimuth). Vector gain is shown in figure 11. 3D eye velocity gain varied between 1.04 ± 0.18 for pitch to 0.52 ± 0.16 for roll. Misalignment varied between $28.2^\circ \pm 0.18$ for roll, to $11.53^\circ \pm 0.51$ for pitch.

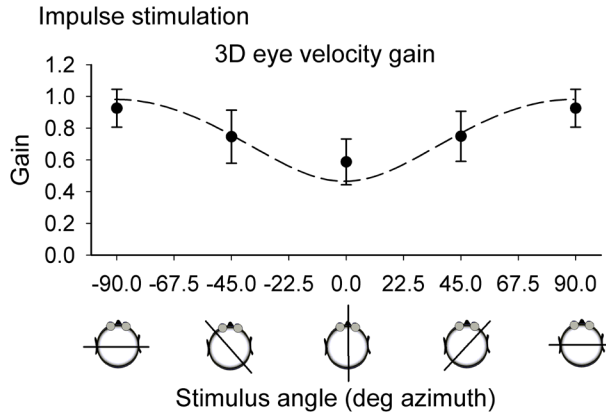


Figure 11: Mean 3D eye velocity gain for all tested horizontal stimulus axes averaged over all subjects (N=6) during impulse stimulation. Dashed line is the vector eye velocity gain response predicted from the vertical and torsion components.

In conclusion, although impulse stimulation causes only a very brief (100 ms) disruption of visual information, the gain and misalignment (figure 12) of eye movements have

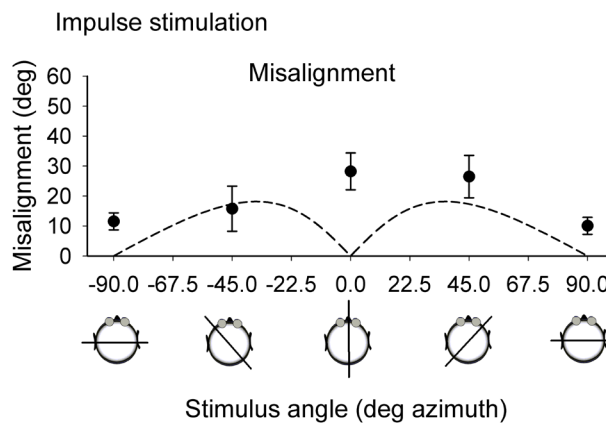


Figure 12: Misalignment of the response axis with respect to the stimulus axis during impulse stimulation. The dashed line in the lower panel represents the predicted misalignment calculated from the vector sum of only vertical and torsion eye velocity components in response to pure pitch and pure roll stimulation, respectively. Error bars indicate one standard deviation

a qualitatively similar pattern as those in response to sinusoidal stimulation in darkness. In both instances the largest misalignment between 3D head and eye rotation axis occurs during roll stimulation.

PATIENTS

3D VOR in non-operated patients

Figure 13 shows the location and the size of the tumor on MRI scans for the three non-operated subjects (see also table 1 in method section). The tumor was in all three cases on the right sided. Subjective complaints of dizziness of these three subjects varied. Subject N1 had an intra-canalicular tumor with the smallest size. He presented himself with unilateral hearing problems and no complaints of vertigo. Subject N2 and N3 did report complaints of vertigo, although neither had complete disorientation problems or vegetative problems.

Figure 14 shows eye position traces for the three non-operated subjects in response to sinusoidal stimulation about a horizontal axis 45° azimuth. Ideally, this stimulus evokes only a combination of vertical and torsional eye movement components and no horizontal eye movements. During stimulation in the light there were few signs of horizontal ocular drift in

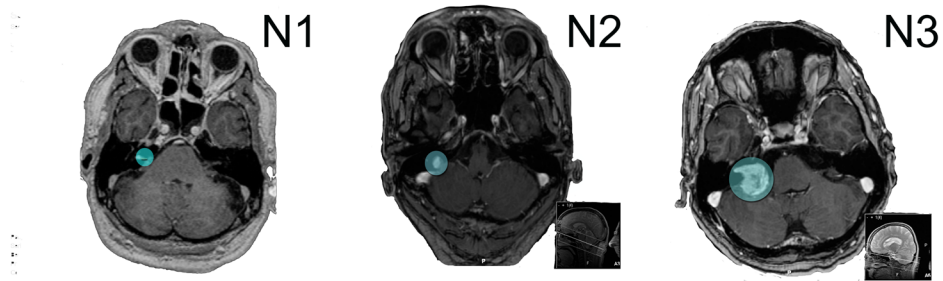


Figure 13: MRI-scans of three patients with untreated Schwannoma's. The Schwannoma is indicated in each scan by the circle.

Table 1: Relevant clinical findings of the six patients who participated in the experiments. The unilateral hearing loss described here was before any therapy and expressed in Fi = Flechter index (mean hearing loss of 500, 1000 and 2000 Hz).

| Subject | Gender | Age (year) | Side of tumor | Tumor size (mm) | Unilateral hearing loss (Fi dB) | Therapy |
|---------|--------|------------|---------------|-----------------|---------------------------------|----------------|
| N1 | male | 61 | right | 4 | 35 | wait and watch |
| N2 | male | 64 | right | 14 | 43 | wait and watch |
| N3 | male | 55 | right | 22 | complete | wait and watch |

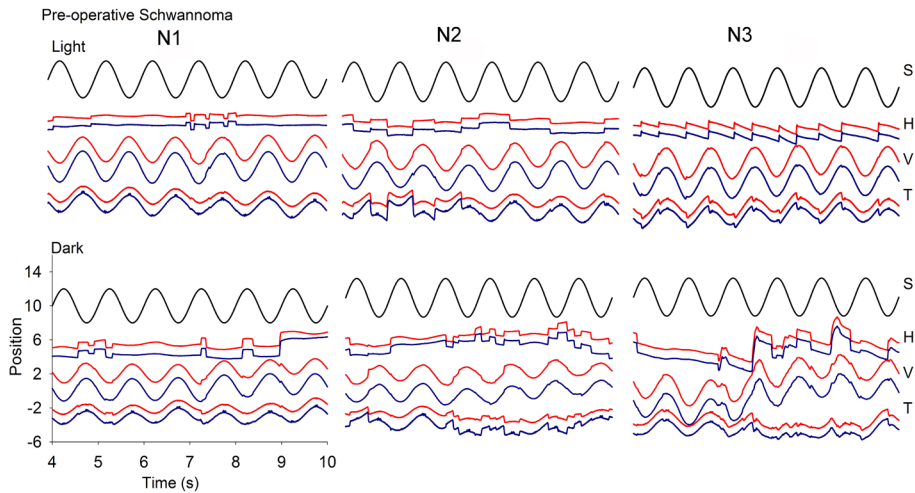


Figure 14: Examples of time series for the three non-operated subjects in response to sinusoidal stimulation about a horizontal axis 45° azimuth. Upper panel row: Light, Lower panel row: Dark. In each panel are plotted the right (red) and left (blue) eye horizontal (H), vertical (V) and torsional (T) eye positions. In this and all subsequent figures eye positions and velocities are expressed in a right-handed, head-fixed coordinate system. In this system clockwise (CW), down and counterclockwise (CCW) eye rotations viewed from the perspective of the subject are defined as positive values. Stimulus motion is indicated in each panel by the top black line.

subjects N1 and N2, whereas subject N3 had a horizontal leftward nystagmus (slow phase to the right) and a CW torsional nystagmus (slow phase CCW). In the dark subject N1 had little or no drift, whereas for subjects N2 and N3 instabilities appeared in the horizontal, vertical and torsional traces. The only weak sign of instability in subject N1 is in torsion, where small corrective torsional saccades were observed that were consistently in CW direction. In subjects N2 and N3 torsional instabilities were larger.

To demonstrate the changes in 3D stability in Schwannoma patients we present for subject N2 in figure 15 the horizontal, vertical and torsional eye velocity gain components (top panel), the 3D gain (centre panel) and misalignment (lower panel). The changes in gain of the individual components have a direct impact on 3D vectorial eye velocity gain and misalignment. The close correspondence between predicted and measured 3D eye velocity and alignment as found in the control subjects no longer holds for Schwannoma patients.

In particular in subjects N2 and N3 the 3D eye velocity gain in darkness was affected. In subject N2 the overall 3D eye velocity gain was lower, which can be explained by the decrease in torsional gain (figure 15). Also in subject N3 the torsion component was affected. His torsional eye velocity gains responses were asymmetric. This resulted in a up to two-fold increase in misalignment.

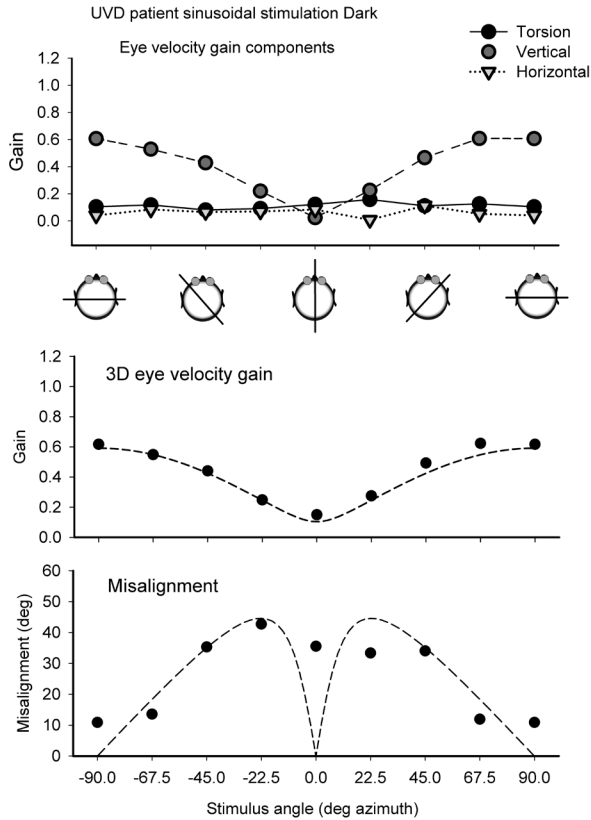


Figure 15: Gain and misalignment of 3D VOR of UVD subject N2 during horizontal axis sinusoidal stimulation in the dark. Top panel: Gain of the horizontal, vertical and torsional eye velocity components. Cartoons underneath give a top view of the orientation of the stimulus axis with respect to the head. Centre panel: Mean 3D eye velocity at each tested stimulus axis orientation. The dashed line represents the vector eye velocity gain response predicted from the vertical and torsional components. Lower panel: Misalignment of the response axis with respect to the stimulus axis.

The dashed line in the lower panel represents the predicted misalignment calculated from the vector sum of vertical and torsional eye velocity components.

Notice the low gain for torsion in the top panel and large misalignment in the lower panel.

DISCUSSION

This paper describes a method to accurately measure 3d angular VOR in response to whole body rotations in humans. The advantage of the method is that it gives quantitative information about gain and misalignment of 3D angular VOR in all three dimensions. The method is useful for fundamental research and has also potential clinical value e.g. for testing patients with vertical canal problems or patients with ill-understood central vestibular problems. Another advantage of the device is the ability to test translational VOR responses

[1] Disadvantages of the system are: 1) the cost aspects in terms of equipment, space and personnel: the current machine was developed for pilot training purposes. 2) Discomfort during the measurements. Accurate eye movement recordings are based on the scleral search coil technique. Due to its superior signal to noise ratio and absence of slip compared to head-mounted infrared camera systems, this is still the only technique to measure VOR responses in humans with high precision. Improvements in slip-free infrared video bases eye tracker systems are badly needed.

The data show that in healthy human subjects the quality of the 3D VOR response varies not only in terms of gain, but also in terms of alignment of the eye rotation axis with head rotation axis. As was also found in other studies on 3D VOR dynamics, there is a high gain for horizontal and vertical eye movements compared to torsion. This general property has also been described in lateral eyed animals (rabbits: [13] and frontal eyed animals (monkeys: [14] and humans [15] [16] [9] [4]. The gain of the VOR for stimulation about the cardinal axes is in close agreement with previous studies in humans [8, 17, 18]. There was a small but significant higher gain for pitch head up, compared to pitch head down impulses. This is possibly related to the fact that our impulses were whole body movements in contrast to previous studies that involved stimulation of the neck [19, 20].

The second main finding is the systematic variation in misalignment between stimulus and response axis. In the light misalignment has minima at roll and pitch, and its maxima at plus and minus 45° azimuth. Quantitatively, the misalignment angles in our study are similar to those reported in monkeys [21, 22]. In the dark and during impulse stimulation there is a twofold increase in misalignment compared to sinusoidal stimulation in the light over the whole range of tested axes. Under dark and impulse stimulus conditions stimulation about the roll axis results in the largest misalignment. The relatively large misalignment during roll axis stimulation in the dark has its origin in a small but consistent horizontal eye movement component that has in combination with low gain for torsion a relatively large contribution to the vector gain [3].

Although subjects viewed a fixation target during impulse stimulation, misalignments were not significantly different (t-test $P > 0.05$) from the sinusoidal stimulation in darkness condition. This means that the relatively mild impulse that we used, briefly interferes with visual fixation. As a result of this the response is similar to sinusoidal stimulation in darkness.

The sensitivity of the method is demonstrated in a small group of patients with unilateral Schwannoma's. In this non-operated group that was on a wait and watch policy, subjective problems were variable and relatively mild in the light. Nevertheless, with this method we were able to show that in the dark the proper 3D gain and alignment of the 3D VOR is impaired. Although the group is very small, our data suggest a correlation between tumor size and severity of 3D VOR abnormalities.

REFERENCES

1. Houben, M.M.J., et al., Angular and linear vestibulo-ocular responses in humans. *Ann NY Acad Sci*, 2005. 1039: p. 68-80.
2. Collewijn, H., et al., Human ocular counterroll: assessment of static and dynamic properties from electromagnetic scleral coil recordings. *Exp Brain Res*, 1985. 59(1): p. 185-96.
3. Goumans, J., et al., Peaks and troughs of three-dimensional vestibulo-ocular reflex in humans. *Journal of the Association for Research in Otolaryngology: JARO*, 2010. 11(3): p. 383-93.
4. Ferman, L., et al., Human gaze stability in the horizontal, vertical and torsional direction during voluntary head movements, evaluated with a three-dimensional scleral induction coil technique. *Vision Res*, 1987. 27(5): p. 811-28.
5. Robinson, D.A., A Method Of Measuring Eye Movement Using A Scleral Search Coil In A Magnetic Field. *IEEE Trans Biomed Eng*, 1963. 10: p. 137-45.
6. Hausteijn, W., Considerations on Listing's Law and the primary position by means of a matrix description of eye position control. *Biol Cybern*, 1989. 60(6): p. 411-20.
7. Haslwanter, T. and S.T. Moore, A theoretical analysis of three-dimensional eye position measurement using polar cross-correlation. *IEEE Trans Biomed Eng*, 1995. 42(11): p. 1053-61.
8. Aw, S.T., et al., Three-dimensional vector analysis of the human vestibuloocular reflex in response to high-acceleration head rotations. II. responses in subjects with unilateral vestibular loss and selective semicircular canal occlusion. *J Neurophysiol*, 1996. 76(6): p. 4021-30.
9. Aw, S.T., et al., Three-dimensional vector analysis of the human vestibuloocular reflex in response to high-acceleration head rotations. I. Responses in normal subjects. *J Neurophysiol*, 1996. 76(6): p. 4009-20.
10. Crawford, J.D. and T. Vilis, Axes of eye rotation and Listing's law during rotations of the head. *Journal of neurophysiology*, 1991. 65(3): p. 407-23.
11. Tabak, S., H. Collewijn, and L.J. Boumans, Deviation of the subjective vertical in long-standing unilateral vestibular loss. *Acta Otolaryngol*, 1997. 117(1): p. 1-6.
12. Tabak, S., et al., Gain and delay of human vestibulo-ocular reflexes to oscillation and steps of the head by a reactive torque helmet. II. Vestibular-deficient subjects. *Acta Otolaryngol*, 1997. 117(6): p. 796-809.
13. Van der Steen, J. and H. Collewijn, Ocular stability in the horizontal, frontal and sagittal planes in the rabbit. *Exp Brain Res*, 1984. 56(2): p. 263-74.
14. Seidman, S.H., et al., Dynamic properties of the human vestibulo-ocular reflex during head rotations in roll. *Vision Res*, 1995. 35(5): p. 679-89.
15. Seidman, S.H. and R.J. Leigh, The human torsional vestibulo-ocular reflex during rotation about an earth-vertical axis. *Brain Res*, 1989. 504(2): p. 264-8.
16. Tweed, D., et al., Rotational kinematics of the human vestibuloocular reflex. I. Gain matrices. *J Neurophysiol*, 1994. 72(5): p. 2467-79.
17. Tabak, S. and H. Collewijn, Human vestibulo-ocular responses to rapid, helmet-driven head movements. *Exp Brain Res*, 1994. 102(2): p. 367-78.
18. Paige, G.D., Linear vestibulo-ocular reflex (LVOR) and modulation by vergence. *Acta Otolaryngol Suppl*, 1991. 481: p. 282-6.
19. Halmagyi, G.M., et al., Impulsive testing of individual semicircular canal function. *Ann NY Acad Sci*, 2001. 942: p. 192-200.
20. Tabak, S. and H. Collewijn, Evaluation of the human vestibulo-ocular reflex at high frequencies with a helmet, driven by reactive torque. *Acta Otolaryngol Suppl*, 1995. 520 Pt 1: p. 4-8.

21. Crawford, J.D. and T. Vilis, Axes of eye rotation and Listing's law during rotations of the head. *J Neurophysiol*, 1991. 65(3): p. 407-23.
22. Migliaccio, A.A., et al., The three-dimensional vestibulo-ocular reflex evoked by high-acceleration rotations in the squirrel monkey. *Exp Brain Res*, 2004. 159(4): p. 433-46.



5

Scaling of compensatory eye movements during translations: virtual versus real depth

Joyce Dits¹, W. Michael King² and Johannes van der Steen¹.

¹ Department of Neuroscience, Erasmus MC, Rotterdam, The Netherlands.

² Department of Otolaryngology, University of Michigan Medical Center, Ann Arbor, MI.

Adapted from:

Neuroscience. 2013 Aug; 246: 73-81.

ABSTRACT

Vestibulo-ocular reflexes are the fastest compensatory reflex systems. One of these is the translational vestibulo-ocular reflex (TVOR) which stabilizes gaze at a given fixation point during whole body translations. For a proper response of the TVOR the eyes have to counter rotate in the head with a velocity that is inversely scaled to viewing distance of the target. It is generally assumed that scaling of the TVOR is automatically coupled to vergence angle at the brainstem level. However, different lines of evidence also argue that in humans scaling of the TVOR also depends on a mechanism that pre-sets gain on a priori knowledge of target distance.

To discriminate between these two possibilities we used a real target paradigm with vergence angle coupled to distance and a virtual target paradigm with vergence angle dissociated from target distance. We compared TVOR responses in six subjects who underwent lateral sinusoidal whole-body translations at 1 and 2 Hz. Real targets varied between distance of 50 and 22.4 cm in front of the subjects, whereas the virtual targets consisting of a green and red LED were physically located at 50 cm from the subject. Red and green LED's were dichoptically viewed. By shifting the red LED relative to the green LED we created a range of virtual viewing distances where vergence angle changed but the ideal kinematic eye velocity was always the same. Eye velocity data recorded with virtual targets were compared to eye velocity data recorded with real targets. We also used flashing targets (flash frequency 1Hz, duration 5 ms). During the real, continuous visible targets condition scaling of compensatory eye velocity with vergence angle was nearly perfect. During viewing of virtual targets, and with flashed targets compensatory eye velocity only weakly correlated to vergence angle, indicating that vergence angle is only partially coupled to compensatory eye velocity during translation. Our data suggest that in humans vergence angle as a measure of target distance estimation has only limited use for automatic TVOR scaling.

INTRODUCTION

In primates, gaze stabilization during translational head movements is mediated by vestibular and visual mechanisms, resulting in compensatory eye movements that minimize retinal image motion across the fovea. The translational vestibulo-ocular reflex (TVOR) responds to linear accelerations sensed by the otoliths of the vestibular system: neural signals relayed by the vestibular nuclei and oculomotor nuclei produce compensatory eye movements at very short latency. The relative contribution of vestibular and visual sensory inputs to gaze stabilization depends on the frequency or acceleration of head motion. Visual systems are mainly active at frequencies up to 1 Hz, whereas the contribution of the translational vestibulo-ocular reflex (TVOR) becomes significant at 1 Hz and increases with frequency [1].

In contrast to the angular VOR, the TVOR gain in the dark without a target is quite low [2]. Presumably, this occurs because the response of the TVOR is viewing distance dependent. Geometry dictates that the amplitude of compensatory eye movements must increase with decreasing viewing distance, which is confirmed by experimental data in humans and non-human primates [1, 3-8].

Many studies claim that vergence angle determines the amplitude of the response [1, 3, 9, 10]. The notion that vergence angle modulates the gain of the TVOR is an attractive hypothesis because vergence angle is directly encoded by neurons located in the brainstem [11, 12] and indirectly by neurons in the vestibular and perihypoglossal nuclei that encode monocular eye position [13, 14]. Findings in favour of an important role for encoded vergence angle include: an increase in TVOR gain after use of prism lenses to dissociate vergence angle from actual target distance [1]; a decrease in gain with inadequate vergence angles [5] scaling of TVOR gain to target distance from the earliest onset of movement during stepwise motion stimuli [9]; and a minor role for monocular visual cues [15].

Although the vergence angle hypothesis is computationally attractive, vergence angle may not directly modulate TVOR gain since other studies in humans describe TVOR gain modulation that cannot be explained solely by vergence angle. Ramat and Zee [5] noticed an increase in gain with a decrease in vergence angle in one of their subjects. Viirre and Demer [16] found a discrepancy between TVOR gain and vergence angle during eccentric rotation up to 2 Hz. These findings suggest that the “gain” setting of the TVOR depends on other cues. For example, Snyder and King (1992) found that anticipation plays an important role in distance scaling. They found scaling to target distance in advance of vergence eye movements a finding that argues against a causal role for vergence angle. Similarly, Clement and Maciel [17] found that target-distance dependent modulation of the angular vestibulo-ocular reflex (AVOR) at 0.8 Hz is more dependent on perceived target distance than on the actual target or fixation distance. It has also been shown that a priori knowledge of the direction of head movement and fixation of a target (head-fixed or earth-fixed) play important roles in gaze stabilization [18, 19]. Furthermore, during predictable motion stimuli, predictive smooth

pursuit eye movements could play a role in target distance dependent TVOR scaling [20, 21]. The TVOR and smooth pursuit system both have foveal dependent responses with similar kinematics and are likely to partially share the same central neural pathways [22]. Other factors that might play a role in scaling TVOR amplitude in relation to target distance are accommodation, motion parallax and visual cues. However, the contribution of these factors has been found less important in humans than in monkey [2, 23]

Recently, it was proposed that an estimate of spatial orientation or internal representation is necessary for perception as well as for the control of reflexive eye movements and postural responses [24]. This implies that scaling of TVOR is not merely a brainstem or cerebellar mediated reflex loop dependent on instantaneous vergence angle, but that its state depends on an internal representation of 3D space built from visual, vestibular and possibly eye position cues related to extraocular proprioception [25, 26]. Thus, an alternative explanation for TVOR scaling is that there is a central representation of a target's spatial location that determines both the vergence angle and the magnitude of the TVOR. In support of this idea, [27] described neurons located in the prearcuate cortex immediately rostral to the frontal eye fields that discharged in relation to vergence eye movements and whose discharge preceded those eye movements by 28 msec. Many of these neurons were also responsive to the visual presentation of a near target prior to any motor response; thus, they encoded a representation of the target's location in depth and could provide a signal to modulate the TVOR. In support of this suggestion, Gamlin and colleagues [28] showed a possible pathway linking the prearcuate cortex to a precerebellar nucleus (nucleus reticularis tegmenti pontis) implicated in the control of voluntary eye movements.

Experimental and theoretical evidence further suggest that different spatial orientation estimates may underlie perception (e.g. target depth) and motor action (e.g., ocular vergence angle) [29, 30]. Also for the TVOR there may not be a tight link between depth perception and binocular eye position information, as vergence eye movements provoked by visual disparity do not need to be accompanied by depth perception [31] [32].

In the present study we address the mechanisms of gaze stabilization during translations in humans. Our aim was to determine the relative contribution of visual, vestibular and eye position cues on the central target representation and its effect on scaling compensatory eye movements.

METHODS

Subjects

Eye movements were recorded from six subjects. Subject 1, male, age 56, is one of the authors (J.S.). The other five subjects (4 males, 1 female, age between 22 and 35 years) were naïve with respect to the goal of the experiment. Written informed consent was obtained from all subjects prior to the experiments. None of the subjects had a history of inner ear pathology or impaired stereoscopic vision (according to the random dot stereo test), and all subjects were able to see the targets clearly. The mean inter-ocular distance of the subjects was 6.5 ± 0.2 cm. Experimental procedures were approved by the Medical Ethical Committee of the Erasmus University Medical Center and adhered to the Declaration of Helsinki for research involving human subjects.

Experimental setup

Visual targets

The experiment was performed in a completely dark room. Visual targets consisted of black-coated 2.3 mm optic fibres, one end of which was connected to a light emitting diode (LED);

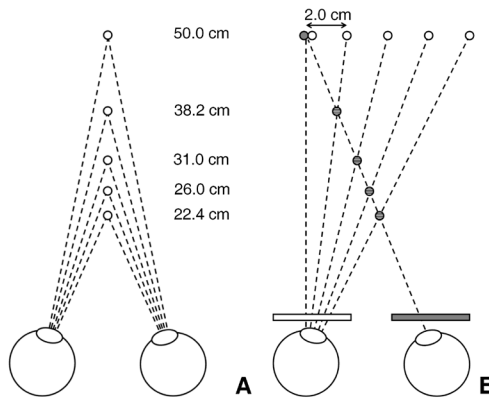


Figure 1: The two real and virtual target paradigms. Panel A shows the real targets that were located at 5 distances from the subject. Panel B shows the ‘virtual targets’; six optic fibre tips (top circles): one green fibre on the left (filled circle) and five red fibres on the right (open circles). These are seen through red and green filters (bottom bars): the left eye could only see the red fibres; the right eye only the green fibre. Only two fibres were switched on at the same time: the green one and one of the red ones. The distance to the intersections of the lines of sight of both eyes (striped circles) was defined as virtual target distance. The target distances of the virtual targets in B matched those of the real targets in A. Note that for the furthest virtual target, the green and red fibre are located at approximately the same position. This target therefore resembles a real target.

the other (open) end pointed towards the observer as a visual target. We used two different kinds of targets: real targets and virtual targets (figure 1).

The real targets were positioned at 22, 26, 31, 38 and 50 cm distance from the centre between the observer's eyes, and were located directly in front of the subject (figure 1A). The virtual target lights were aligned horizontally and perpendicular to straight-ahead gaze at a distance of 50 cm from the observer (figure 1B). These targets consisted of a green light aligned with the left eye and five red lights spaced at 2 cm intervals towards the right of the green target. Virtual targets were shown pairwise (the green light in combination with one of the five red lights). Subjects viewed the paired targets through red-green anaglyphic filters such that each eye saw one of the two lights. The LED targets were arranged in such a way that the vergence angles needed to fuse the virtual targets were identical to the vergence angles needed to fixate the real targets. Thus, when subjects viewed the virtual targets, vergence angles were dissociated from physical target distance allowing us to study the effect of vergence angle independent of target distance. The distance between the observers' eyes and the theoretical interception of the lines of sight of both eyes was defined as virtual fixation distance. The virtual fixation distance thus reflected the vergence angle of the eyes needed to fuse the virtual targets and not the physical location of the targets.

In addition to the continuously illuminated targets, we presented flashing real and virtual targets. These targets had a flash frequency of 1 Hz and a flash duration of 5 ms. These values were chosen based on data from pilot experiments which showed that higher flash frequencies or longer flash durations resulted in higher gains, probably due to an increase in visual feedback. Another advantage of the 1 Hz flash frequency is that during 1 and 2 Hz platform motion the visual target appeared at the same location relative to the platform with each flash. This also minimized the possible predictive effects of storage of planned eye movements in working memory by the subject. To eliminate long-term memory effects we presented the flashing target paradigms prior to the continuous target condition. Target distances were presented in a random order.

Motion stimuli

During the experiment, the subject was seated in a chair on a six degrees of freedom motion platform (FCS-Moog, Nieuw-Vennep, The Netherlands) [33]. The subject's body was securely fastened with a 5-point harness. In addition, a vacuum cushion and an individually moulded bite board were used to completely immobilize the head relative to the platform [33, 34]. The platform delivered sinusoidal sideward whole-body translations at 1 and 2 Hz, with a peak-to-peak amplitude of 5 and 2.5 cm, respectively. The duration of each movement was 20 seconds and contained a fade-in and fade-out period of 2 s (a linear increase/decrease in amplitude).

The motion platform was equipped with a laser device at backside of the platform base aimed at a photocell mounted on the wall. This photocell produced a light intensity related voltage. This voltage level was sampled along with the eye movement data (see below) and enabled us to time the actual delivered motion stimuli with the eye movement responses within a millisecond [33, 34].

Eye movement recordings

Eye movements were recorded with scleral search coils. We used a standard 25-kHz two-field coil system (Model EMP3020; Skalar Medical, Delft, The Netherlands) based on the amplitude detection method by Robinson. The field coils were mounted on the motion platform so the search coils recorded eye position relative to the head. Standard dual coils embedded in a silicone annulus (Skalar Medical, Delft) were inserted in each eye. Before insertion, the eyes were anesthetized with a few drops of oxybuprocain (0.4%) in HCl (pH 4.0). Both coils were pre-calibrated in vitro by mounting them on a gimbal system placed in the center of the magnetic fields. We sampled the coil data at 1000 Hz on a CED system (Cambridge Electronic Design, Cambridge, UK). Subjects were instructed to fixate a series of five targets (central target and a target at 10 degrees left, right, up and down). Targets were back projected onto a translucent screen at 186 cm distance. The subjects fixated each target for ten seconds. Data were stored to a hard disk for further analysis.

Data analysis

Eye movements made to a 5-point calibration pattern were used to transform voltage into Fick angles. After calibration, we digitally smoothed the data by applying a 2-point moving average. After smoothing, saccades were removed using velocity and acceleration (typically $2000^\circ \cdot s^{-2}$) thresholds and a duration criterion (10-185 ms). Eye movement parameters (amplitude and frequency) were obtained by conversion of the data to the frequency domain using a Fast Fourier Transform (FFT). Peak eye velocity was calculated by multiplying the amplitude of the eye movement by the fundamental frequency of the stimulus motion.

To compare data from individual subjects with ideal performance, a computer model was constructed with Matlab's SimuLink to compute the eye velocity needed to accurately compensate for head translation for each of the virtual and real target positions. Next, for each subject, a linear regression of eye velocity as a function of vergence angle was performed for each of the real or virtual experimental conditions (real or virtual targets viewed continuously or strobed X 2 frequencies = 8 conditions). For statistical analysis, data were pooled across all subjects for each condition so as to compare group performance in each paradigm.

RESULTS

Real and virtual target paradigms were tested under two conditions: continuous lighting and flashing of the targets. Examples of raw eye movement recordings under the different

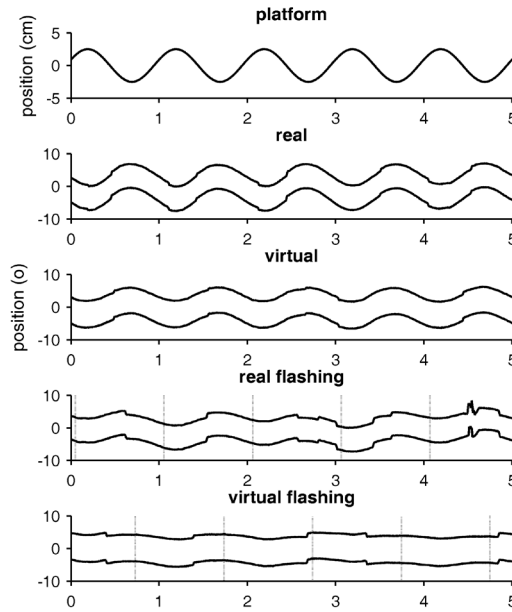


Figure 2: Example (subject 2) of platform position (upper panel), and eye movements (lower four panels) recorded with the search coil system, under the four different target conditions: real continuous, virtual continuous, real flashed and virtual flashed. Upper traces in each panel represent left eye positions, the lower traces right eye positions. Dashed vertical lines indicate the moments in time at which the flashes occurred. Upward deflections: rightward horizontal eye movements.

conditions are shown in figure 2. For both real and virtual target paradigms there were major differences in response amplitude in the continuous and flashing target conditions. The response amplitude to the flashing targets was always smaller than to the continuously illuminated targets.

The other major difference in eye movement response between the real and virtual targets was their dependency of viewing distance. The real targets had response amplitudes that were directly related to viewing distance. This relation is shown in the top panel of figure 3. In this plot vergence angle is plotted on the y-axis (zero vergence at top), whereas the gaze angles of the left (blue) and right (red) eyes are plotted on the X-axis. The panel shows an increase in gaze amplitude and vergence angle as a function of viewing distance.

Gaze trajectories become larger for near viewing distances, consistent with the geometrical requirement for keeping the eyes on target during the linear translations.

The lower panel of figure 3 shows an example a gaze vergence plot of eye movements in response to the targets at all presented virtual distances. For any virtual distance, the gaze amplitude of the right and left eye remained the same regardless of the vergence angle required to fuse the virtual target by shifting the left eye (blue traces) to the right.

To determine the relationship between peak eye velocity and real and virtual viewing distance, we plotted for each subject's eye velocity as a function of vergence and fitted the data with a linear regression. The slope of this regression line estimates the extent to which eye velocity is related to vergence angle.

Figure 4 shows the peak eye velocity as a function of vergence angle. The solid line in each panel shows the expected eye velocity for the continuously viewed real target condition. The

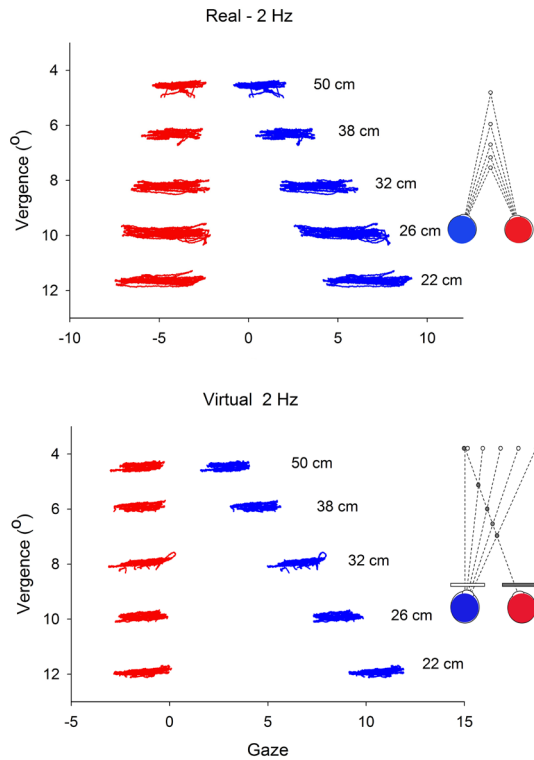


Figure 3: Gaze versus vergence angle during whole-body translations at 2 Hz. In this plot vergence angle is plotted on the y-axis (zero vergence at top), whereas the gaze positions of the left (blue) and right (red) eyes are plotted on the X-axis. The panel shows that for real targets (upper panel) there is an increase in gaze amplitude and vergence angle as a function of vergence. Gaze trajectories become larger for near viewing distances, consistent with the geometrical requirement for keeping the eyes on target during the linear translations.

slope of this line, $4.92^\circ/\text{s}$ per degree of vergence represents the expected ideal relationship between eye velocity and vergence angle. The horizontal dotted line at $35^\circ/\text{s}$ is the expected eye velocity for the virtual target condition. Since the virtual targets are all located at the same distance from the subject, there is no effect of vergence angle on the expected eye velocity (slope=zero).

As expected, under continuously viewed real target conditions, eye velocity scaled well with vergence angle (square symbols in the upper panels of figure 4). The slope of the pooled regression line was $2.8^\circ/\text{s}$ per degree of vergence for 1 Hz translations (upper left panel) and was highly significant ($p < 0.001$). For 2 Hz translations, the slope was reduced ($1.9^\circ/\text{s}$ per degree of vergence) but still highly significant ($p < 0.001$). In contrast, despite a similar range of vergence angles, there was a much weaker relationship between eye velocity and

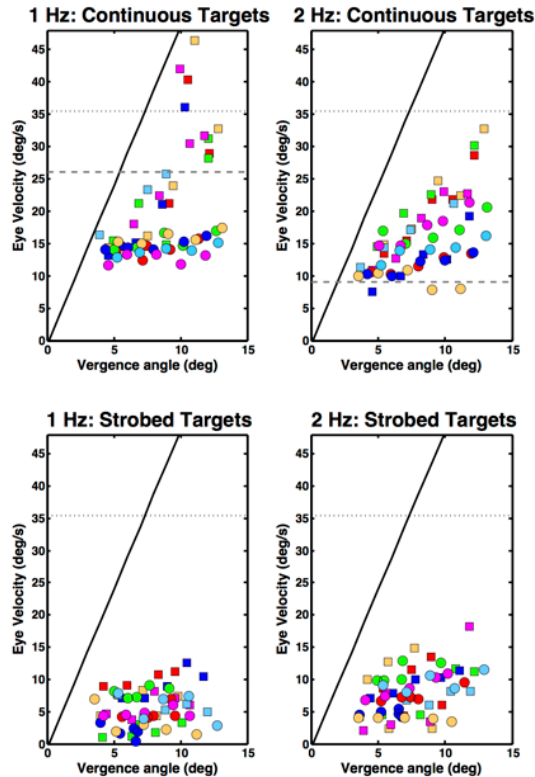


Figure 4: Peak eye velocity as a function of vergence angle during 1 and 2 Hz sinusoidal translations (left and right panels respectively). The solid line in each panel shows the expected eye velocity for the continuously viewed real target condition. The slope of this line, $4.92^\circ/\text{s}$ per degree of vergence represents the expected ideal relationship between eye velocity and vergence angle. The dashed line is the expected eye velocity for the virtual target condition. Data from individual subjects are indicated with different colours. Squares: real targets, Circles: virtual targets. Upper panels: continuously lit targets, Lower panels: strobed targets.

vergence for continuously viewed virtual targets at either frequency. For 1 and 2 Hz translations, the slopes of the pooled regressions were statistically significant ($p < 0.01$) but significantly smaller (1 Hz: $0.27^\circ/s$ per degree of vergence; 2Hz: $0.58^\circ/s$ per degree of vergence) than the slopes for real targets (circular symbols). When the real targets were flashed, the slopes of the regression lines were further reduced (figure 4, lower panels) and were not significantly different from zero ($p < 0.01$, see table 1) for either real or virtual targets at either frequency.

Table 1

| | 1 Hz | | | | | 2 Hz | | | | |
|------------------------|------|-----------|-------|-------|-------|-----------|-------|-------|-------|--|
| | N | Intercept | Slope | r^2 | p | Intercept | Slope | r^2 | p | |
| Real Targets | | | | | | | | | | |
| Continuous | 6 | 0.24 | 2.8 | 0.61 | 0.000 | 2.3 | 1.9 | 0.69 | 0.000 | |
| Strobed | 6 | 3.4 | 0.38 | 0.09 | 0.120 | 2.6 | 0.69 | 0.18 | 0.020 | |
| Virtual Targets | | | | | | | | | | |
| Continuous | 6 | 12.1 | 0.28 | 0.27 | 0.003 | 8.7 | 0.58 | 0.23 | 0.008 | |
| Strobed | 6 | 4.9 | -0.02 | 0.0 | 0.924 | 4.1 | 0.47 | 0.16 | 0.028 | |

DISCUSSION

Our results show that during translational passive whole body motion the gain of horizontal compensatory eye movements is proportional to target distance. Eye velocity scales with vergence angle for real targets when there is continuous visual feedback, but this relationship is weakened when vergence angle is changed without changing target distance and breaks down completely when targets are flashed so as to eliminate visual feedback.

TVOR scaling and vergence angle

In several studies it was concluded that the amplitude of TVOR compensatory eye movements scale with target distance and that this scaling is mediated by vergence angle. Paige et al. [4] tried to isolate the TVOR from visual cues by using imagined targets. Initially, a target was seen during sinusoidal self-motion, then it disappeared and subjects were asked to continue to fixate the target in their imagination. During fixation of these imagined targets, vergence angle as well as the gain of the eye movements decreased considerably. They concluded that the change in eye speed was the result of the decrease in vergence angle. However, it is also plausible that in this study decreases in both vergence and eye speed had the same cause: an inability to fixate the imagined target or to accurately remember its spatial location. In agreement with Paige [1], Wei et al. [10] using high frequency stimulation and Ramat et

al. [5] concluded that vergence angle was the most important factor contributing to TVOR scaling. However, in the latter study, other possibilities could not be excluded. Indeed, in a later report, Ramat et al. [18] emphasized a possible role of cognitive factors in determining TVOR eye velocity.

The new aspect of our study is that we used a virtual target paradigm that dissociated vergence from other target distance cues in order to directly test the hypothesis that vergence angle determines TVOR eye velocity scaling. The virtual target paradigm is different from two other widely used target arrangements, head-fixed (HF) and earth fixed (EF) [1], that either promoted the TVOR (EF) or required its suppression (HF). The virtual target paradigm enables us to dissociate the magnitude of the vergence angle from the kinematical correct TVOR amplitude; TVOR eye speed should not be scaled in relation to vergence angle, but is also not suppressed. We believe this paradigm is fundamentally different since complete suppression of the TVOR could be due to a mechanism other than modulation of TVOR gain.

The results of our experiment show that there is only a weak correlation of vergence angle to scaling of the TVOR. Furthermore, the data during fixation of flashing virtual targets, suggest that in contrast to monkeys, vergence angle in humans is not nearly as strong a determinant of eye velocity as in monkeys [9].

Our data also agree very well with the findings of Ramat and Zee [5] who used side-to-side velocity steps (heave). Steps have a broad frequency spectrum, and the fact that Ramat

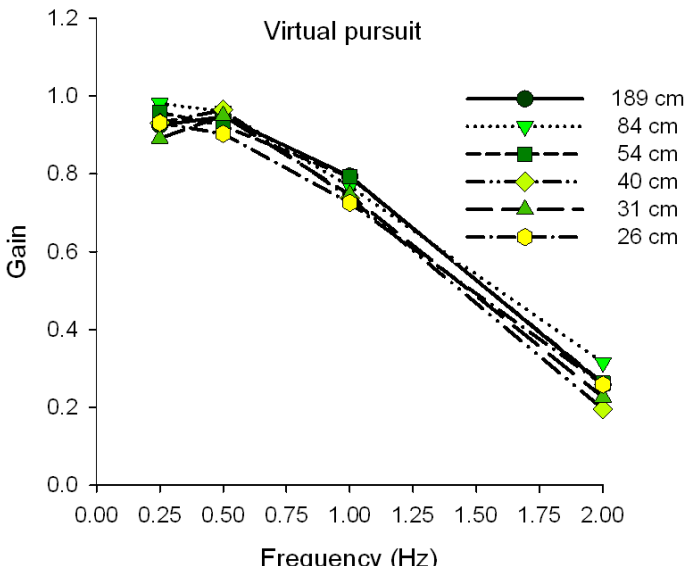


Figure 5: Smooth pursuit gain as function of sinusoidal stimulation frequency and viewing distance. Frequency range was between 0.25 and 2.0 Hz. Viewing distance varied between 189 and 26 cm. Smooth pursuit gain decreases as a function of frequency is not modulated by target distance or vergence angle.

and Zee found only partial compensation is a further argument in favour of a weak vergence angle related TVOR scaling across the whole frequency spectrum.

Paige et al. [4] studied visuo-vestibular interactions using two target paradigms: earth-fixed (EF) and head-fixed (HF) targets, and compared compensatory eye movements when real or imagined targets were viewed. Based on their findings, smooth pursuit and/or predictive mechanisms could have contributed to our subject's responses over the frequency range we employed. We believe, however, that this is unlikely. We asked stationary subjects to track moving targets located at distances comparable to those used in the TVOR experiments.

Figure 5 illustrates smooth pursuit gain for a typical subject over a frequency range of 0.25 to 2.0 Hz. The data show (1) that smooth pursuit gain decreases as a function of frequency (gain \sim 0.7 at 1 Hz and \sim 0.25 at 2 Hz) and (2) smooth pursuit gain is essentially unmodulated by target distance or vergence angle. Based on these data, we can estimate the eye velocity needed to track the virtual targets with smooth: at 1 Hz, the expected eye velocity is $0.7 \times 35^\circ/\text{s} = 24.5^\circ/\text{s}$ (figure 4, dashed gray line); at 2 Hz, the expected eye velocity is $0.3 \times 35^\circ/\text{s} = 10.5^\circ/\text{s}$, figure 4,, dashed gray line). Clearly, at 1 Hz actual eye velocity is less than predicted and at 2 Hz, eye velocity is greater than predicted. Furthermore, smooth pursuit of targets (Figure 5) was associated with a frequency dependent phase lag ranging from $14.6 \pm 8.3^\circ$ at 1 Hz to $42.3 \pm 14.2^\circ$ at 2 Hz. In contrast, the phase lag of the TVOR for the virtual targets was independent of frequency ($3.7 \pm 7.0^\circ$ at 1 Hz; $11.8 \pm 10.2^\circ$ at 2 Hz).

We also used flashing target conditions in order to eliminate the influence of smooth pursuit (figure 4, lower panels). A similar experimental manoeuvre to reduce the influence of smooth pursuit was performed before by Han et al. [35] who used stroboscopic illumination at 4 Hz, with a flash duration of 30 ms. In their experiments flash frequency was increased with increasing frequency of head movements in order to keep the same number of flashes per cycle of head movement. These higher frequencies and relatively long flash durations could, however, also increase the visual feedback and lead to an overestimate of the vestibular contribution to compensatory eye velocity. To minimize visual feedback, we flashed our targets at 1 Hz, regardless of the frequency of head (and body) movement. Moreover, we used a shorter flash duration of 5 ms, which had an additional advantage: the subject saw an effectively stationary visual target, once per cycle (1 Hz) or once per two cycles (2 Hz head movement). Thus, the stationary target provided no information to the smooth pursuit system about the required velocity of the eye movements, (e.g., zero as in the HF paradigm) but did provide feedback about target distance. In this way, we selectively shut down the smooth pursuit system without suppression of the TVOR.

TVOR and accommodation

Wei et al. [15] demonstrated that despite comparable vergence angles TVOR scaling was more accurate when real targets were viewed than when virtual targets were viewed. In agreement

with our data, in their “vergence-only” condition, vergence was dissociated from actual target distance and the TVOR still scaled with viewing distance (see their figure 6). Since the scaling was insufficient to match vergence angle, they concluded that a signal related to accommodation must have been used to correct TVOR eye velocity toward a value appropriate for the actual distance of the target. In contrast to the hypothesis of Wei et al, we do not find an important influence of accommodation since eye velocity was much less than expected based on vergence angle when subjects viewed flashed near targets. Unfortunately, we are not able to precisely determine the influence of accommodation for two reasons. First, the cut end fibre optic target presented a poor accommodative point stimulus, whereas Wei et al. [15] used a fixation dot as well as an array of dots filling the peripheral retina. Furthermore, during the virtual target condition, accommodation would be compromised because vergence was dissociated from accommodation, which is a non-physiological situation [36]. We therefore conclude that accommodation does not contribute to TVOR scaling.

TVOR scaling and visual cues

Motor signals related to vergence angle or accommodation, sensory cues such as disparity or motion parallax, or perceptual information might be used to determine target distance and scale the TVOR. Wei et al. [15] evaluated the relative importance of all these different factors. In that study, monkeys were translated laterally at 5 Hz while they viewed a variety of visual stimuli that included real targets projected onto a movable screen and an array of visual backgrounds (random dot stereograms) designed to present texture and disparity cues that were consistent or inconsistent with vergence. Their main conclusion was that visual cues that accurately or inaccurately cued target distance were relatively ineffective in scaling TVOR responses. Our study suggests that in humans, however, visual cues are important for TVOR scaling: a single point visual stimulus is sufficient to produce significant TVOR scaling. The key difference with the study of Wei et al. [15] is that we presented only a foveal fixation target, whereas visual backgrounds are whole retina stimuli that may contribute to spatial knowledge but would not necessarily determine target depth in a laboratory environment.

Cognitive factors

Ramat et al. [18] found that TVOR gains can be enhanced or suppressed by cognition. In their paradigm, prior knowledge of the direction of head movement and the context of the target (earth-fixed or head-fixed) influenced the TVOR response within 100 ms of the onset of head movement [7]. This result suggests an influence of cognition on the TVOR at the earliest stage of the response, either via a direct cortical connection to the vestibular nuclei or indirectly via the cerebellum (e.g., by a pathway similar to that described by Gamlin and colleagues [28]). Previously, Zhou et al. [19] found rapid contextual TVOR learning in the monkey. Cognition is

a factor that is difficult to rule out. On the one hand, all of the subjects knew that they were sinusoidal translated and that the targets were earth fixed. On the other hand, the Angelaki experiments [37] and Ramat et al. [18] experiments only required discrimination of earth from head fixed targets. As in the study of Paige [1], this task is fundamentally less complex than our task which required recognition of target distance in the absence of any other visual reference and scaling of the TVOR response with target distance.

REFERENCES

1. Paige, G.D., The influence of target distance on eye movement responses during vertical linear motion. *Exp Brain Res*, 1989. 77(3): p. 585-93.
2. Paige, G.D., Linear vestibulo-ocular reflex (LVOR) and modulation by vergence. *Acta Otolaryngol Suppl*, 1991. 481: p. 282-6.
3. Crane, B.T. and J.L. Demer, Human horizontal vestibulo-ocular reflex initiation: effects of acceleration, target distance, and unilateral deafferentation. *J Neurophysiol*, 1998. 80(3): p. 1151-66.
4. Paige, G.D., et al., Human vestibuloocular reflex and its interactions with vision and fixation distance during linear and angular head movement. *J Neurophysiol*, 1998. 80(5): p. 2391-404.
5. Ramat, S. and D.S. Zee, Ocular motor responses to abrupt interaural head translation in normal humans. *J Neurophysiol*, 2003. 90(2): p. 887-902.
6. Schwarz, U. and F.A. Miles, Ocular responses to translation and their dependence on viewing distance. I. Motion of the observer. *J Neurophysiol*, 1991. 66(3): p. 851-64.
7. Snyder, L.H. and W.M. King, Effect of viewing distance and location of the axis of head rotation on the monkey's vestibuloocular reflex. I. Eye movement responses. *J Neurophysiol*, 1992. 67(4): p. 861-74.
8. Telford, L., S.H. Seidman, and G.D. Paige, Dynamics of squirrel monkey linear vestibuloocular reflex and interactions with fixation distance. *J Neurophysiol*, 1997. 78(4): p. 1775-90.
9. Angelaki, D.E., Eyes on target: what neurons must do for the vestibuloocular reflex during linear motion. *J Neurophysiol*, 2004. 92(1): p. 20-35.
10. Wei, M. and D.E. Angelaki, Viewing distance dependence of the vestibulo-ocular reflex during translation: extra-otolith influences. *Vision Res*, 2004. 44(9): p. 933-42.
11. Gamlin, P.D. and R.J. Clarke, Single-unit activity in the primate nucleus reticularis tegmenti pontis related to vergence and ocular accommodation. *J Neurophysiol*, 1995. 73(5): p. 2115-9.
12. Mays, L.E., Neural control of vergence eye movements: convergence and divergence neurons in midbrain. *J Neurophysiol*, 1984. 51(5): p. 1091-1108.
13. McConville, K., et al., Eye position signals in the vestibular nuclei: consequences for models of integrator function. *J Vestib Res*, 1994. 4(5): p. 391-400.
14. Zhou, W. and W.M. King, Premotor commands encode monocular eye movements. *Nature*, 1998. 393(6686): p. 692-5.
15. Wei, M., G.C. DeAngelis, and D.E. Angelaki, Do visual cues contribute to the neural estimate of viewing distance used by the oculomotor system? *J Neurosci*, 2003. 23(23): p. 8340-50.
16. Viirre, E.S. and J.L. Demer, The human vertical vestibulo-ocular reflex during combined linear and angular acceleration with near-target fixation. *Exp Brain Res*, 1996. 112(2): p. 313-24.
17. Clement, G. and F. Maciel, Adjustment of the vestibulo-ocular reflex gain as a function of perceived target distance in humans. *Neurosci Lett*, 2004. 366(2): p. 115-9.
18. Ramat, S., D. Straumann, and D.S. Zee, Interaural translational VOR: suppression, enhancement, and cognitive control. *J Neurophysiol*, 2005. 94(4): p. 2391-402.
19. Zhou, H.H., M. Wei, and D.E. Angelaki, Motor scaling by viewing distance of early visual motion signals during smooth pursuit. *J Neurophysiol*, 2002. 88(5): p. 2880-5.
20. Barnes, G.R. and G.D. Paige, Anticipatory VOR suppression induced by visual and nonvisual stimuli in humans. *J Neurophysiol*, 2004. 92(3): p. 1501-11.
21. Yasui, S. and L.R. Young, On the predictive control of foveal eye tracking and slow phases of optokinetic and vestibular nystagmus. *J Physiol*, 1984. 347: p. 17-33.

22. Adeyemo, B. and D.E. Angelaki, Similar kinematic properties for ocular following and smooth pursuit eye movements. *J Neurophysiol*, 2005. 93(3): p. 1710-7.
23. Hine, T. and F. Thorn, Compensatory eye movements during active head rotation for near targets: effects of imagination, rapid head oscillation and vergence. *Vision Res*, 1987. 27(9): p. 1639-57.
24. MacNeilage, P.R., N. Ganesan, and D.E. Angelaki, Computational approaches to spatial orientation: from transfer functions to dynamic Bayesian inference. *Journal of neurophysiology*, 2008. 100(6): p. 2981-96.
25. Wang, X., et al., The proprioceptive representation of eye position in monkey primary somatosensory cortex. *Nature neuroscience*, 2007. 10(5): p. 640-6.
26. Xu, Y., et al., The time course of the tonic oculomotor proprioceptive signal in area 3a of somatosensory cortex. *Journal of neurophysiology*, 2011.
27. Gamlin, P.D. and K. Yoon, An area for vergence eye movement in primate frontal cortex. *Nature*, 2000. 407(6807): p. 1003-7.
28. Gamlin, P.D., K. Yoon, and H. Zhang, The role of cerebro-ponto-cerebellar pathways in the control of vergence eye movements. *Eye (Lond)*, 1996. 10 (Pt 2): p. 167-71.
29. Merfeld, D.M., et al., Vestibular perception and action employ qualitatively different mechanisms. II. VOR and perceptual responses during combined Tilt&Translation. *J Neurophysiol*, 2005. 94(1): p. 199-205.
30. Zupan, L.H. and D.M. Merfeld, Human ocular torsion and perceived roll responses to linear acceleration. *J Vestib Res*, 2005. 15(4): p. 173-83.
31. Collewijn, H., J. van der Steen, and L.J. van Rijn, Binocular eye movements and depth perception. *Representations of Vision. Trends and Tacit Assumptions in Vision Research.*, ed. G. A.1991, Cambridge: Cambridge University Press. 165-183.
32. Erkelens, C.J. and H. Collewijn, Motion perception during dichoptic viewing of moving random-dot stereograms. *Vision Res*, 1985. 25(4): p. 583-8.
33. Houben, M.M.J., et al., Angular and linear vestibulo-ocular responses in humans. *Ann NY Acad Sci*, 2005. 1039: p. 68-80.
34. Goumans, J., et al., Peaks and troughs of three-dimensional vestibulo-ocular reflex in humans. *Journal of the Association for Research in Otolaryngology: JARO*, 2010. 11(3): p. 383-93.
35. Han, Y.H., et al., Vestibular and non-vestibular contributions to eye movements that compensate for head rotations during viewing of near targets. *Exp Brain Res*, 2005. 165(3): p. 294-304.
36. Hung, G.K., J.L. Semmlow, and K.J. Ciuffreda, The near response: modeling, instrumentation, and clinical applications. *IEEE transactions on bio-medical engineering*, 1984. 31(12): p. 910-9.
37. Angelaki, D.E., H.H. Zhou, and M. Wei, Foveal versus full-field visual stabilization strategies for translational and rotational head movements. *J Neurosci*, 2003. 23(4): p. 1104-8.



6

Memory-guided saccade-vergence interactions after
passive whole-body rotations and translations

Joyce Dits, Johan J.M. Pel and Johannes van der Steen.

Department of Neuroscience, Erasmus MC, Rotterdam, The Netherlands.

Submitted in Neuroscience, January 2014

ABSTRACT

Visual orientation to novel or remembered objects in our environment (spatial updating) requires accurate control of binocular changes in gaze direction (version) and ocular distance (vergence).. When a gaze shift from memory is executed under static conditions, the abducting eye is the eye that is most accurate in direction whereas the adducting eye gives the distance. Under dynamic conditions spatial updating is a more complex situation where visual and vestibular cues have to be combined. The combination of multimodal cues can be achieved at the planning stage or at the motor execution stage. To test between these two alternatives we compared in six subjects spatial updating under stationary (visual spatial memory only) and dynamic (visual spatial memory in combination with intervening whole-body translations and rotations) conditions. Dynamic trials consisted of passive Gaussian velocity whole body rotations ($A=10^\circ$, $V_{max}=33^\circ/s$) in yaw and sideways translations ($A=10\text{cm}$, $V_{max}=0.3\text{m/s}$) produced with a six degrees of freedom motion platform. Subjects were instructed to fixate a platform-fixed visual target in front of the left eye, either at 94cm ("far") or at 31cm ("near") in depth. A space-fixed target, left of the platform-fixed target sight line at 45cm viewing depth, was flashed (80ms) before platform motion onset. Subjects were instructed to make a saccade to the remembered locations of the space-fixed target after the platform-fixed target was dimmed, during randomized "near" or "far" fixation trials. We found that spatial update performance was significantly better after rotations compared with translations. During binocular memory-guided gaze shifts, the abducting eye is the most accurate eye both in stationary and dynamic spatial updating tasks. Errors in vergence from memory are mainly at the expense of the adducting eye.

INTRODUCTION

Visual orienting towards novel or remembered objects in our environment is important for our interaction with the world. Our visual system stores the spatial locations of objects around us in internal spatial memory. This enables us to view or grasp objects even when they are temporarily not visible. During daily activities objects can change their position with respect to our body because the move, or that our head and body are moving. Spatial representations in our brain need to be continuously updated using visual [1-3] and other sensory cues [4-6] in order to maintain a constant accurate representation of the three-dimensional space around us. For example, when we drive our car, we cannot constantly direct our eyes to surrounding traffic, because we also have to maintain focus on the road in front of us. Yet, we can integrate our own motion with memorized positions of visual objects in our environment.

Eye movements are an important mechanism to keep track on where objects are located in our surrounding environment. For visual orientation in a three-dimensional world, saccades are used to guide the direction of gaze, whereas vergence eye movements are used to binocularly foveate an object at the correct viewing distance with respect to our body (depth).

During most gaze shifts, saccadic and vergence movements are made in combination. The two systems interact, where saccade speed slows down and vergence speed goes up compared to isolated saccade or vergence movements [7].

So far, not much is known about saccade/vergence interactions during memorized gaze shifts. Kumar et al. showed that version/vergence peak velocity ratios between visually-guided and memory-guided gaze shifts are different. [8]. We recently demonstrated that under static conditions memory-guided binocular gaze shifts are different from visually-guided gaze shifts in several aspects [9]. During memory-guided gaze shifts the abducting eye is the most accurate in obtaining correct gaze direction, whereas most of the required vergence is mediated by the adducting eye.

Binocular memory-guided eye movements are even more complex when intervening head or whole-body movements occur. Spatial updating after intervening movements has been studied after (passive and active) rotational motion [5, 10, 11]. These studies show that saccades can be accurately programmed from memory after intervening gaze shifts, and after intervening active (e.g. self-induced locomotion) or passive (e.g. whole body displacements) movements of the head or body. In particular spatial updating of binocular gaze signals during linear movements are complicated. During translations, images of objects closer to the eyes move faster across our retinas than the images of far objects (motion parallax). Indeed it has been shown that target distance is taken into account in spatial updating after linear lateral [12, 13], depth [14, 15] and translations [6]. Although these studies show that extra-retinal position information from other sensory sources is used, little is known about the relative contribution of version and vergence in spatial memory tasks that require integration

of visual and vestibular memory cues. In this study we investigated the accuracy and interaction of combined saccade-vergence movements during spatial updating tasks consisting of intervening passive whole body rotations and translations. Multimodal cues such as visually memorized target positions with vestibular information can be combined at the planning stage or at the motor execution stage. In the first condition a target position stored in spatial memory is updated with a vestibular signal that corrects for the amount of head displacement or rotation and that updated target position is then used to execute the required version and vergence. Alternatively the vestibular signal is added after version-vergence command signal has been planned based on stored target position. To test between these two alternatives we investigated spatial updating in six subjects who underwent stationary (visual spatial memory only) and dynamic (visual spatial memory in combination with intervening whole-body translations and rotations) trials. If addition is at the planning stage, we expect no differences between spatial updating under static and dynamic conditions. On the other hand, if vestibular updating is more downstream, we expect that updating under dynamic conditions is less accurate than under static conditions.

METHODS

Subjects

Eye movements were recorded from six subjects (4 male, 2 female, age 40 ± 15 years), naïve with respect to the goal of the experiment. Written informed consent was obtained from all subjects prior to the experiments. None of the subjects had a history of oto-vestibular pathology or mastoidectomy, or impaired stereoscopic vision. All subjects had normal or corrected-to-normal vision. The inter-ocular distance of the subjects was 6.5 ± 0.2 cm (mean \pm SD). Experimental procedures were approved by the Medical Ethical Committee of Erasmus MC and adhered to the Declaration of Helsinki for research involving human subjects.

Experimental setup

Motion stimuli

The subject was seated in a chair that was fixated on a six degrees of freedom motion platform (FCS-MOOG, Nieuw Vennep, The Netherlands) in a completely darkened room [16]. Each subject's body was firmly fastened with a 5-point harness. In addition, a vacuum cushion and an individually moulded bite board were used to completely immobilize the head. The platform delivered rightward Gaussian velocity whole-body sway translations (sway amplitude = 10 cm, $V_{\max} = 0.3$ m/s) and yaw rotations (rotation angle = 10° , $V_{\max} = 33^\circ/s$). Three subjects also participated in control trials in which counter clockwise rotations and leftward translations

were delivered. The motion platform was equipped with a laser device for recording the exact timing of the actual delivered motion stimuli.

Visual targets

Three Light-Emitting Diodes (LEDs) placed at the eye level at different viewing distance from the subject served as visual stimuli (figure 1). Two platform-fixed red LEDs functioned as fixation point (platform-fixed LEDs) and were placed on a wooden frame that was attached to the front of the platform. The platform-fixed LEDs were placed in line with the subject's left eye: one at the distance of 94 cm ("far") and one at the distance of 31 cm ("near") in depth. One other white LED served as a peripheral space-fixed flash target (space-fixed LED). At the initial platform position, the location of this target was 45 cm in depth and 3 cm to the left relative to the subject's left eye. The space-fixed LED was flashed for the duration of 80 ms and the

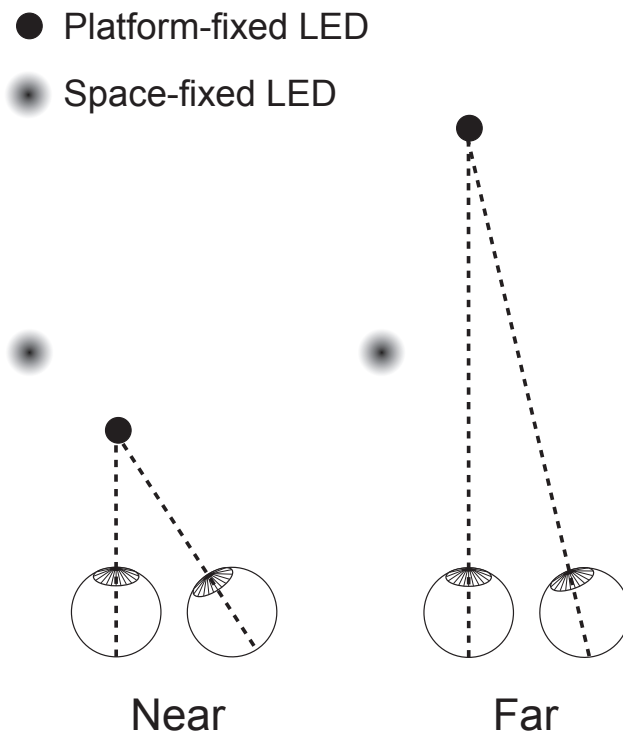


Figure 1: Schematic top view of visual targets. The fixation targets are illustrated with the black closed circles and were placed in line with the subject's left eye: one at the distance of 94 cm ("far") and one at the distance of 31 cm ("near") in depth. The space-fixed (flash) target is illustrated with the gradient closed circles. At the initial platform position, the location of this target was 45 cm in depth and 3 cm to the left relative to the subject's left eye.

subject's task was to remember its location. We ensured that the space-fixed LED stimulated both retinas during the experiment.

Eye movement recordings

Eye positions were recorded with scleral search coils. We used a standard 25-kHz two-field coil system (Model EMP3020; Skalar Medical, Delft, The Netherlands) based on the amplitude detection method by Robinson [17]. Standard dual coils embedded in a silicone annulus (Combi Coils; Skalar Medical) were inserted in each eye. Before insertion, the eyes were anesthetized with a few drops of oxybuprocain (0.4%) in HCl (pH 4.0). Both coils were precalibrated in vitro by mounting them on a gimbal system placed in the center of the magnetic fields. We sampled the coil data at 1000 Hz on a CED system (Cambridge Electronic Design, Cambridge, UK). Prior to each experiment a calibration trial was performed. Subjects were instructed to fixate a series of five targets (central target and a target at 10 degrees left, right, up and down). Targets were back projected onto a translucent screen at 186 cm distance. The subjects fixated each target for ten seconds. Data were stored on a hard disc for further off-line analysis.

Experimental procedure

Experiments were designed to test spatial updating for translational as well as rotational motion. Subjects were instructed to perform memory-guided eye movements under two conditions, referred to as stationary and dynamic trials. In figure 2 the different trials are presented for the translational movement and "near" fixation.

Before the experimental trials started, we presented two fixation trials (figure 2A). The platform first moved to the final position used in the dynamic trials. Then the space-fixed LED was presented for 4 seconds. Subjects were instructed to fixate the space-fixed LED. Fixation trials were used to calculate the errors in gaze and vergence toward the space-fixed LED (see data analysis).

Stationary (control) trials (figure 2B) were used to measure the accuracy of memory-guided saccades without intervening movement. Thus, these trials served as control situations for the dynamic trials. The platform was placed in the final position that was used in the dynamic (rotation or translation) trials in order to create the same positions of the visual targets. The subjects were asked to fixate the platform-fixed LED while the space-fixed LED was flashed for 80 ms. Subjects had to maintain fixation on the platform-fixed fixation LED, but remember the location of the peripheral flashed space-fixed LED. 1800 ms after the space-fixed LED was extinguished, the platform-fixed LED was turned off and the subject had to make a saccade to the remembered location of the space-fixed LED.

During the dynamic (updating) trials (figure 2C) we tested spatial memory updating. The subjects' task corresponded to the stationary trials, but in the dynamic trials the platform

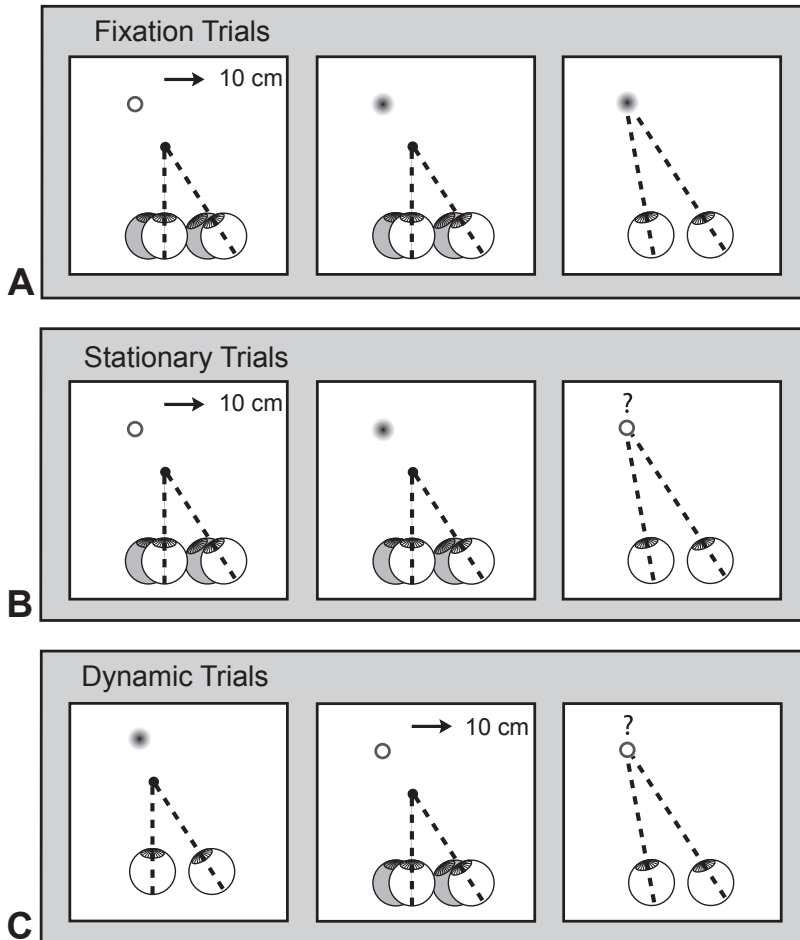


Figure 2: Setup of trials. Trials are illustrated for translational movement during “near” fixation. A. Fixation trials: First, the platform moved to the final position that was used in the dynamic trials. Next, subjects were instructed to fixate the space-fixed target that was presented. Fixation trials were used to calculate the errors in eye position and vergence toward the space-fixed target. B. Stationary trials: The platform was placed in the final position that was used in the dynamic trials. The subjects were asked to fixate the platform-fixed target while the space-fixed target was flashed for 80ms. Subjects had to maintain fixation on the platform-fixed target, and at the same time remember the location of the peripheral flashed space-fixed target. 1800ms after the space-fixed target was extinguished, the platform-fixed targets were turned off and the subject had to make a saccade to the remembered location of the flashed (space-fixed) target. These trials served as control situations for the dynamic trials. C. Dynamic trials: The subjects’ task corresponded to the stationary trials, but in the dynamic trials, movement of the platform intervened the memory task. The platform produced a rotational or translational movement, 1200ms after the flash of the space-fixed target was dimmed. During the movement of the platform, subjects had to fixate the platform-fixed targets that remained illuminated. 800ms after the platform had reached its final position, the platform-fixed targets were extinguished and the subjects had to make a saccade to the remembered location of the space-fixed target.

movement intervened the memory task. 1200 ms after the flash of the space-fixed LED was dimmed, the platform produced a rotational or translational movement. During the movement of the platform, subjects had to fixate the platform-fixed LED that remained illuminated. 800 ms after the platform had reached its final position, the platform-fixed LED was extinguished and the subjects had to make a saccade to the remembered location of the space-fixed LED.

In each experiment, subjects participated in stationary trials, rotations and translations. Sixty trials were recorder per experiment, and all conditions were randomly presented. This resulted in five repetitions of each condition. No visual feedback of the location of the space-fixed LED was provided after each trial and therefore no learning effect was possible.

Control experiments

Two control experiments were performed in which 3 subjects participated:

(1) Lateralization effects:

To exclude possible left-right differences in performance due to eye dominance, we presented the space-fixed LED on the right side of the subject. The space-fixed LED was placed 45 cm in depth and 3 cm to the right relative to the right eye and platform movements were leftward / counter-clockwise with the same amplitude. All other test conditions and trial numbers were identical to the stationary and dynamic trails.

(2) Peripheral visual cueing effects:

To test the influence of depth cues on localization of the flash target, a light source consisting of 8 bright white LEDs was placed on a frame above the subject's head. The light source illuminated the environment before and during the period the flash target was turned on.

Data analysis

Data were analyzed off-line using self-written Matlab (Mathworks) routines. Eye movements to the 5-point calibration pattern, retrieved during the calibration task, were used to transform voltage into Fick angles. After calibration, the data were digitally smoothed using a 2-point moving average. We excluded trials by the following criteria: the subject did not keep their eye directed at the platform-fixed LED, did not make a saccade after the platform-fixed LED was extinguished or when the subject made a saccade before the platform-fixed LED was extinguished.

We computed the eye position of the left and right eye separately. We calculated eye positions of fixed points during each task using the following criteria (figure 3): the initial gaze when the eyes were fixated on the platform-fixed LED (t_1) and after the eye movement to the location of the memorized space-fixed LED, but before slow drifting movements (t_2). Saccades were detected by calculating the eye velocity signal from the gaze signal. Vergence angles were calculated as the difference between left and right (L-R) horizontal gaze.

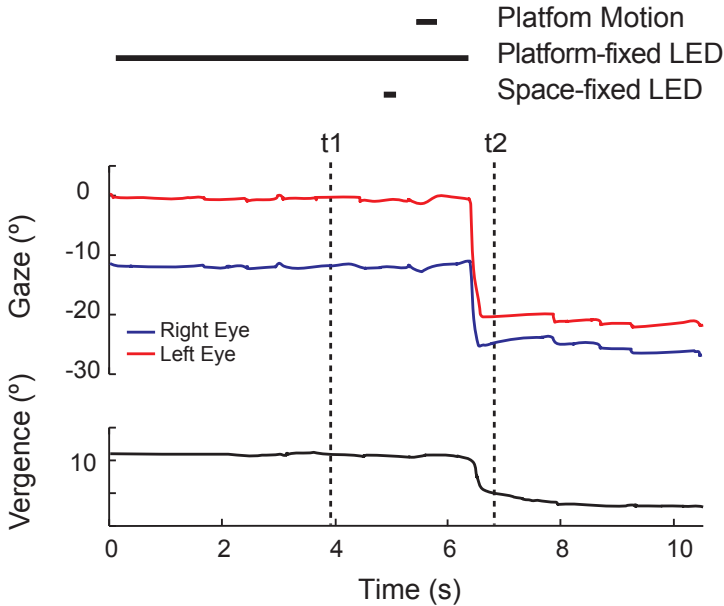


Figure 3: Points in time for error determination. Simulation of gaze and vergence against time. We calculated eye positions of fixed points during each task: the initial position when the eyes were fixated on the fixation target (t_1), the position before (t_2) and after (t_3) the first saccade to the location of the memorized space-fixed target and the end position after multiple saccades (t_4).

Errors in direction (horizontal gaze)

After retrieving eye positions at time t_1 and t_2 , we calculated the errors in gaze direction for each trial. We determined normalized gaze using the following equation:

$$\text{Gaze ratio} = (\text{gaze}(t_2) - \text{gaze}(t_1)) / (\text{control gaze} - \text{gaze}(t_1)) \quad (\text{eq. 1})$$

This results in a normalized ratio of correct gaze positions. Ratios in gaze were calculated for both eyes. Subject specific control gaze values were obtained from the fixation trials. A ratio of 1 indicates a 100% correct eye movement from memory. A ratio < 1 corresponds to an undershoot in direction (eye movement was too small); while a ratio > 1 corresponds to an overshoot.

Errors in depth (vergence)

Normalized change in vergence was determined with the following equation:

$$\text{Vergence ratio} = \text{Vergence}(t_2) / \text{Vergence control} \quad (\text{eq. 2})$$

This results in a ratio of the correct vergence angle. Again subject specific control vergence was obtained from the fixation trials. Vergence ratio of 1 indicates perfect vergence adjustment. A ratio > 1 indicates vergence angle is too large, while a ratio < 1 indicates that vergence change is too small.

Update ratios

Each trial was conducted under stationary and dynamic conditions, i.e. with an intervening translational or rotational movement. We quantified the effect of the intervening movement by calculating a spatial update ratio (UR), defined as:

$$\text{Gaze UR} = \text{Dynamic (gaze (t}_2) - \text{gaze (t}_1)) / \text{Stationary (gaze (t}_2) - \text{gaze (t}_1)) \quad (\text{eq. 3})$$

$$\text{Vergence UR} = \text{Dynamic vergence} / \text{Stationary vergence} \quad (\text{eq. 4})$$

This ratio characterized updating performance. If the update ratio is 1, the intervening movement is properly taken into account (perfect spatial memory updating). A ratio < 1 indicates that stationary trials result in smaller errors than dynamic trials (0 indicates no updating after intervening movement). The update ratios were computed for vergence and horizontal gaze of both eyes separately.

Statistics

The mean and standard deviation position error of each specific spatial task was group-wise calculated and tested for a normal distribution. Differences between position errors or vergence, e.g. Rotation versus Translation, near versus far or binocular versus monocular, were tested for significance using a paired-sample t-test (SPSS). The update ratio and the vergence ratio were compared to the test value 1 using a one-sample t-test. P-values < 0.05 were considered statistically significant. Univariate analysis of variance (ANOVA) analyses was used to test the effect of fixation distance, left vs right eye and intervening movements on update ratio.

RESULTS

The eye movements of six subjects were measured. Three subjects also participated in control experiments including counter-clockwise or leftward platform motions or peripheral visual cueing effects. We excluded ~ 10% of the experimental trials on the basis that subjects did not perform the task correctly, e.g. at the onset of a trial they did not accurately fixate the platform-fixed LED. We calculated the errors during the stationary and the dynamic trials for gaze direction, vergence and their interactions. The errors during the stationary trials reflected the accuracy of gaze-shifts from memory, i.e. no updating of spatial memory. These

errors were compared to those made during the dynamic with the errors during the dynamic trials to test spatial updating which was also assessed by calculating update ratios.

Errors in gaze direction

Examples of the dynamic trials are shown in figure 4 and 5, for translations and rotations respectively. The horizontal gaze of both eyes and vergence is plotted against time. In the top part (figure 4A and 5A, "Far") the platform-fixed LED was behind the space-fixed LED, while in the bottom part (figure 4B and 5B, "Near") the platform-fixed LED was in front of the space-fixed LED. In all the demonstrated conditions, the platform moved rightward or clockwise,

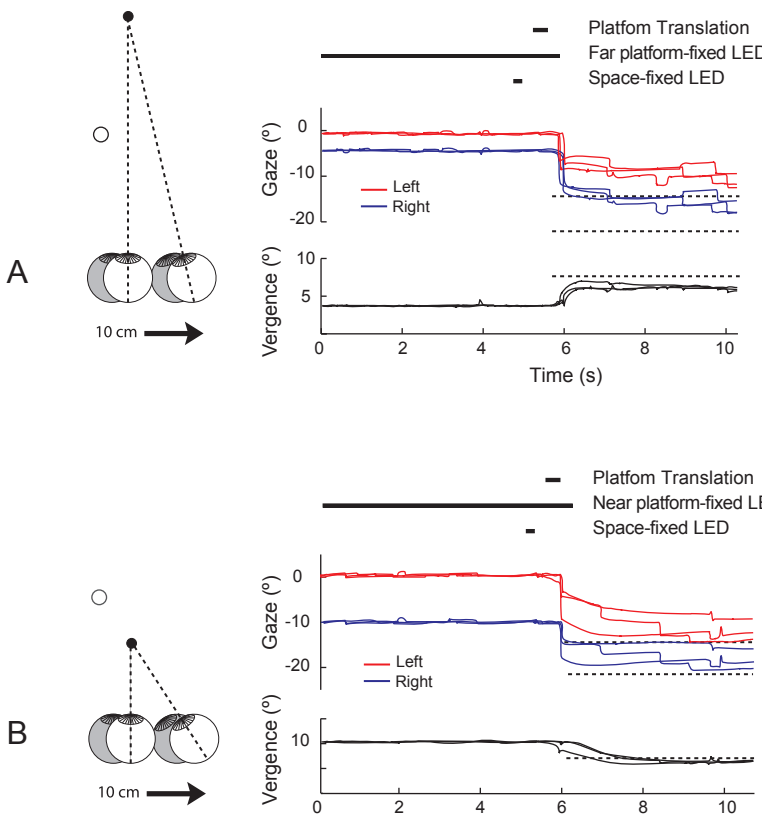


Figure 4: Example of translation trials. "Far" and "near" fixation conditions are illustrated in panel A and B respectively and are obtained from one subject. In all the demonstrated conditions, the platform translated rightward, and leftward eye movements were made towards the memorized location of the space-fixed target. The horizontal eye positions of both eyes are plotted against time in the top traces. Vergence is plotted against time in the bottom traces. In the "near" fixation condition (B) vergence decreased, whereas in the "far" fixation condition (A) convergent eye movements were made toward the location of the remembered space-fixed target. The correct eye positions, retrieved from each subject in the fixation trials, are also plotted as a reference.

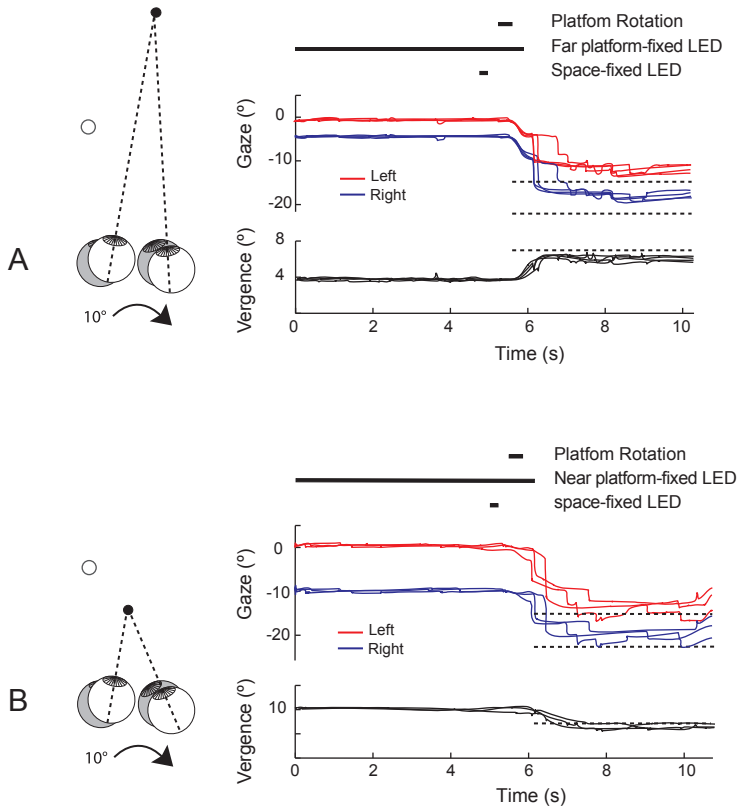


Figure 5: Example of rotation trials. “Far” and “near” fixation conditions are illustrated in panel A and B respectively and are obtained from one subject. In all the demonstrated conditions, the platform produced clockwise rotations, and leftward eye movements were made towards the memorized location of the space-fixed target.

and leftward gaze shifts were made toward the memorized location of the space-fixed LED. The correct eye positions, retrieved from each subject in the fixation trials, are also plotted as a reference.

Stationary (control) trials

The errors in direction were calculated as the proportional eye movement of the correct eye positions by equation 2 (see methods) and expressed as gaze ratio (presented in table 1). During the stationary trials, there was no intervening movement, and no updating of spatial memory was necessary.

In “near” fixation condition, we found a mean gaze ratio of $0.99 (\pm 0.20)$ and $0.92 (\pm 0.25)$, of the left and the right eye respectively. Thus, the gaze-shifts towards the space-fixed LED were 99% and 92% correct for the left and the right eye respectively. These gaze-shifts were not significant different from 1.0, indicating that no significant error was made during the

“near” fixation trials. In the “far” fixation condition gaze ratios of the eye position were 0.99 and 0.89, left and right eye respectively. In this condition only the gaze ratio of the right eye was significantly different from 1 ($p < 0.001$; one sample t-test).

Dynamic trials

Movement in the dynamic trials consisted of either translations or rotations. After translational platform movement, all gaze ratios of both eye positions were significantly less than unity (table 1).

Thus, in both “near” and “far” fixation condition the translational platform movement resulted in a significant error in gaze direction. After platform rotation no significant error was made in the “near” fixation condition 1.00 (left eye) / 0.92 (right eye). In the “far” condition gaze ratio was 0.92 (left eye) / 0.88 (right eye) of which the gaze ratio of the right eye was significantly different from 1. Note that this difference in significance between the left and right eye was also present in the stationary trials. In control experiments, in which the platform moved counterclockwise or leftward, the opposite was found: the left eye caused significant

Table 1: Normalized gaze and vergence ratios

| | Normalized gaze | | Normalized vergence | |
|----------------------------|-----------------|-----------|---------------------|-----------|
| | Mean \pm SD | P-value* | Mean \pm SD | P-value* |
| Near fixation (divergence) | | | | |
| Stationary | | | | |
| Left eye | 0.99 \pm 0.20 | P=0.81 | 0.85 \pm 0.21 | P < 0.001 |
| Right eye | 0.92 \pm 0.25 | P=0.06 | | |
| Translation | | | | |
| Left eye | 0.85 \pm 0.23 | P < 0.01 | 0.83 \pm 0.17 | P < 0.001 |
| Right eye | 0.73 \pm 0.30 | P < 0.001 | | |
| Rotation | | | | |
| Left eye | 1.00 \pm 0.20 | P=0.93 | 0.81 \pm 0.31 | P < 0.05 |
| Right eye | 0.92 \pm 0.25 | P=0.18 | | |
| Far fixation (convergence) | | | | |
| Stationary | | | | |
| Left eye | 0.99 \pm 0.22 | P=0.74 | 0.71 \pm 0.24 | P < 0.001 |
| Right eye | 0.89 \pm 0.14 | P < 0.001 | | |
| Translation | | | | |
| Left eye | 0.74 \pm 0.25 | P < 0.001 | 0.85 \pm 0.24 | P < 0.01 |
| Right eye | 0.72 \pm 0.22 | P < 0.001 | | |
| Rotation | | | | |
| Left eye | 0.93 \pm 0.24 | P=0.13 | 0.78 \pm 0.27 | P < 0.001 |
| Right eye | 0.88 \pm 0.19 | P < 0.01 | | |

Normalized values are mean \pm SD, n=6. * Difference with 1.0. See methods for equations.

larger gaze errors than the right eye ($p < 0.05$; paired sample t-test). Finally, comparing the gaze ratios after translations with those after rotations resulted in significantly larger errors in gaze direction after translational platform movements ($p < 0.05$; paired sample t-test).

Errors in vergence

Vergence is plotted against time in the lower panels of figures 4 and 5. In the “near” condition vergence decreased, whereas in the “far” condition a convergence eye movement was made toward the location of the remembered space-fixed LED. Errors in vergence were calculated using equation 4 and expressed as vergence ratio (table 1, right column). In the “near” fixation condition vergence ratios were all significant smaller than 1. That is 0.85, 0.83 and 0.81 for respectively the stationary, translation and rotation condition. Thus, in the “near” fixation conditions vergence decreased too much, indicating significant overshoots in divergent eye movements. In the “far” fixation condition the vergence ratio was also significantly less than 1 (0.71, 0.85 and 0.78 for respectively the stationary, translation and rotation condition). This significant undershoot in convergence, indicates that vergence did not increase adequately.

To test for a possible learning effect during the experiment, we plotted for each subject normalized vergence ratios as a function of trial number. The slope of the fitted regression lines was on average 0.00 ± 0.07 , indicating that no learning effect influenced the measurement series presented.

Update ratio

The update ratios were calculated by dividing dynamic with the stationary performance, see methods, equation 5 and 6. The closer the update ratio is to 1, the better spatial updating after a given intervening movement. The gaze update ratios are illustrated in the top box-plots of figure 6.

In the “near” condition, the update ratios for eye position were 0.77 ± 0.15 (left eye) / 0.68 ± 0.24 (right eye) after translation, and 1.01 ± 0.11 (left eye) / 0.99 ± 0.14 (right eye) after rotation. The update ratio was significantly below unity ($p < 0.05$; one sample t-test) after translation, but not after rotation ($p = 0.81$ / $p = 0.90$; one-sample t-test). In conclusion, spatial updating was most accurate after platform rotations.

In the “far” condition the update ratios were 0.75 ± 0.33 (left eye) / 0.81 ± 0.28 (right eye) after translation, and 0.97 ± 0.15 (left eye) / 1.00 ± 0.14 (right eye) after rotation. Thus also for this condition, spatial updating was significantly better after rotations than after translations. A univariate ANOVA, with fixation condition (near / far), eye (left / right), platform motion (rotation / translation), platform direction (leftward-CCW / rightward-CW) as fixed factors and update ratio as dependent variable, indicated no effect of fixation condition ($F(1,71) = 0.79$,

$P=0.38$), eye ($F(1,71)=0.25, P=0.88$), and platform direction ($F(1,71)=0.138, P=0.712$), but a significant effect of platform motion ($F(1,71)=11.19, P<0.01$).

We also calculated vergence update ratios. These update ratios are illustrated in the bottom panels of figure 6. In the “near” fixation trials all update ratios were not significant different from unity (1.03 ± 0.18 after translation and 0.90 ± 0.18 after rotation).

In the “far” condition update ratios were: 1.25 ± 0.22 after translation (significant different from unity) and 1.09 ± 0.22 after rotation (not significant different from unity). A univariate ANOVA, with fixation condition (near / far), platform motion (rotation / translation), platform direction (leftward-CCW / rightward-CW) as fixed factors and update ratio as dependent variable, indicated no effect of fixation condition ($F(1,35)=3.31, P=0.08$), platform motion ($F(1,35)=0.15, P=0.70$) and platform direction ($F(1,35)=0.07, P=0.79$). In conclusion, in particularly during translations there are differences in updating the depth component: When the eyes start in a converged position and have to diverge, spatial updating in depth was

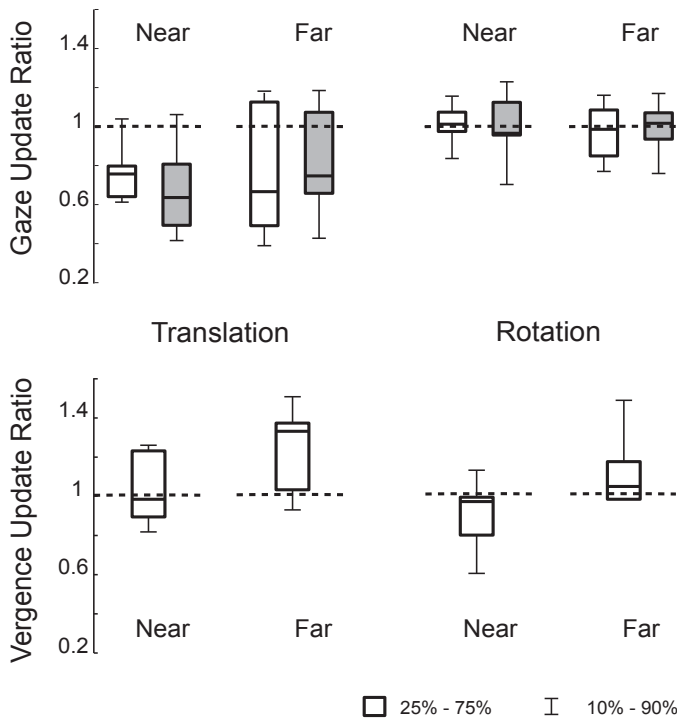


Figure 6: Update performance. Mean gaze and vergence update ratios. Data of update ratios are presented as box-whisker plots. Each box represents the 25th to 75th percentile of the data. The band near the middle of the box is the 50th percentile. The whiskers (or error bars) represent the 5th and 95th percentile of the data. In the top panel gaze update ratios of the left and right eye are illustrated by the white and grey boxes respectively. Update ratios were calculated by dividing the dynamic error with the stationary error. The closer the update ratio is to 1, the better spatial updating after a given intervening movement. Gaze update ratios after translations were significant lower than after rotations.

more accurate than when the eyes started in nearly parallel position and were required to converge.

DISCUSSION

The aim of our study was to assess accuracy and relative contribution of combined saccade and vergence movements towards memorized visual targets in combination with intervening passive whole-body translations and rotations. Our results support previous findings that memory-guided eye movements are not only guided by stored visual cues under static conditions, but can be integrated with motion cues from the vestibular system, thus contributing to spatial constancy [6, 18-20].

We previously showed that the abducting eye is more accurate than the adducting eye in lining itself up with the target during stationary memory-guided gaze shifts [9]. In the present experiment updating was more complex, because passive intervening whole-body movements were added. Nevertheless, also during dynamic updating, memorized targets were more accurately fixated with the abducting eye than with the adducting eye. This shows that there are no differences in the execution of binocular gaze changes to memorized targets under static and dynamic conditions.

Within the same group of subjects errors in gaze direction were significantly larger for spatial memory updating after translations than after rotations. The difference between spatial update performance after translations and rotations may originate in the differences in anatomy and physiology involved in processing the motion components. Translational and rotational responses are not only located in different parts of the vestibular apparatus, they also have different sensory properties and separate brainstem and cortical circuits [21-23]. The differences reflect the specialized functions of the two systems: global versus foveal stabilization in response to rotational versus translational involuntary head movements [24]. Foveal stabilization implies stabilization of the eyes at a single fixation point at variable viewing distance. Therefore, for translations the gain of the signals that code direction is also variable and is a context dependent signal for spatial memory updating.. Our results suggest that vestibular information is used for translational passive spatial updating, but insufficient to provide accurate spatial updating of binocular gaze.

When we compare our data with previous, spatial update ratios for translations our results are comparable with data from Medendorp and Klier [6, 12]. Our update ratios for rotations were more accurate than reported in previous work [18, 19]. These differences suggest an effect of stimulus acceleration and amplitude magnitude, as we used higher acceleration and the larger stimulus amplitude compared to earlier studies.

For rotations our data are consistent with a central updating of memorized target position in 3D space. The small difference in updating under static and dynamic conditions are

in favor of a central updating mechanism that takes into account multisensorial cues (visual and vestibular). Nevertheless the performance accuracy depends on the conditions. We compared the situation in which the initial point of fixation of both eyes was at far distance, thus requiring convergent eye movements towards remembered target, versus the situation in which the initial point of fixation was at near distance, requiring divergent eye movements from memory. We found that in particularly in the dynamic tasks requiring divergence, the error in vergence was significantly smaller than when convergence was required. In all test conditions the eyes had a tendency to diverge, which suggests that releasing vergence is easier than enhancing vergence. This is in line with the fact that without visual input, and thereby without visual disparity signals, the brain generally favors a small vergence angle, which is less than required for fixation of the near target [25].

Spatial updating after intervening movements occurs under natural conditions, continuous visual information of the surrounding world is present, even if the visual target is not available. The limitations of the vestibular system to process motion are overcome using other sensory cues, most importantly visual cues [26]. The multisensory integration of visual-vestibular input is especially important after translation motion, because the foveal stabilization of the visual target is more dependent on visual feedback (disparity). How vestibular signals are integrated and used for spatial updating remains unclear. Although the posterior parietal cortex is mostly related to vision, it also combines signals from multiple modalities (e.g. vision, vestibular information) to create a representation of space [27-30]. Also the prefrontal cortex has a three-dimensional representation [31, 32]. Many brain regions carry signals related to both optic and motion information. The extrastriate areas MST (medial superior temporal area) and VIP (ventral interparietal area) contain representations of self-motion based on visual and vestibular cues [33, 34]. Vestibular interconnected cortical areas, the “vestibular cortex”, [35, 36] and PIVC [37] receive vestibular information, but do not respond to optic information and are therefore not believed to be involved in multisensory integration.

The overall conclusion is that spatial updating after passive whole-body vertical axis rotation is nearly perfect, while significant update errors occur after lateral translations. During binocular memory-guided gaze shifts, both in stationary and spatial updating tasks, the abducting eye is most accurate, and errors in vergence from memory are mainly at the expense of the adducting eye.

REFERENCES

1. Hallett, P.E. and A.D. Lightstone, Saccadic eye movements to flashed targets. *Vision Res*, 1976. 16(1): p. 107-14.
2. Schlag, J., M. Schlag-Rey, and P. Dassonville, Saccades can be aimed at the spatial location of targets flashed during pursuit. *J Neurophysiol*, 1990. 64(2): p. 575-81.
3. Smith, M.A. and J.D. Crawford, Implications of ocular kinematics for the internal updating of visual space. *J Neurophysiol*, 2001. 86(4): p. 2112-7.
4. Angelaki, D.E. and K.E. Cullen, Vestibular system: the many facets of a multimodal sense. *Annu Rev Neurosci*, 2008. 31: p. 125-50.
5. Klier, E.M., D.E. Angelaki, and B.J. Hess, Human visuospatial updating after noncommutative rotations. *J Neurophysiol*, 2007. 98(1): p. 537-44.
6. Klier, E.M., B.J. Hess, and D.E. Angelaki, Human visuospatial updating after passive translations in three-dimensional space. *J Neurophysiol*, 2008. 99(4): p. 1799-809.
7. Collewijn, H., C.J. Erkelens, and R.M. Steinman, Voluntary binocular gaze-shifts in the plane of regard: dynamics of version and vergence. *Vision Res*, 1995. 35(23-24): p. 3335-58.
8. Kumar, A.N., et al., Tests of Hering- and Helmholtz-type models for saccade-vergence interactions by comparing visually guided and memory-guided movements. *Ann N Y Acad Sci*, 2005. 1039: p. 466-9.
9. Dits, J., et al., Version-vergence interactions during memory-guided binocular gaze shifts. *Invest Ophthalmol Vis Sci*, 2013. 54(3): p. 1656-64.
10. Medendorp, W.P., et al., Rotational remapping in human spatial memory during eye and head motion. *J Neurosci*, 2002. 22(1): p. RC196.
11. Van Pelt, S., J.A. Van Gisbergen, and W.P. Medendorp, Visuospatial memory computations during whole-body rotations in roll. *J Neurophysiol*, 2005. 94(2): p. 1432-42.
12. Medendorp, W.P., D.B. Tweed, and J.D. Crawford, Motion parallax is computed in the updating of human spatial memory. *J Neurosci*, 2003. 23(22): p. 8135-42.
13. Li, N., M. Wei, and D.E. Angelaki, Primate memory saccade amplitude after intervened motion depends on target distance. *J Neurophysiol*, 2005. 94(1): p. 722-33.
14. Li, N. and D.E. Angelaki, Updating visual space during motion in depth. *Neuron*, 2005. 48(1): p. 149-58.
15. Van Pelt, S. and W.P. Medendorp, Updating target distance across eye movements in depth. *J Neurophysiol*, 2008.
16. Houben, M.M., et al., Angular and linear vestibulo-ocular responses in humans. *Ann N Y Acad Sci*, 2005. 1039: p. 68-80.
17. Robinson, D.A., A Method Of Measuring Eye Movement Using A Scleral Search Coil In A Magnetic Field. *IEEE Trans Biomed Eng*, 1963. 10: p. 137-45.
18. Blouin, J., et al., Updating visual space during passive and voluntary head-in-space movements. *Exp Brain Res*, 1998. 122(1): p. 93-100.
19. Klier, E.M., B.J. Hess, and D.E. Angelaki, Differences in the accuracy of human visuospatial memory after yaw and roll rotations. *J Neurophysiol*, 2006. 95(4): p. 2692-7.
20. Wei, M., et al., Deficits and recovery in visuospatial memory during head motion after bilateral labyrinthine lesion. *J Neurophysiol*, 2006. 96(3): p. 1676-82.
21. Angelaki, D.E., Eyes on target: what neurons must do for the vestibuloocular reflex during linear motion. *J Neurophysiol*, 2004. 92(1): p. 20-35.

22. Angelaki, D.E., A.M. Green, and J.D. Dickman, Differential sensorimotor processing of vestibulo-ocular signals during rotation and translation. *J Neurosci*, 2001. 21(11): p. 3968-85.
23. Uchino, Y., et al., Utricular input to cat extraocular motoneurons. *Acta Otolaryngol Suppl*, 1997. 528: p. 44-8.
24. Angelaki, D.E., H.H. Zhou, and M. Wei, Foveal versus full-field visual stabilization strategies for translational and rotational head movements. *J Neurosci*, 2003. 23(4): p. 1104-8.
25. Rosenfield, M., Tonic vergence and vergence adaptation. *Optom Vis Sci*, 1997. 74(5): p. 303-28.
26. DeAngelis, G.C. and D.E. Angelaki, Visual-Vestibular Integration for Self-Motion Perception, in *The Neural Bases of Multisensory Processes*, M.M. Murray and M.T. Wallace, Editors. 2012: Boca Raton (FL).
27. Andersen, R.A., Multimodal integration for the representation of space in the posterior parietal cortex. *Philos Trans R Soc Lond B Biol Sci*, 1997. 352(1360): p. 1421-8.
28. Cohen, Y.E. and R.A. Andersen, A common reference frame for movement plans in the posterior parietal cortex. *Nat Rev Neurosci*, 2002. 3(7): p. 553-62.
29. Duhamel, J.R., C.L. Colby, and M.E. Goldberg, The updating of the representation of visual space in parietal cortex by intended eye movements. *Science*, 1992. 255(5040): p. 90-2.
30. Medendorp, W.P., et al., Gaze-centered updating of visual space in human parietal cortex. *J Neurosci*, 2003. 23(15): p. 6209-14.
31. Fukushima, J., et al., The vestibular-related frontal cortex and its role in smooth-pursuit eye movements and vestibular-pursuit interactions. *J Vestib Res*, 2006. 16(1-2): p. 1-22.
32. Fukushima, K., J. Fukushima, and T. Warabi, Vestibular-related frontal cortical areas and their roles in smooth-pursuit eye movements: representation of neck velocity, neck-vestibular interactions, and memory-based smooth-pursuit. *Front Neurol*, 2011. 2: p. 78.
33. Bremmer, F., et al., Visual-vestibular interactive responses in the macaque ventral intraparietal area (VIP). *Eur J Neurosci*, 2002. 16(8): p. 1569-86.
34. Duffy, C.J. and R.H. Wurtz, Response of monkey MST neurons to optic flow stimuli with shifted centers of motion. *J Neurosci*, 1995. 15(7 Pt 2): p. 5192-208.
35. Akao, T., et al., Latency of vestibular responses of pursuit neurons in the caudal frontal eye fields to whole body rotation. *Exp Brain Res*, 2007. 177(3): p. 400-10.
36. Guldin, W.O. and O.J. Grusser, Is there a vestibular cortex? *Trends Neurosci*, 1998. 21(6): p. 254-9.
37. Grusser, O.J., M. Pause, and U. Schreiter, Vestibular neurones in the parieto-insular cortex of monkeys (*Macaca fascicularis*): visual and neck receptor responses. *J Physiol*, 1990. 430: p. 559-83.



7

General discussion

Visual orientation in a three-dimensional world requires accurate control of eye movements of both eyes. To visually focus a new target of interest, we have to make a gaze-shift from our current point of fixation towards a point that has a different direction and depth. Changes in direction are made with saccadic eye movements (version) and in depth with vergence movements. We, as humans, are constantly in motion and although our frontally placed eyes are eminently suited for binocular vision, we cannot always view the complete visual scene. For this reason eye movements are also made to targets from our memory. Since retinal stability of our visual field becomes disturbed during motion, we depend on our vestibular system, which is important for three-dimensional stabilization of visual information. Thus, three-dimensional images stabilization under stationary and dynamic conditions requires a complex interaction between visual and vestibular stabilizations systems in order to achieve optimal binocular alignment of the eyes. The focus of the thesis is on version and vergence, when eye movements interact with spatial memory and whole body movements, and when the extra-retinal information is disturbed.

Binocular vision needs independent eye movements to maintain binocular correspondence

In human binocular vision, both eyes are normally aimed at the same point in visual space [1]. To visually orient in a three-dimensional environment, eye movements are made either in the same direction (version) or in opposite direction to change depth (vergence). For sharp binocular vision, corresponding retinal coordinates are necessary to construct a single representation of the visual world [2]. Disparity is important for binocular vision, but is limited by the fusional range of images [3, 4]. In chapter 2 we demonstrated that to sustain binocular vision, slow phase eye movements with independent motion directions are generated. Dichoptic visual stimuli with orthogonal motion direction were used (vertical motion left eye – horizontal motion right eye). In contrast to the independent slow phase eye movements, the perceived direction was the vector sum of the two images (diagonal motion). This paradoxical situation can be explained when we take into account that independent slow phase eye movements only occur when images were fusible. Without the ability to fuse images (anti-correlated stimuli) conjugate eye movements were made. Thus, the purpose of the independent slow phase eye movements was to maintain retinal binocular correspondence.

The question is how the independent disjunctive eye movements are controlled. Are they really independent, or are these movements the result of asymmetrical vergence (Hering-Helmholtz debate) Lesion and physiological data have shown that different neuronal populations exist for conjugate gaze and vergence [5-9]. In this context, the data in chapter 2 could be explained by assuming that horizontal and vertical vergence centers are able to send adjustable signals to the left and right oculomotor neurons. This has also been suggested

earlier for horizontal binocular eye movements [10]. In contrast, there is also an ongoing debate that control of eye movements is partially uni-ocular [11].

Regardless of what the final common pathway is, the independent disjunctive eye movements depend on cortical binocular visual processing. In cortical area V1 disparity sensitive cells are present, that might be the key to binocular control of disjunctive eye movements [12-14]. The disparity cells are sensitive to both horizontal and vertical disparity [15]. They are dependent on visual feedback by fusing images and hereby maintaining binocular correspondence.

Vergence is the compromising factor in memory-guided eye movements

Although binocular eye movements can be made very accurately towards targets that are visually available, problems occur when the eyes are directed towards targets from memory. Memory-guided saccades are, besides the small systemic errors, quite accurate [16, 17]. In chapter 3, we studied the accuracy of combined saccadic-vergence gaze shift from memory. In our test setup, the subjects were placed in a darkened room, so little depth cues (eg familiar of size) were available. During the visually-guided experiment, a single LED target produces adequate stimuli to drive both version and vergence toward an accurate eye position. In contrast, when visual feedback of the target location was absent and binocular eye movements were driven from memory, significant errors occurred in vergence, while version movements remained accurate. The errors in vergence were reflected in the adducting eye. Thus, the abducting eye accurately produced a gaze shift in direction, but because vergence adjustment is insufficient, errors were found in the adducting eye. By comparing the trials requiring convergence and divergence eye movements, we found that in each condition the eyes tended to diverge, reducing the vergence angle. This resulted in larger errors during the trials requiring convergence.

The asymmetry in accuracy in memory-guided combined saccade-vergence movements has not been demonstrated before. Dynamic studies of visually-guided saccades demonstrated higher peak velocity of the abducting eye [18]. The differences in neural pathways that are involved in the control of abducting and adducting eye movements offer a plausible explanation for this finding. Innervation of the lateral rectus muscle, which abducts the eye, is a directly driven pathway by the abducens nucleus and nerve (VI), whereas the medial rectus muscle (which adducts the eye) is indirectly controlled by the abducens nucleus via the medial longitudinal fasciculus (MLF) and the oculomotor nucleus (III). Chen et al. [19] tested the role of the MLF in saccade-vergence interactions and found that horizontal saccades were governed first by disjunctive signals, preceded by an initial, high acceleration conjugate transient and followed by a slow vergence component. Patients with MLF lesions (INO, internuclear ophthalmoplegia) were unable to modulate adducting velocity when eye movements to different viewing conditions were made. This is in accordance with our findings

in chapter 3; vergence was adjusted after the initial saccade. In the memory-guided trials the slow vergence adjustment, which occurs in the adducting eye, was lacking. This resulted in gaze errors in the adducting eye. How our findings rule on to the Hering-Helmholtz binocular coordination debate [for review; 11], is difficult. When a slow vergence signal is lacking, which is suggested by our data, the abducting eye is directed accurately toward the memorized target location. If an equal vergence signal was added to both eyes, the abducting eye would be less accurate. To achieve the required binocular eye movement, the adducting eye has to be adjusted to a greater extent than the abducting eye. Thus, each eye has to receive its own vergence signal, which is more in agreement with the Helmholtz theory [20].

Visual disparity is the strongest drive for vergence [21], but this is not available in a dark environment during a memory-guided eye movement. The disparity signal that could be derived from the briefly presented visual target prior to the eye movement, had to be stored in spatial memory, but was insufficient to accurately drive vergence movements from memory. Previous research has demonstrated that disparity memorization decays after 2 seconds [22, 23]. For this reason we used an interval between target presentation and initiation of the eye movement below 2 seconds. Memorization on disparity can be improved by training [22], but this was not the aim of our research. The question remains where disparity memorization occurs. Recent study involving transcranial magnetic stimulation (TMS) has demonstrated that besides saccades, also vergence was affected by TMS of the frontal eye fields (FEF) [24], which was already demonstrated in primates [25]. Also the posterior parietal cortex has been indicated to be involved in the initiation of vergence [26, 27]. Recent experiments have identified vergence neurons in the rostral superior colliculus, which might play a role in the generation of signals to precisely align the eyes toward targets in 3D space [28].

Vergence movements are under voluntary control, but are mainly performed without being aware of them [29]. Our data suggests that when eye movements are made from memory, the eyes are directed to the memorized target location by a conjugate or disjunctive saccade. Subsequently when visual feedback becomes available and disparity is signaled, vergence and accommodation are adjusted to gain a sharp and foveated image of the visual target. Thus, in our natural environment, we are to a great extent dependent of visual feedback to accurately drive vergence to the visual target location.

The role of the vestibular system in seeing the three-dimensional world

When we move in three-dimensional space, compensatory eye movements are necessary to stabilize our visual field. The vestibular system measures angular and linear accelerations within six degrees of freedom. The vestibulo-ocular reflexes (VORs) provide fast compensatory eye movements during translations and rotations. Rotational motion is detected by the semicircular canals, while the otolith organs detect linear acceleration (translation). Compensation for translations is different from rotations during the VOR. During the rotational

VOR, eye movements opposite to head velocity can stabilize an entire visual field. Thus, also without visual information (eg dark room) compensatory eye movements can be made, although with lower gain, based on vestibular information of the rotational head motion. The translational VOR on the other hand, stabilizes a given fixation point in space, to keep images stable on two foveae [30-32]. For this reason, the translational VOR has more correspondence to foveal / binocular vision than the rotational VOR [33]. In chapter 4 a method is described to measure the three-dimensional VOR in humans, using a six degree of freedom motion simulator. Although the method can be used for both translations and rotations, chapter 4 describes measurement of the angular (rotational) VOR. The motion platform is used in combination with the sclera search coils to measure the eye movements [34]. This measurement setup provides a sensitive and novel method to perform fundamental research, but also to test vestibular function in patients with vestibular problems. Our results are in accordance with other VOR research [35-38] and demonstrate accurate compensation for horizontal and vertical rotations, compared to torsional motion which resulted in lower VOR gain.

Linear motion: a challenge for visual-vestibular interaction

Vestibular compensation for translations is computationally more difficult than rotations, because the translational VOR stabilizes a given point in space instead of the whole visual field as in rotational motion. A proper translational VOR response is achieved when the eyes counter rotate with a velocity inversely scaled to viewing distance [30, 39-42]. To measure the gain of the translational VOR, information of the visual target location is necessary. When imagined or previously presented visual targets are used, the brain has to retain the target distance to produce the correct compensatory eye movements. In chapter 3 however, we concluded that vergence cannot voluntarily be maintained at a desired angle from memory in an environment without visual cues (dark room). Similar findings were demonstrated during translational VOR experiments using fixation on imagined targets. When the visual target was dimmed, the vergence angle and gain of the VOR decreased significantly [43]. It was concluded [41, 44, 45] that TVOR scales with vergence angle. In chapter 5 we studied scaling of the translational VOR using real and virtual targets. We found that when visual targets are continuously available, eye velocity scales almost perfect with vergence. However, when vergence is changed without changing target distance or when the visual target is flashed and visual feedback is compromised, the relationship between vergence and eye velocity breaks down.

Our vestibular system detects and processes translations, and subsequently the compensatory eye movements are generated according to the visual requirements. Under natural conditions, viewing distance is the most important factor to set the translational VOR, but it can be influenced by visual cues and cognitive factors [45, 46]. Thus, the translational VOR, driven by vestibular input, interacts closely with our visual need to stabilize the visual image

of a target at a given distance in 3D space. Vestibular information of translations without visual feedback is insufficient to guide compensatory eye movements of visual space, demanding a close visual-vestibular interaction.

Vestibular information is used, but insufficient for accurate binocular visuospatial updating

Visuospatial updating is a process that enables us to keep track of locations of objects in space, even though we are constantly moving, by taking our intervening movements into account. This allows us to interact with the environment in an accurate way. By focusing on self-motion, a distinction between active and passive motion has to be made. During active self-motion, efference copies of intended motor commands could be used for spatial updating [47-50]. This thesis focused on passive self-motion in spatial updating tasks. The use of passive whole-body motion eliminated the use of efference motor copy signals and enabled us to study the influence of sensory information used for spatial updating, especially vestibular information. Previous research has shown that our vestibular system, among others, plays an important role in spatial updating [51-54]. In chapter 6, the difference between passive spatial updating after upright whole body yaw rotations and lateral translations was described. As for the vestibule-ocular reflex, spatial updating of translational motion is also more complicated to take into account than rotations. During translations, the distance from target to observer is altered, requiring changes in vergence angles. Furthermore, targets closer to the subjects require larger changes in version, than objects at farther distance (motion parallax), thus target distance has to be taken into account. Motion parallax was demonstrated to be taken into account in updating of spatial memory [55]. Separate previous research has studied passive whole-body translations and rotation along different axes [51-53, 55-57]. However, the accuracy of spatial updating after translational and rotational movement was not compared within the same subject group. We used yaw rotations and horizontal translations for two reasons: 1) gravity cues are small and comparable, and 2) they are most used during natural movement. We demonstrated that spatial update performance of gaze direction after whole-body rotations was significantly more accurate than after translations. When comparing our results with previous research, we found comparable spatial update ratios for translations [53, 55], but more accurate update ratios for rotations [51, 52]. This difference could be based on the difference in delivered acceleration and amplitude of the motion platform. Our results suggest that vestibular information is used for translational passive spatial updating, but insufficient to provide accurate spatial updating measured by eye movements. Other sensory and motor cues must be used to complement the deficiency of the vestibular system. The fact that during translation, our brain is more dependent on visual feedback than during rotation, was also found during the VOR.

In contrast to directional eye movements, vergence was less affected in the spatial updating tasks. Especially in the translational motion trials this would be expected based on motion parallax. The vergence errors in memory-guided eye movements, as described in chapter 3, are not increased after passive whole-body rotations and translations (chapter 6). This suggests that vergence system is at least partially dependent on visual feedback to obtain a disparity signal and direct the eyes to the adequate vergence angle. It does not indicate that vergence is insufficiently taken into account during intervening whole-body movements. Thus even though significant vergence errors are made during memory-guided binocular eye movements, vergence is adequately taken into account during passive intervening whole-body lateral translations and yaw rotations.

General conclusion

When version and vergence interact during binocular eye movements, the abducting eye has a leading role in directing version, whereas the adducting eye is used to adjust for the vergence component. Vergence movements are accurate when visual cues are present to drive disparity, but memorization of disparity is insufficient to accurately guide memory-guided vergence in absent of visual cues. Processing of translational motion is dependent on adequate vestibular-visual interaction, both in compensatory eye movements (VOR) and voluntary eye movements in spatial updating.

REFERENCES

1. Erkelens, C.J., R.M. Steinman, and H. Collewijn, Ocular vergence under natural conditions. II. Gaze shifts between real targets differing in distance and direction. *Proc R Soc Lond B Biol Sci*, 1989. 236(1285): p. 441-65.
2. Howard, I.P., B.J. Rogers, and Oxford University Press., *Seeing in depth* 2008, New York: Oxford University Press. 1275.
3. Erkelens, C.J., Fusional limits for a large random-dot stereogram. *Vision Res*, 1988. 28(2): p. 345-53.
4. Schor, C., T. Heckmann, and C.W. Tyler, Binocular fusion limits are independent of contrast, luminance gradient and component phases. *Vision Res*, 1989. 29(7): p. 821-35.
5. Goebel, H.H., et al., Lesions of the pontine tegmentum and conjugate gaze paralysis. *Arch Neurol*, 1971. 24(5): p. 431-40.
6. Hepp, K. and V. Henn, Spatio-temporal recoding of rapid eye movement signals in the monkey paramedian pontine reticular formation (PPRF). *Exp Brain Res*, 1983. 52(1): p. 105-20.
7. Mays, L.E., Neural control of vergence eye movements: convergence and divergence neurons in midbrain. *J Neurophysiol*, 1984. 51(5): p. 1091-1108.
8. Mays, L.E., et al., Neural control of vergence eye movements: neurons encoding vergence velocity. *J Neurophysiol*, 1986. 56(4): p. 1007-21.
9. Zee, D.S., Brain stem and cerebellar deficits in eye movement control. *Trans Ophthalmol Soc U K*, 1986. 105 (Pt 5): p. 599-605.
10. Erkelens, C.J., A dual visual-local feedback model of the vergence eye movement system. *J Vis*, 2011. 11(10).
11. King, W.M., Binocular coordination of eye movements – Hering's Law of equal innervation or unioocular control? *Eur J Neurosci*, 2011. 33(11): p. 2139-46.
12. Cumming, B.G. and A.J. Parker, Responses of primary visual cortical neurons to binocular disparity without depth perception. *Nature*, 1997. 389(6648): p. 280-3.
13. Erkelens, C.J. and H. Collewijn, Eye movements and stereopsis during dichoptic viewing of moving random-dot stereograms. *Vision Res*, 1985. 25(11): p. 1689-700.
14. Poggio, G.F. and B. Fischer, Binocular interaction and depth sensitivity in striate and prestriate cortex of behaving rhesus monkey. *J Neurophysiol*, 1977. 40(6): p. 1392-405.
15. Barlow, H.B., C. Blakemore, and J.D. Pettigrew, The neural mechanism of binocular depth discrimination. *J Physiol*, 1967. 193(2): p. 327-42.
16. Baker, J.T., T.M. Harper, and L.H. Snyder, Spatial memory following shifts of gaze. I. Saccades to memorized world-fixed and gaze-fixed targets. *J Neurophysiol*, 2003. 89(5): p. 2564-76.
17. White, J.M., D.L. Sparks, and T.R. Stanford, Saccades to remembered target locations: an analysis of systematic and variable errors. *Vision Res*, 1994. 34(1): p. 79-92.
18. Collewijn, H., C.J. Erkelens, and R.M. Steinman, Binocular co-ordination of human horizontal saccadic eye movements. *J Physiol*, 1988. 404: p. 157-82.
19. Chen, A.L., et al., The role of the medial longitudinal fasciculus in horizontal gaze: tests of current hypotheses for saccade-vergence interactions. *Exp Brain Res*, 2011. 208(3): p. 335-43.
20. Helmholtz, H., *Helmholtz's treatise on physiological optics* (English translation of "Handbuch der physiologischen Optik", 1910), 1910/1962, New York: Dover.
21. Leigh, R.J. and D.S. Zee. *The neurology of eye movements*. 2006; 4th:[x, 763].
22. Bucci, M.P., et al., Disconjugate memory-guided saccades to disparate targets: temporal aspects. *Exp Brain Res*, 2000. 134(1): p. 133-8.
23. Israel, I., Memory-guided saccades: what is memorized? *Exp Brain Res*, 1992. 90(1): p. 221-4.

24. Yang, Q. and Z. Kapoula, Distinct control of initiation and metrics of memory-guided saccades and vergence by the FEF: a TMS study. *PLoS One*, 2011. 6(5): p. e20322.
25. Gamlin, P.D. and K. Yoon, An area for vergence eye movement in primate frontal cortex. *Nature*, 2000. 407(6807): p. 1003-7.
26. Kapoula, Z., et al., Role of the posterior parietal cortex in the initiation of saccades and vergence: right/left functional asymmetry. *Ann N Y Acad Sci*, 2005. 1039: p. 184-97.
27. Yang, Q. and Z. Kapoula, TMS over the left posterior parietal cortex prolongs latency of contralateral saccades and convergence. *Invest Ophthalmol Vis Sci*, 2004. 45(7): p. 2231-9.
28. Van Horn, M.R., D.M. Waitzman, and K.E. Cullen, Vergence neurons identified in the rostral superior colliculus code smooth eye movements in 3D space. *J Neurosci*, 2013. 33(17): p. 7274-84.
29. Schor, C.M. and K.J. Ciuffreda, Vergence eye movements: basic and clinical aspects 1983, Boston: Butterworth. xxx, 726.
30. Angelaki, D.E., H.H. Zhou, and M. Wei, Foveal versus full-field visual stabilization strategies for translational and rotational head movements. *J Neurosci*, 2003. 23(4): p. 1104-8.
31. Seidman, S.H., G.D. Paige, and D.L. Tomko, Adaptive plasticity in the naso-occipital linear vestibulo-ocular reflex. *Exp Brain Res*, 1999. 125(4): p. 485-94.
32. Tomko, D.L. and G.D. Paige, Linear vestibuloocular reflex during motion along axes between naso-occipital and interaural. *Ann N Y Acad Sci*, 1992. 656: p. 233-41.
33. Miles, F.A., The neural processing of 3-D visual information: evidence from eye movements. *Eur J Neurosci*, 1998. 10(3): p. 811-22.
34. Collewijn, H., et al., Human ocular counterroll: assessment of static and dynamic properties from electromagnetic scleral coil recordings. *Exp Brain Res*, 1985. 59(1): p. 185-96.
35. Aw, S.T., et al., Three-dimensional vector analysis of the human vestibuloocular reflex in response to high-acceleration head rotations. I. Responses in normal subjects. *J Neurophysiol*, 1996. 76(6): p. 4009-20.
36. Ferman, L., et al., Human gaze stability in the horizontal, vertical and torsional direction during voluntary head movements, evaluated with a three-dimensional scleral induction coil technique. *Vision Res*, 1987. 27(5): p. 811-28.
37. Seidman, S.H. and R.J. Leigh, The human torsional vestibulo-ocular reflex during rotation about an earth-vertical axis. *Brain Res*, 1989. 504(2): p. 264-8.
38. Tweed, D., et al., Rotational kinematics of the human vestibuloocular reflex. I. Gain matrices. *J Neurophysiol*, 1994. 72(5): p. 2467-79.
39. Paige, G.D. and S.H. Seidman, Characteristics of the VOR in response to linear acceleration. *Ann N Y Acad Sci*, 1999. 871: p. 123-35.
40. Paige, G.D. and D.L. Tomko, Eye movement responses to linear head motion in the squirrel monkey. II. Visual-vestibular interactions and kinematic considerations. *J Neurophysiol*, 1991. 65(5): p. 1183-96.
41. Ramat, S. and D.S. Zee, Ocular motor responses to abrupt interaural head translation in normal humans. *J Neurophysiol*, 2003. 90(2): p. 887-902.
42. Zhou, W., et al., Rapid motor learning in the translational vestibulo-ocular reflex. *J Neurosci*, 2003. 23(10): p. 4288-98.
43. Paige, G.D., et al., Human vestibuloocular reflex and its interactions with vision and fixation distance during linear and angular head movement. *J Neurophysiol*, 1998. 80(5): p. 2391-404.
44. Paige, G.D., The influence of target distance on eye movement responses during vertical linear motion. *Exp Brain Res*, 1989. 77(3): p. 585-93.

45. Wei, M., G.C. DeAngelis, and D.E. Angelaki, Do visual cues contribute to the neural estimate of viewing distance used by the oculomotor system? *J Neurosci*, 2003. 23(23): p. 8340-50.
46. Ramat, S., D. Straumann, and D.S. Zee, Interaural translational VOR: suppression, enhancement, and cognitive control. *J Neurophysiol*, 2005. 94(4): p. 2391-402.
47. Duhamel, J.R., C.L. Colby, and M.E. Goldberg, The updating of the representation of visual space in parietal cortex by intended eye movements. *Science*, 1992. 255(5040): p. 90-2.
48. Mays, L.E. and D.L. Sparks, Saccades are spatially, not retinocentrically, coded. *Science*, 1980. 208(4448): p. 1163-5.
49. Medendorp, W.P., et al., Rotational remapping in human spatial memory during eye and head motion. *J Neurosci*, 2002. 22(1): p. RC196.
50. Van Pelt, S. and W.P. Medendorp, Gaze-centered updating of remembered visual space during active whole-body translations. *J Neurophysiol*, 2007. 97(2): p. 1209-20.
51. Blouin, J., et al., Updating visual space during passive and voluntary head-in-space movements. *Exp Brain Res*, 1998. 122(1): p. 93-100.
52. Klier, E.M., B.J. Hess, and D.E. Angelaki, Differences in the accuracy of human visuospatial memory after yaw and roll rotations. *J Neurophysiol*, 2006. 95(4): p. 2692-7.
53. Klier, E.M., B.J. Hess, and D.E. Angelaki, Human visuospatial updating after passive translations in three-dimensional space. *J Neurophysiol*, 2008. 99(4): p. 1799-809.
54. Wei, M., et al., Deficits and recovery in visuospatial memory during head motion after bilateral labyrinthine lesion. *J Neurophysiol*, 2006. 96(3): p. 1676-82.
55. Medendorp, W.P., D.B. Tweed, and J.D. Crawford, Motion parallax is computed in the updating of human spatial memory. *J Neurosci*, 2003. 23(22): p. 8135-42.
56. Bloomberg, J., et al., Vestibular-contingent voluntary saccades based on cognitive estimates of remembered vestibular information. *Adv Otorhinolaryngol*, 1988. 41: p. 71-5.
57. Glasauer, S. and T. Brandt, Noncommutative updating of perceived self-orientation in three dimensions. *J Neurophysiol*, 2007. 97(4): p. 2958-64.



8

Summary / Samenvatting

SUMMARY

In our daily environment objects are located in different directions and at different viewing distances from our body. Humans have their eyes placed frontally and for this reason we have the ability to look at these objects using combined images of two eyes. This is called binocular vision. To obtain sharp vision, objects of interest have to be projected on the fovea of both retinas, where photoreceptor density is highest. In order to maintain clear and sharp binocular vision of during object- or self-motion it is essential to keep track of the location of objects around us. Eye movements are the most essential tool in accomplishing these goals. Eye movements are necessary to compensate for motion and direct the lines of sight of both eyes to new objects of interest. This interaction between processing of visual information and making eye movements is an ongoing process, which allows us to continuously update all changes in our visual environment. We also rely on our spatial memory to remember the locations of objects around us, when they are temporarily out of sight.

The aim of this thesis is to study the interaction between the gaze direction of both eyes (version) and the angle between both eyes (vergence) when eye movements interact with visual spatial memory, (intervening) whole body movements and the vestibular system. This thesis focuses on binocular eye movements in healthy human volunteers, to targets that are close to our eyes in 3-dimensional space.

Humans are normally unable to voluntarily move the eyes independently from one another. In chapter 2 we investigated to what extent humans have independent binocular control and what are the required conditions for this behavior. To test this a two-dimensional dichoptic visual stimulation paradigm was used. We demonstrated that to sustain binocular correspondence, humans can generate slow phase eye movements with independent motion directions and with different frequencies. The perceived direction of binocular motion can be dissociated from control of eye movement.

Orienting eye movements towards visible or remembered visual targets require binocular gaze changes that are accurate in direction (version) and ocular distance (vergence). In chapter 3 the accuracy and contribution of abducting and adducting eye during binocular gaze shifts towards memorized targets in three-dimensional space was determined and compared memorized binocular gaze shifts with visually-guided binocular gaze shifts. Visually-guided binocular gaze shifts are faster and more accurate than memory-guided binocular gaze shifts. In memory-guided gaze shifts the abducting eye is most accurate and has a leading role in version movements. Vergence errors are reflected in the adducting eye and an intra-saccadic vergence component during convergence was absent.

The vestibulo-ocular reflex (VOR) is a compensatory eye movement reflex, used to stabilize gaze during head and body motion in three dimensional space. In chapter 4 a six degrees of freedom motion platform is presented as a method for testing the three-dimensional vestibulo-ocular reflex in humans. The gain and misalignment of the 3D angular VOR provide a direct measure of the quality of vestibular function during movements in 3D space.

Translational (linear) and rotational (angular) head movements are detected and processed differently. The rotational VOR stabilizes gaze during rotations, by producing eye movements that are opposite to head movements. The rotational VOR can stabilize the whole visual field on the retina. In contrast to the rotational VOR, compensatory eye movements during the translational VOR stabilizes gaze at a given fixation point during whole body translations. Chapter 5 presents the influence of vergence angle and target distance on gaze stabilization during translations in humans. During translational passive whole body motion the gain of horizontal compensatory eye movements is appropriate to target distance. Eye velocity scales nearly perfectly with vergence angle for real targets when there is continuous visual feedback, but this relationship breaks down under conditions where vergence angle is changed without changing target distance, or when visual targets are flashed eliminating visual feedback.

When we move around, we have no difficulty in keeping track of objects around us, even when they are temporarily out of sight. To maintain accurate orientation we have to update our spatial representation, by taking intervening movements into account. In chapter 6 spatial memory updating after rotational and translational passive whole body movements was compared, by using a 6DF motion platform. Spatial update performance after passive whole-body vertical axis rotation was nearly perfect, while significant update errors occur after lateral translations. The abducting eye is most accurate during binocular memory-guided gaze shift in spatial updating tasks.

The following general conclusions are made in this thesis. Independent control of slow phase binocular eye movements is required to maintain binocular correspondence. When version and vergence interact during binocular eye movements, the abducting eye has a leading role in directing version, whereas the adducting eye is used to adjust for the vergence component. Vergence movements are accurate when visual cues are present to drive disparity, but memorization of disparity is insufficient to accurately guide memory-guided vergence in absence of visual cues. Processing of translational motion is dependent on adequate vestibular-visual interaction, both in compensatory eye movements (VOR) and voluntary eye movements in spatial updating.

SAMENVATTING

In onze omgeving bevinden objecten zich op verschillende afstanden ten opzichte van ons lichaam. Bij mensen zitten de ogen frontaal (aan de voorzijde van ons hoofd), waardoor we met beide ogen een beeld van een object kunnen vormen. Dit noemen we binoculair zien. Om een voorwerp scherp te zien, moet het beeld hiervan op de fovea (gele vlek) van beide retina's (netvliezen) worden geprojecteerd. In de fovea zijn de meeste fotoreceptoren aanwezig. Tijdens beweging is het van groot belang om voorwerpen te volgen, zodat onze visus scherp blijft. Oogbewegingen spelen hierin een essentiële rol. Door middel van oogbewegingen compenseren we continu voor bewegingen van voorwerpen en van ons lichaam zelf. Deze continue interactie zorgt ervoor dat we onze omgeving scherp zien en veranderingen in de omgeving waar kunnen nemen. Ons spatiële geheugen helpt ons de locatie van objecten vast te houden, zelfs wanneer deze tijdelijk uit ons gezichtsveld zijn. Het doel van dit proefschrift is om de interacties tussen onze kijkrichting (versie) en de hoek tussen onze ogen (vergentie, diepte) te onderzoeken, terwijl onze ogen samenwerken met het spatiële geheugen en het vestibulair systeem (evenwichtsorgaan). In dit proefschrift worden binoculaire oogbewegingen van gezonde proefpersonen onderzocht, naar objecten in de nabije 3-dimensionale ruimte.

Mensen kunnen de ogen niet bewust onafhankelijk van elkaar bewegen. In hoofdstuk 2 wordt onderzocht in welke mate mensen onafhankelijke binoculaire controle hebben en wanneer dit vereist is. Door middel van twee-dimensionale dichoptische stimuli laten we zien dat mensen langzame oogbewegingen kunnen maken met ieder oog in verschillende richting en frequentie.

Voor oriënterende oogbewegingen naar voorwerpen (reëel of vanuit ons geheugen) zijn nauwkeurige oogbewegingen in richting (versie) en diepte (vergentie) nodig. In hoofdstuk 3 wordt de nauwkeurigheid van binoculaire oogbewegingen naar objecten vergeleken met oogbewegingen naar een doel vanuit ons geheugen. Het abducerende en het adducerende oog worden vergeleken. Fouten worden met name in vergentie gemaakt, welke ook tot uiting komen de richting van het adducerende oog.

De vestibulo-oculaire reflex (VOR) is een snelle oogbeweging die zorgt voor blik stabilisatie tijdens bewegingen van ons hoofd en lichaam. In hoofdstuk 4 wordt het bewegingsplatform gepresenteerd, welke 6 vrijheidsgraden bezit. Met behulp van dit platform is het mogelijk de VOR in 3D te testen bij mensen. Door middel van de VOR kan het vestibulair systeem in meerdere aspecten worden onderzocht.

Draaibewegingen (rotatoir) en lineaire bewegingen worden op verschillende manieren verwerkt door het lichaam. In hoofdstuk 5 wordt de invloed van vergentie (kijkhoek) en

kijkafstand op de lineaire vestibulaire-oculaire reflex getest. Er wordt een directie relatie gevonden tussen vergentie en kijkafstand wanneer het doel continu aanwezig is. Bij kortdurend dimmen van het doel, vervaagt deze relatie.

In hoofdstuk 6 wordt het spatiële geheugen getest na verstoringen door tussenkomende (passieve) bewegingen van het bewegingsplatform. Er worden grotere fouten gemaakt na lineaire bewegingen van het platform. Hieruit blijkt dat rotatoire bewegingen gemakkelijker worden verwerkt en gecompenseerd dan lineaire bewegingen.

De volgende conclusies worden in dit proefschrift getrokken. Om binoculaire retinale correspondentie te behouden zijn onafhankelijke oogbewegingen tijdens gladde volgbewegingen mogelijk. Tijdens binoculaire oogbewegingen, bepaalt het abducerende oog de richting van de oogbeweging, terwijl het adducerende oog wordt gebruikt om vergentie aan te passen. Accurate vergentie is in hoge mate afhankelijk van visuele feedback, waardoor het vrijwel onmogelijk is om oogbewegingen in diepte te maken in afwezigheid hiervan. Het verwerken van lineaire beweging is afhankelijk van adequate vestibulaire-visuele interactie, zowel in compensatoire oogbewegingen (VOR) als bewuste oogbewegingen vanuit het geheugen.

CURRICULUM VITAE

Joyce Dits werd geboren op 2 december 1984 te Rotterdam, waar ze ook opgegroeid is. In 2003 behaalde zij haar V.W.O. diploma aan het Sint Montfoort College te Rotterdam, waarna zij startte met de opleiding geneeskunde aan de Erasmus Universiteit te Rotterdam. Tijdens deze studie werd haar interesse gewekt voor het zenuwstelsel en de hersenen, waardoor zij besloot een extra research master in de neurowetenschappen te volgen (Master of Neuroscience). Deze master werd afgerond in 2008, waarna zij in 2010 het artsexamen Cum Laude behaalde. Tijdens haar co-schappen werd duidelijk dat ondanks haar interesse voor de neurowetenschappen, het vak neurologie minder tot haar verbeelding sprak. Toch besloot zij haar met veel plezier gestarte onderzoek op de afdeling neurowetenschappen door de zetting in de vorm van een promotie traject onder supervisie van Prof.dr. J. van der Steen en Dr.ir. J.J.M. Pel. Door ervaring op te doen als arts niet in opleiding tot specialist (ANIOS) op de spoedeisende hulp afdeling van het Franciscus Ziekenhuis te Roosendaal, werd uiteindelijk duidelijk dat het beroep longarts goed bij haar past. Per januari 2013 is zij gestart met de specialisatie tot longarts aan het Erasmus Medisch Centrum, onder opleider Prof.dr. H.C. Hoogsteden. De eerste twee jaar vooropleiding interne geneeskunde worden momenteel gevolgd in het Ikazia Ziekenhuis in Rotterdam, onder opleider Dr. A.A.M. Zandbergen.

PHD PORTFOLIO

Summary of PhD training and teaching

| | | | |
|-------------------|--------------|--------------|---------------------------|
| Name PhD student: | Drs. J. Dits | PhD period: | 2009 – 2014 |
| Research School: | Erasmus MC | Promotor: | Prof.dr. J. Van Der Steen |
| Department: | Neuroscience | Co-promotor: | Dr.ir. J.J.M. Pel |

| 1. PhD training | Year | Workload (Hours) |
|--|-----------|------------------|
| Courses | | |
| Shanghai PhD summer program | 2011 | 80 |
| (Inter)national conferences | | |
| - NCM Seville (poster presentation) | 2008 | 40 |
| - NCM Hawaii (poster presentation) | 2009 | 40 |
| - NCM Puerto Rico (poster presentation) | 2011 | 40 |
| - ECVP Utrecht (poster presentation) | 2008 | 10 |
| - Dag van de Perceptie Eindhoven (poster presentation) | 2011 | 10 |
| Seminars and workshops | | |
| - Labtalks and seminars department neuroscience | 2009-2013 | 60 |
| - Helmholtz Lectures | 2010-2012 | 3 |
| - Lof der Geneeskunst | 2009 | 5 |
| Presentations | | |
| - Neuroscience labtalk | 2011 | 25 |
| - International PhD program Shanghai (oral presentation) | 2011 | 30 |
| - 5 poster presentation | 2010-2012 | 150 |
| 2. Teaching | | |
| Lecturing | | |
| - Workshop motion platform | 2011 | 5 |
| - Lab presentation neuroscience summerschool | 2010 | 10 |
| Supervising practicals and excursions, Tutoring | | |
| - Medicine practical on the visual and vestibular system | 2010-2011 | 30 |
| Supervising Master's theses | | |
| - Master neuroscience | 2011 | 50 |
| - Summerschool | 2010 | 5 |
| Total | | 593 |

LIST OF PUBLICATIONS

J. Dits, M.M. Houben, J. van der Steen,

“Three dimensional vestibular ocular reflex testing using a six degree of freedom motion platform”

Journal of Visualized Experiments. 2013 May 23;(75).

J. Dits, W.M. King, J. van der Steen

“Scaling of compensatory eye movements during translations± virtual versus real depth.”

Neuroscience. 2013 Aug 29;246:73-81

J. Dits, A. Remmers, J.J. Pel, J. van der Steen

“Version-vergence interactions during memory-guided binocular gaze shifts.”

Investigative Ophthalmology and Visual Science. 2013 Mar 5;54(3):1656-64.

J. van der Steen and J. Dits

“Binocular eye movement control and motion perception: what is being tracked?”

Investigative Ophthalmology and Visual Science. 2012 Oct 19;53(11):7268-75.

J. Goumans, M.M.J. Houben, J. Dits, J. van der Steen

“Peaks and troughs of three-dimensional vestibuloocular reflex in humans”

Journal of Association for Research in Otolaryngology. 2010 Sep;11(3):383-93.

DANKWOORD

Na ruim 3 jaar is het dan zo ver, mijn proefschrift is af! Zonder de steun van mensen om mij heen had ik de weg, die soms wat ongebruikelijk was, niet kunnen bewandelen.

Graag begin ik met het bedanken van mijn promotor, Hans van der Steen. Tijdens de Master of Neuroscience heb jij met het enorme bewegingsplatform mijn interesse gewekt voor het evenwichtsorgaan en oogbewegingen. Sinds vorig jaar ga jij als professor door het leven en ik vind het een grote eer om jouw eerste promovendus te zijn. Hans, bedankt voor je vertrouwen en de mogelijkheden die je me hebt geboden om mijn doel te bereiken.

Johan Pel, mijn co-promotor, zonder jou had ik een paar jaar geleden ongetwijfeld de handdoek in de ring gegooid. Bedankt voor je support, kritische blik, statistische kennis, gezelligheid en vriendschap. Als ik terug denk aan het gesmolten schepijs in Hawaï krijg ik weer kramp in mijn lachspieren.

Alle neuroscience collega's, bedankt voor de gezelligheid op het lab! Fleur, ik was vereerd jouw paranimf te zijn. Jammer dat je niet op mijn ceremonie aanwezig kunt zijn. Angelique, het was erg leuk om met jou te brainstormen en aan het platform te knutselen.

Professor Hoogsteden, bedankt voor de extra motivatie die u mij heeft gegeven om dit proefschrift af te maken en het vertrouwen in mij om mij op te leiden tot longarts.

I should also like to thank professor Mike King for reading my thesis and travelling to the Netherlands in order to participate in the committee. Graag wil ik ook de overige leden van de promotie commissie bedanken voor het beoordelen van mijn proefschrift.

Bedankt Dr. Zandbergen, Adrienne, voor de prettige opleidingsgesprekken en de mogelijkheid die ik heb gekregen om mijn vooropleiding op mijn eigen manier te doorlopen. Het promoveren naast mijn opleiding heeft veel van mij gevraagd. Interne collega's in het Ikazia, bedankt voor jullie gezelligheid en natuurlijk jullie flexibiliteit bij het uitvoeren van de laatste loodjes.

Niet te vergeten mijn vrienden en vriendinnen. Bedankt paranimfen, Marlijn, Marleen en Miriam, voor jullie vriendschap, begrip en steun. Marlijn, erg tof dat je samen met je kleine, mijn paranimf wilt zijn. Ik hoop dat je aanwezig kunt zijn tijdens de ceremonie. En Marleen, mijn reserve-paranimf, bedankt dat je deze taak zo hartelijk in ontvangst hebt genomen. Lieve meiden: Elke, Nina, Rianne, Hilde, Simone, Jennifer en Marieke, onze groep is gedurende de afgelopen jaren steeds hechter geworden. Ook jouw vriendschap, Dee, blijft

voor mij waardevol en bijzonder. Jullie hebben mijn gehele promotietraject vanaf de zijlijn meegemaakt. Dank voor al jullie support. Vanaf nu is er meer tijd voor gezellige avondjes en borrels. Jippie!

Lieve pap en mam, bedankt voor jullie eindeloze vertrouwen en steun. Zoals in heel mijn leven, hebben jullie ook tijdens dit promotietraject altijd voor mij klaar gestaan. Mam, bedankt voor het meedenken en ontwerpen van de omslag!

Als laatste bedank ik jou, lieve Dennis, mijn allergrootste steun. De afgelopen jaren heb ik meerdere carrière keuzes moeten maken. Jouw eindeloze geduld en begrip heeft het voor mij mogelijk gemaakt de juiste beslissingen te nemen en tevens dit boekje af te maken. Ik bewonder je enorme inlevingsvermogen. Dank je wel voor alles.

